

Gluon Double-Spin Asymmetry in the Longitudinally Polarized $p + p$ Collisions

Yuri V. Kovchegov^{1,*} and Ming Li^{1,†}

¹*Department of Physics, The Ohio State University, Columbus, OH 43210, USA*

We derive the first-ever small- x expression for the inclusive gluon production cross section in the central rapidity region of the longitudinally polarized proton-proton collisions. The cross section depends on the polarizations of both protons, therefore comprising the numerator of the longitudinal double-spin asymmetry A_{LL} for the produced gluons. The cross section is calculated in the shock wave formalism and is expressed in terms of the polarized dipole scattering amplitudes on the projectile and target protons. We show that the small- x evolution corrections are included into our cross section expression if one evolves these polarized dipole amplitudes using the double-logarithmic helicity evolution derived in [1–4]. Our calculation is performed for the gluon sector only, with the quark contribution left for future work. When that work is complete, the resulting formula will be applicable to longitudinally polarized proton-proton and proton-nucleus collisions, as well as to polarized semi-inclusive deep inelastic scattering (SIDIS) on a proton or a nucleus. Our results should allow one to extend the small- x helicity phenomenology analysis of [5] to the jet/hadron production data reported for the longitudinally polarized proton-proton collisions at RHIC and to polarized SIDIS measurements at central rapidities to be performed at the EIC.

CONTENTS

I. Introduction	1
II. Gluon production in the shock wave formalism	3
A. The scattering amplitude	3
B. Inclusive gluon production cross section	5
C. Target–projectile symmetric form for the gluon production cross section	9
D. Lowest-order calculations	13
III. Including small- x evolution	16
A. Target side	17
B. Projectile side	17
IV. Conclusions and outlook	18
Acknowledgments	19
A. Ultraviolet contribution to $(D + E) A_{\text{eik}}^* + \text{c.c.}$ interference terms	19
B. Small- x limit of twist-3 gluon helicity-flip TMD	20
C. Gluon production in an adjoint dipole scattering on a polarized target	22
1. \mathcal{F}^{12} -type dipole projectile	22
2. $(\mathcal{D}^i - \tilde{\mathcal{D}}^i)$ -type dipole projectile	25
References	30

I. INTRODUCTION

Understanding helicity distributions for quarks and gluons at small values of Bjorken x is an integral part of the proton spin puzzle [6–17]. Since the current and future experiments can only probe these helicity distributions down to some small value of $x = x_{\text{min}}$, and would not be able to reach all the way down to $x = 0$ due to the finite energy

* Email: kovchegov.1@osu.edu

† Email: li.13499@osu.edu

coverage [9, 11, 13–15, 17], there appears to be a need for a theoretically controlled extrapolation of the helicity distributions down to very small x values. A promising approach to accomplishing this goal is in using the small- x evolution equations, which can predict the parton distributions at small x given some initial conditions at the larger $x = x_0$ and assuming that the strong coupling is sufficiently small (see [18–30] for spin-independent small- x evolution equations and [31–38] for reviews).

The past decade has seen a significant advancement of our theoretical understanding of helicity evolution at small x [1–4, 39–50] in the framework of the shock wave/ s -channel evolution formalism [21–30, 51–53]. The sub-eikonal and, in some cases, sub-sub-eikonal (suppressed by one or two powers of the center-of-mass energy squared s) corrections to the eikonal scattering of quarks and gluons on a background field have been found in [3, 42, 54–67]. This informed the in-parallel development of the small- x evolution for the sub-eikonal operators related to the quark and gluon flavor-singlet helicity distribution functions $\Delta\Sigma(x, Q^2)$ and $\Delta G(x, Q^2)$, and to the g_1 structure function [1–4, 39–50]. (Flavor non-singlet helicity evolution in the s -channel formalism was derived in [2].) The corresponding formalism, involving sub-eikonal and sub-sub-eikonal operators on the light-cone, has been referred to as the light-cone operator treatment (LCOT) [1–4, 61, 63].

The leading-order helicity evolution derived in [1–4] is in the double-logarithmic approximation (DLA): it sums up powers of $\alpha_s \ln^2(1/x)$, where α_s is the strong coupling constant. Its original version was derived in [1–3] (KPS), and has recently been modified in [4] (KPS-CTT). A resummation of the single-logarithmic corrections (power of $\alpha_s \ln(1/x)$) for helicity evolution was attempted in [48], but needs to be revised in light of the recent modifications of the DLA evolution found in [4].

The evolution equations [1–4] close in the large- N_c [68] and large- $N_c \& N_f$ [69] limits, with N_c and N_f the numbers of quark colors and flavors, respectively. The evolution equations have been solved numerically and analytically [4, 49] for large N_c and numerically [50] for large $N_c \& N_f$. The resulting intercepts driving the small- x asymptotics of the helicity parton distribution functions (hPDFs) $\Delta\Sigma(x, Q^2)$ and $\Delta G(x, Q^2)$, and the g_1 structure function appear to be close to but slightly differ (at the $< 1\%$ level at large N_c [4, 49] and $< 3\%$ level at large $N_c \& N_f$ [50]) from those found earlier in the pioneering work by Bartels, Ermolaev and Ryskin (BER) [70, 71], in which hPDFs at small x were calculated employing an entirely different approach, the infrared evolution equations (IREE) formalism from Refs. [72–77]. The origin of this minor disagreement is not yet clear: see the Appendices of Refs. [2, 49] for the possible reasons for the discrepancy. (There appears to be no disagreement between the flavor non-singlet helicity PDFs asymptotics found in [70] using IREE and in [2] using LCOT at large N_c . A disagreement between the BER formalism for the flavor-singlet distributions and the exact calculation of the 3-loop polarized anomalous dimension was observed earlier in [78, 79], but was shown to be attributable to scheme dependence.)

Since the disagreements between the LCOT and BER approaches outlined above are numerically small, it appears that the degree of agreement between the two approaches is sufficient to perform phenomenological analyses of the data based on these formalisms. Such analyses based on the BER formalism had been performed in Refs. [76, 80–84], before the LCOT approach was developed. More recently, a phenomenological analysis of the polarized deep inelastic scattering (DIS) and semi-inclusive DIS (SIDIS) data was performed in Ref. [5] using the large- $N_c \& N_f$ KPS-CTT evolution with running coupling (see also [85] for a similar “proof-of-principle” analysis of the polarized DIS data only using the earlier KPS evolution). The analysis of [5] resulted in a successful fit of the world polarized DIS and SIDIS data for $x < 0.1$ and with the photon virtuality $Q^2 > 1.69 \text{ GeV}^2$. At the same time, the analysis in [5] found the existing polarized DIS and SIDIS data insufficient to completely fix the initial conditions for small- x helicity evolution. This resulted in a significant spread of the predictions achieved in [5] for the hPDFs and the proton g_1 structure function at lower values of x than probed in the present or past experiments, reducing the advantage of the small- x evolution approach over the more standard Q^2 -evolution approaches [86–100] based on the (spin-dependent) Dokshitzer-Gribov-Lipatov-Altarelli-Parisi (DGLAP) evolution equations [101–103], which cannot predict hPDFs at very small x .

One way to address this issue is to wait for the future Electron-Ion Collider (EIC) [9, 11, 15, 17] to generate more polarized DIS and SIDIS data. However, to better test theoretical predictions, it would be desirable to reduce the spread found in [5] before the start of the EIC experimental program. To this end, one may try utilizing the data on the jets and pion production in polarized proton-proton collisions reported by the experiments at the Relativistic Heavy Ion Collider (RHIC) (see [104, 105] along with [13, 14] for a summary of those results). However, to describe the RHIC Spin data in the small- x formalism, one needs to derive an expression for the numerator of the double-spin asymmetry A_{LL} , preferably in terms of the so-called polarized dipole scattering amplitudes entering the helicity evolution equations [1–4] and employed in the polarized DIS and SIDIS analysis of [5]. The double-spin asymmetry is defined by

$$A_{LL} = \frac{d\sigma(++) - d\sigma(+-)}{d\sigma(++) + d\sigma(+-)}, \quad (1)$$

where $d\sigma(++)$ ($d\sigma(+-)$) is the differential cross section with the colliding protons having the same (opposite) helicities. We see that to find the numerator of A_{LL} one needs to calculate the part of the particle production cross section in the

$p + p$ collisions dependent on the helicities of the colliding protons. This is an inclusive particle production observable, different, for instance, from the total scattering DIS cross section needed to calculate the structure functions. While the SIDIS process analyzed in [5] also involves inclusive hadron production, the calculation there was simplified since in most of the existing polarized SIDIS data the hadron is produced in the current fragmentation region (i.e., in the forward direction for the virtual photon). Motivated by the RHIC data [13, 14, 104, 105], we would like to calculate hadron production in the central rapidity region, far (in rapidity) from the fragmentation regions of both colliding protons. Similar analytic calculations have been carried out at small x in the unpolarized case in [106–116]. Specifically, for gluon production in unpolarized proton–proton collisions, the target–projectile symmetric expression for inclusive gluon production cross section in the small- x /saturation formalism was obtained in [108, 110]. The result of [108, 110] can be used in the denominator of the double-spin asymmetry A_{LL} in Eq. (1).

Our calculation will follow the standard technique for small- x inclusive hadron production cross section calculations outlined in [37], with the exception that we are now interested in the sub-eikonal correction to this cross section, dependent on the helicities of the colliding protons. We will employ the operator formalism in the LCOT framework. For simplicity, in this paper we will work in the gluon sector only. Hence, the colliding polarized protons for us will be dominated by gluons, and the produced particle will be a gluon as well. Since quarks also contribute to the small- x helicity evolution in the DLA, they will certainly contribute to hadron production too. We leave the inclusion of the quark contributions to future work, concentrating only on the gluons here.

We derive the inclusive gluon production cross section in the polarized-particle scattering in Sec. II, employing the shock wave formalism [21], treating one of the scattering particles as a fast-moving projectile and another one as a target shock wave. For simplicity, we take the incoming particle to be a (longitudinally polarized) gluon. After obtaining an expression for the inclusive gluon production cross section in Sec. IIB (see Eq. (29)), we recast it in the projectile–target symmetric form in Eq. (55) from Sec. IIC, in the process expressing it in terms of the polarized dipole amplitudes for scattering on the projectile and on the target. These polarized dipole amplitudes can be evaluated in the quasi-classical approximation of the Glauber–Gribov–Mueller (GGM) scattering/McLerran–Venugopalan (MV) model [117–120] by using the helicity-dependent version [46] of the MV model: this would give a quasi-classical approximation to inclusive gluon production in the polarized $p + p$ collisions, not shown explicitly below. In Sec. IID we cross-check our result (55) at the lowest non-trivial order by comparing it to the calculations existing in the literature (which we also redo in a different gauge): we find a complete agreement between all lowest-order results.

The small- x helicity evolution [1–4] is included into the expression (55) for the inclusive cross section in Sec. III in the large- N_c approximation. Similar to the unpolarized case [37, 110], the evolution effects leave the expression (55) for the production cross section unchanged, and are accounted for by evolving the polarized dipole amplitudes entering this expression using the large- N_c KPS-CTT evolution. The rapidity intervals between the produced gluon and the target and between the produced gluon and the projectile are different, requiring evolution up to different values of rapidity for the projectile and target polarized dipole amplitudes. We summarize our main results and conclude in Sec. IV.

II. GLUON PRODUCTION IN THE SHOCK WAVE FORMALISM

A. The scattering amplitude

The diagrams contributing to inclusive gluon production in the scattering of a longitudinally polarized gluon on a longitudinally polarized target are shown in Fig. 1. The produced gluon is denoted by a cross. As usual, the shaded rectangle denotes the shock wave of the target fields. The black circle denotes the sub-eikonal helicity-dependent vertex, while the small white square denotes the sub-eikonal interaction with the shock wave. This is the same notation as that used in [1–4, 39–46, 48]. As mentioned above, throughout this paper we will be working in the gluon sector: this is why the quark-mediated contributions are not included in Fig. 1.

To calculate the diagrams in Fig. 1 we will employ the sub-eikonal expansion of the S -matrix for a high-energy gluon scattering in the background quark and gluon fields [3, 55, 57, 60, 61]. Following the notation of [4] we write the high-energy gluon’s S -matrix as

$$(U_{\underline{x}, \underline{y}; \lambda', \lambda})^{ba} \equiv (U_{\underline{x}})^{ba} \delta^2(\underline{x} - \underline{y}) \delta_{\lambda, \lambda'} + \lambda \delta_{\lambda, \lambda'} (U_{\underline{x}}^{\text{pol}[1]})^{ba} \delta^2(\underline{x} - \underline{y}) + \delta_{\lambda, \lambda'} (U_{\underline{x}, \underline{y}}^{\text{pol}[2]})^{ba} + \mathcal{O}\left(\frac{1}{s^2}\right) \quad (2)$$

keeping terms up to and including the sub-eikonal order (that is, up to and including order- $1/s$ terms in the expansion in inverse powers of the center of mass energy squared s for the projectile–target scattering). Here $b(a)$ and $\lambda'(\lambda)$ are the final(initial) gluon colors and polarizations. The transverse vectors are denoted by $\underline{v} = (v^1, v^2)$. The adjoint

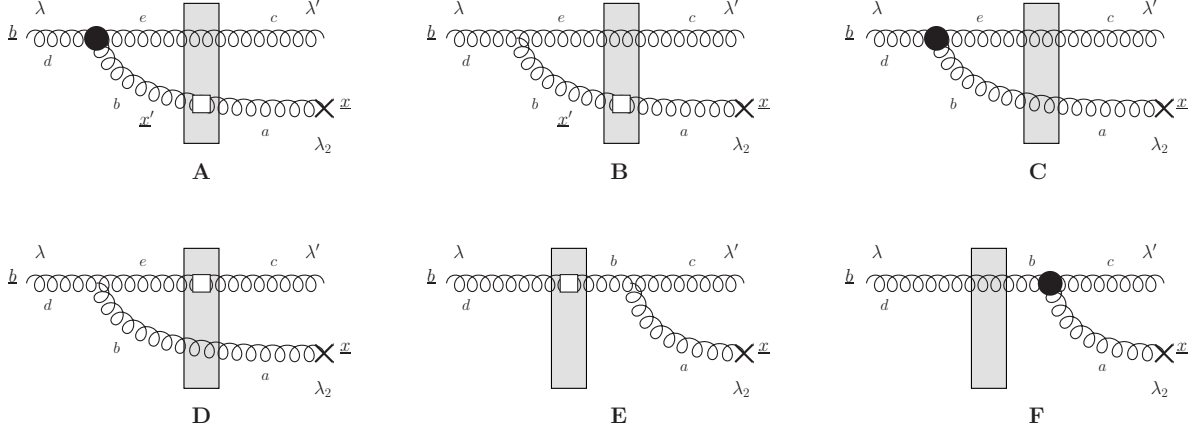


FIG. 1. Diagrams contributing to gluon production in the polarized hadron–hadron scattering in the pure glue picture. The rectangle denotes the shock wave, while the produced gluon is indicated by a cross.

light-cone Wilson line is defined by

$$U_{\underline{x}}[x_f^-, x_i^-] = \mathcal{P} \exp \left[ig \int_{x_i^-}^{x_f^-} dx^- \mathcal{A}^+(0^+, x^-, \underline{x}) \right] \quad (3)$$

with the gluon field $\mathcal{A}^\mu = \sum_a A^{a\mu} T^a$, where T^a are the adjoint $SU(N_c)$ generators, $(T^a)_{bc} = -if^{abc}$. Here \mathcal{P} is the path ordering operator and g is the QCD coupling constant. The light-cone coordinates are defined by $x^\pm = (t \pm z)/\sqrt{2}$. The gluon in Eq. (2) is predominantly moving in the light-cone minus direction. The infinite light-cone Wilson line is $U_{\underline{x}} = U_{\underline{x}}[\infty, -\infty]$: this is the eikonal (order- $(1/s)^0$) contribution coming from the first term on the right of Eq. (2).

The sub-eikonal (order- $1/s$) contribution is given by the second and third terms on the right of Eq. (2). They are referred to as the polarized Wilson lines of the first and second kind. As in [4], we separate the quark and gluon sub-eikonal operator contributions by writing

$$U_{\underline{x}}^{\text{pol}[1]} = U_{\underline{x}}^{\text{G}[1]} + U_{\underline{x}}^{\text{q}[1]}, \quad U_{\underline{x}, \underline{y}}^{\text{pol}[2]} = U_{\underline{x}, \underline{y}}^{\text{G}[2]} + U_{\underline{x}, \underline{y}}^{\text{q}[2]} \delta^2(\underline{x} - \underline{y}), \quad (4)$$

with

$$(U_{\underline{x}}^{\text{G}[1]})^{ba} = \frac{2igp_1^+}{s} \int_{-\infty}^{\infty} dx^- (U_{\underline{x}}[\infty, x^-])^{bb'} (\mathcal{F}^{12})^{b'a'}(x^-, \underline{x}) (U_{\underline{x}}[x^-, -\infty])^{a'a}, \quad (5a)$$

$$(U_{\underline{x}}^{\text{q}[1]})^{ba} = \frac{g^2 p_1^+}{2s} \int_{-\infty}^{\infty} dx_1^- \int_{x_1^-}^{\infty} dx_2^- (U_{\underline{x}}[\infty, x_2^-])^{bb'} \bar{\psi}(x_2^-, \underline{x}) t^{b'} V_{\underline{x}}[x_2^-, x_1^-] \gamma^+ \gamma^5 t^{a'} \psi(x_1^-, \underline{x}) (U_{\underline{x}}[x_1^-, -\infty])^{a'a} + \text{c.c.}, \quad (5b)$$

$$(U_{\underline{x}, \underline{y}}^{\text{G}[2]})^{ba} = -\frac{ip_1^+}{s} \int_{-\infty}^{\infty} dz^- d^2z (U_{\underline{x}}[\infty, z^-])^{bb'} \delta^2(\underline{x} - \underline{z}) \tilde{\mathcal{D}}^{b'c}(z^-, \underline{z}) \mathcal{D}^{ca'}(z^-, \underline{z}) (U_{\underline{y}}[z^-, -\infty])^{a'a} \delta^2(\underline{y} - \underline{z}), \quad (5c)$$

$$(U_{\underline{x}}^{\text{q}[2]})^{ba} = -\frac{g^2 p_1^+}{2s} \int_{-\infty}^{\infty} dx_1^- \int_{x_1^-}^{\infty} dx_2^- (U_{\underline{x}}[\infty, x_2^-])^{bb'} \bar{\psi}(x_2^-, \underline{x}) t^{b'} V_{\underline{x}}[x_2^-, x_1^-] \gamma^+ t^{a'} \psi(x_1^-, \underline{x}) (U_{\underline{x}}[x_1^-, -\infty])^{a'a} - \text{c.c.} \quad (5d)$$

Here p_1^+ is the large momentum component of the target proton, ψ and $\bar{\psi}$ are the quark and anti-quark background fields, $\mathcal{D}_i^{ab} = \partial_i \delta^{ab} - ig(T^c)_{ab} A_i^c$ and $\tilde{\mathcal{D}}_i^{ab} = \tilde{\partial}_i \delta^{ab} + ig(T^c)_{ab} A_i^c$ are the right- and left-acting adjoint covariant derivatives, \mathcal{F}^{12} is a component of the adjoint field-strength tensor, and t^a are the fundamental $SU(N_c)$ generators. The fundamental light-cone Wilson lines are defined similarly to Eq. (3) by

$$V_{\underline{x}}[x_f^-, x_i^-] = \mathcal{P} \exp \left[ig \int_{x_i^-}^{x_f^-} dx^- A^+(0^+, x^-, \underline{x}) \right] \quad (6)$$

with the gluon field given by $A^\mu = \sum_a A^{\mu} t^a$. It is useful to define the abbreviation $V_{\underline{x}} = V_{\underline{x}}[\infty, -\infty]$ for infinite lines.

Since we are interested in the sub-eikonal polarization-dependent cross section, we will need to keep only the contributions to the diagrams A, C, D, E, and F in Fig. 1 which depend on the polarization λ of the incoming gluon. In terms of the operators, this means that the black circle in diagrams A, C and F denotes the insertion of the sub-eikonal operator containing \mathcal{F}^{12} from Eq. (5a), while the white box in diagrams D and E brings in the entire $U_{\underline{b}}^{G[1]}$ operator.

Using the notation outlined above, the diagrams in Fig. 1 contribute as follows in the $A^- = 0$ gauge for the minus-moving projectile and plus-moving target:

$$iA = -\frac{g}{\pi} \lambda \delta_{\lambda, \lambda'} \frac{k^-}{p_2} (U_{\underline{b}} T^b)^{cd} \epsilon^{ij} \epsilon_{\lambda_2}^{j*} \left\{ \frac{(x-b)^i}{|\underline{x}-\underline{b}|^2} \left[\lambda_2 \left(U_{\underline{x}}^{\text{pol}[1]} \right)^{ab} + \left(U_{\underline{x}}^{\text{q}[2]} \right)^{ab} \right] + \int d^2 x' \frac{(x'-b)^i}{|\underline{x}'-\underline{b}|^2} \left(U_{\underline{x}, \underline{x}'}^{G[2]} \right)^{ab} \right\}, \quad (7a)$$

$$iB = \frac{ig}{\pi} \delta_{\lambda, \lambda'} (U_{\underline{b}} T^b)^{cd} \epsilon_{\lambda_2}^{i*} \left\{ \frac{(x-b)^i}{|\underline{x}-\underline{b}|^2} \left[\lambda_2 \left(U_{\underline{x}}^{\text{pol}[1]} \right)^{ab} + \left(U_{\underline{x}}^{\text{q}[2]} \right)^{ab} \right] + \int d^2 x' \frac{(x'-b)^i}{|\underline{x}'-\underline{b}|^2} \left(U_{\underline{x}, \underline{x}'}^{G[2]} \right)^{ab} \right\}, \quad (7b)$$

$$iC = -\frac{g}{\pi} \lambda \delta_{\lambda, \lambda'} \frac{k^-}{p_2} (U_{\underline{b}} T^b)^{cd} \epsilon^{ij} \epsilon_{\lambda_2}^{j*} \frac{(x-b)^i}{|\underline{x}-\underline{b}|^2} (U_{\underline{x}})^{ab}, \quad (7c)$$

$$iD = \frac{ig}{\pi} \lambda \delta_{\lambda, \lambda'} \frac{\epsilon_{\lambda_2}^* \cdot (x-b)}{|\underline{x}-\underline{b}|^2} (U_{\underline{x}})^{ab} \left(U_{\underline{b}}^{\text{pol}[1]} T^b \right)^{cd}, \quad (7d)$$

$$iE = -\frac{ig}{\pi} \lambda \delta_{\lambda, \lambda'} \frac{\epsilon_{\lambda_2}^* \cdot (x-b)}{|\underline{x}-\underline{b}|^2} \left(T^a U_{\underline{b}}^{\text{pol}[1]} \right)^{cd}, \quad (7e)$$

$$iF = \frac{g}{\pi} \lambda \delta_{\lambda, \lambda'} \frac{k^-}{p_2} (T^a U_{\underline{b}})^{cd} \epsilon^{ij} \epsilon_{\lambda_2}^{j*} \frac{(x-b)^i}{|\underline{x}-\underline{b}|^2} = \frac{g}{\pi} \lambda \delta_{\lambda, \lambda'} \frac{k^-}{p_2} (U_{\underline{b}} T^b)^{cd} \epsilon^{ij} \epsilon_{\lambda_2}^{j*} \frac{(x-b)^i}{|\underline{x}-\underline{b}|^2} (U_{\underline{b}})^{ab}. \quad (7f)$$

The diagram contributions are given in the mixed representation: they are in the transverse position space while in the longitudinal momentum space. We are keeping only the sub-eikonal contributions, and only the projectile helicity-dependent terms in diagrams A, C, D, E, F. For the future reference, we are keeping the quark contributions in the polarized Wilson lines: they will be discarded shortly below. Our amplitudes are normalized as $A = M/(2s)$ [37] compared to the standard normalization for the scattering amplitudes M : this makes the eikonal contribution to the amplitudes energy-independent.

Here k^- is the minus momentum of the produced gluon, while p_2^- is the momentum of the incoming (projectile) one. We assume that $k^- \ll p_2^-$. The gluon polarization four-vector is $\epsilon_{\lambda}^{\mu} = (\epsilon_{\lambda} \cdot \underline{k}/k^-, 0^-, \epsilon_{\lambda})$ with $\epsilon_{\lambda} = -(1/\sqrt{2})(\lambda, i)$ [121] for a gluon with momentum k^{μ} and polarization λ . The incoming gluon is at the transverse position \underline{b} , while the produced one is at \underline{x} to the right of the shock wave and at \underline{x}' to the left (in diagrams A and B only). The color indices and polarizations are shown in Fig. 1. Latin indices denote the transverse directions, $i, j = 1, 2$, while ϵ^{ij} is the transverse Levi-Civita symbol. In simplifying the expression for the diagram F we have used the following Wilson-line identity:

$$(U_{\underline{x}})^{ab} T^b = U_{\underline{x}}^{\dagger} T^a U_{\underline{x}}. \quad (8)$$

As one can show, emissions of the produced gluon from inside the shock wave are suppressed by one power of the logarithm of its transverse momentum [67]. Therefore, they are not included in Fig. 1 and in our analysis here.

The relevant contributions to the net scattering amplitude are

$$A(\underline{x}, \underline{b}) = A_{\text{eik}} + A + B + \dots + F. \quad (9)$$

where the eikonal unpolarized gluon emission at the same order- g in the coupling is [106]

$$iA_{\text{eik}}(\underline{x}, \underline{b}) = \frac{ig}{\pi} \delta_{\lambda, \lambda'} \frac{\epsilon_{\lambda_2}^* \cdot (x-b)}{|\underline{x}-\underline{b}|^2} \left[(U_{\underline{x}})^{ab} - (U_{\underline{b}})^{ab} \right] (U_{\underline{b}} T^b)^{cd}. \quad (10)$$

B. Inclusive gluon production cross section

The inclusive gluon production cross section is [37]

$$\frac{d\sigma(\lambda)}{d^2 k_T dy} = \frac{1}{2(2\pi)^3} \int d^2 x d^2 y d^2 b e^{-ik \cdot (x-y)} \langle A(\underline{x}, \underline{b}) A^*(\underline{y}, \underline{b}) \rangle \quad (11)$$

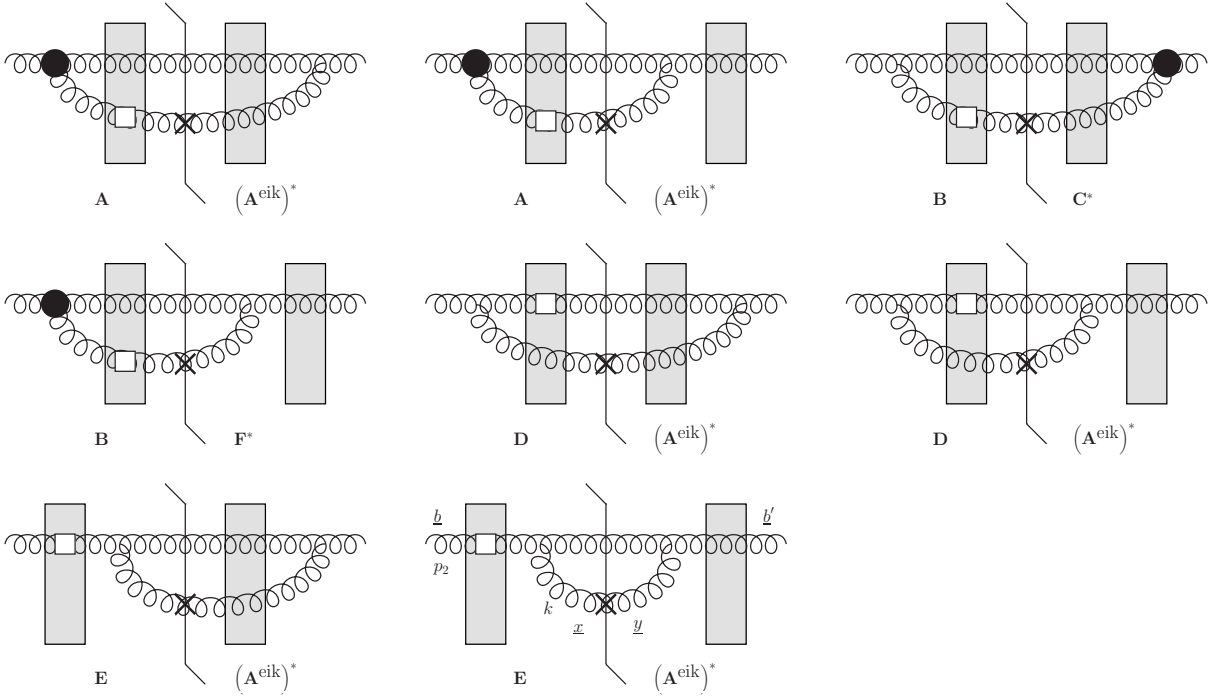


FIG. 2. Diagrams contributing to the gluon production cross section in the polarized hadron-hadron scattering in the pure glue picture. The thin straight vertical line indicates the final state cut. Complex conjugate contributions are implied but not shown.

in terms of the mixed-representation scattering amplitudes we employ normalized as described above. Here k^μ is the produced gluon's 4-momentum with $k_T = |k|$, while $y = (1/2) \ln(k^-/k^+)$ is its rapidity. We are only interested in the part which depends on the polarization λ of the incoming gluon and on the polarization of the target. Restricting the calculation to the sub-eikonal order we write the relevant contributions schematically as

$$A(\underline{x}, \underline{b}) A^*(\underline{y}, \underline{b}) = (A + D + E) A_{\text{eik}}^* + B(C^* + F^*) + \text{c.c.} \quad (12)$$

This is illustrated diagrammatically in Fig. 2.

Dropping the quark contributions in Eqs. (7) we rewrite them as

$$A = \frac{ig}{\pi} \lambda \delta_{\lambda, \lambda'} \frac{k^-}{p_2^-} (U_{\underline{b}} T^b)^{cd} \epsilon^{ij} \epsilon_{\lambda_2}^{j*} \left[\frac{(x-b)^i}{|\underline{x}-\underline{b}|^2} \lambda_2 (U_{\underline{x}}^{\text{G}[1]})^{ab} + \int d^2 x' \frac{(x'-b)^i}{|\underline{x}'-\underline{b}|^2} (U_{\underline{x}, \underline{x}'}^{\text{G}[2]})^{ab} \right], \quad (13a)$$

$$B = \frac{g}{\pi} \delta_{\lambda, \lambda'} (U_{\underline{b}} T^b)^{cd} \epsilon_{\lambda_2}^{i*} \left[\frac{(x-b)^i}{|\underline{x}-\underline{b}|^2} \lambda_2 (U_{\underline{x}}^{\text{G}[1]})^{ab} + \int d^2 x' \frac{(x'-b)^i}{|\underline{x}'-\underline{b}|^2} (U_{\underline{x}, \underline{x}'}^{\text{G}[2]})^{ab} \right], \quad (13b)$$

$$C = \frac{ig}{\pi} \lambda \delta_{\lambda, \lambda'} \frac{k^-}{p_2^-} (U_{\underline{b}} T^b)^{cd} \epsilon^{ij} \epsilon_{\lambda_2}^{j*} \frac{(x-b)^i}{|\underline{x}-\underline{b}|^2} (U_{\underline{x}})^{ab}, \quad (13c)$$

$$D = \frac{g}{\pi} \lambda \delta_{\lambda, \lambda'} \frac{\epsilon_{\lambda_2}^* \cdot (\underline{x}-\underline{b})}{|\underline{x}-\underline{b}|^2} (U_{\underline{x}})^{ab} (U_{\underline{b}}^{\text{G}[1]} T^b)^{cd}, \quad (13d)$$

$$E = -\frac{g}{\pi} \lambda \delta_{\lambda, \lambda'} \frac{\epsilon_{\lambda_2}^* \cdot (\underline{x}-\underline{b})}{|\underline{x}-\underline{b}|^2} (T^a U_{\underline{b}}^{\text{G}[1]})^{cd}, \quad (13e)$$

$$F = -\frac{ig}{\pi} \lambda \delta_{\lambda, \lambda'} \frac{k^-}{p_2^-} (U_{\underline{b}} T^b)^{cd} \epsilon^{ij} \epsilon_{\lambda_2}^{j*} \frac{(x-b)^i}{|\underline{x}-\underline{b}|^2} (U_{\underline{b}})^{ab}. \quad (13f)$$

Concentrating on individual contributions to the production cross section from Eq. (12) we begin with the diagram A and get, after a considerable algebra similar to that in [4],

$$\begin{aligned} \frac{d\sigma^{A A_{\text{eik}}^* + \text{c.c.}}(\lambda)}{d^2 k_T dy} &= \lambda \frac{4\alpha_s}{(2\pi)^4} \frac{k^-}{p_2^-} \frac{N_c}{N_c^2 - 1} \int d^2 x d^2 y d^2 b e^{-ik \cdot (\underline{x}-\underline{y})} \left\{ \frac{\underline{x}-\underline{b}}{|\underline{x}-\underline{b}|^2} \cdot \frac{\underline{y}-\underline{b}}{|\underline{y}-\underline{b}|^2} \langle \text{Tr} [U_{\underline{y}}^\dagger U_{\underline{x}}^{\text{G}[1]}] - \text{Tr} [U_{\underline{b}}^\dagger U_{\underline{x}}^{\text{G}[1]}] \rangle \right. \\ &\quad \left. + i \int d^2 x' \frac{\underline{x}'-\underline{b}}{|\underline{x}'-\underline{b}|^2} \times \frac{\underline{y}-\underline{b}}{|\underline{y}-\underline{b}|^2} \langle \text{Tr} [U_{\underline{y}}^\dagger U_{\underline{x}, \underline{x}'}^{\text{G}[2]}] - \text{Tr} [U_{\underline{b}}^\dagger U_{\underline{x}, \underline{x}'}^{\text{G}[2]}] \rangle \right\} + \text{c.c.} \end{aligned}$$

$$\begin{aligned}
&= \lambda \frac{\alpha_s}{2\pi^4} \frac{1}{s} N_c \int d^2x d^2y d^2b e^{-ik \cdot (x-y)} \left\{ \frac{\underline{x}-\underline{b}}{|\underline{x}-\underline{b}|^2} \cdot \frac{\underline{y}-\underline{b}}{|\underline{y}-\underline{b}|^2} \left[G_{\underline{x},\underline{y}}^{\text{adj}}(2k^- p_1^+) - G_{\underline{x},\underline{b}}^{\text{adj}}(2k^- p_1^+) \right] \right. \\
&\quad \left. - 2i k^i \frac{\underline{x}-\underline{b}}{|\underline{x}-\underline{b}|^2} \times \frac{\underline{y}-\underline{b}}{|\underline{y}-\underline{b}|^2} G_{\underline{x},\underline{b}}^{i \text{adj}}(2k^- p_1^+) \right\}. \tag{14}
\end{aligned}$$

In arriving at Eq. (14) we have employed $\sum_{\lambda_2} \lambda_2 \epsilon_{\lambda_2}^{j*} \epsilon_{\lambda_2}^k = i \epsilon^{jk}$ and $\sum_{\lambda_2} \epsilon_{\lambda_2}^{j*} \epsilon_{\lambda_2}^k = \delta^{jk}$, along with

$$\int d^2b \frac{\underline{x}'-\underline{b}}{|\underline{x}'-\underline{b}|^2} \times \frac{\underline{y}-\underline{b}}{|\underline{y}-\underline{b}|^2} = 0. \tag{15}$$

The cross product is defined by $\underline{u} \times \underline{v} = \epsilon^{ij} u^i v^j = u^1 v^2 - u^2 v^1$, the QCD coupling is $\alpha_s = g^2/4\pi$, c.c. stands for complex conjugate, while Tr denotes a trace of adjoint matrices.

We have also defined the following adjoint *polarized dipole amplitudes* in the pure-gluon sector [1, 3, 4]:

$$G_{\underline{x},\underline{y}}^{\text{adj}}(\beta s) \equiv \frac{1}{2(N_c^2 - 1)} \text{Re} \left\langle \left\langle \text{T Tr} \left[U_{\underline{y}} U_{\underline{x}}^{\text{G}[1]\dagger} \right] + \text{T Tr} \left[U_{\underline{x}}^{\text{G}[1]} U_{\underline{y}}^\dagger \right] \right\rangle \right\rangle (\beta s), \tag{16a}$$

$$G_{\underline{x},\underline{y}}^{i \text{adj}}(\beta s) \equiv \frac{1}{2(N_c^2 - 1)} \text{Re} \left\langle \left\langle \text{T Tr} \left[U_{\underline{y}} U_{\underline{x}}^{i \text{G}[2]\dagger} \right] + \text{T Tr} \left[U_{\underline{x}}^{i \text{G}[2]} U_{\underline{y}}^\dagger \right] \right\rangle \right\rangle (\beta s), \tag{16b}$$

with the new polarized Wilson line of the second kind [4, 42]

$$U_{\underline{z}}^{i \text{G}[2]} \equiv \frac{p_1^+}{2s} \int_{-\infty}^{\infty} dz^- U_{\underline{z}}[\infty, z^-] \left[\mathcal{D}^i(z^-, \underline{z}) - \bar{\mathcal{D}}^i(z^-, \underline{z}) \right] U_{\underline{z}}[z^-, -\infty]. \tag{17}$$

The argument βs of the polarized dipole amplitudes in Eqs. (16) denotes a fraction β of the projectile–target center of mass energy squared s . Since our projectile is minus-moving, here $\beta = k^-/p_2^-$, such that $\beta s = 2k^- p_1^+$ with p_1^+ the large plus momentum of the target. The double angle brackets denote the averaging in the shock wave, now with the polarized target, multiplied by a factor of energy, such that $\left\langle \left\langle \dots \right\rangle \right\rangle = \beta s \langle \dots \rangle$ (see [1] for details).

Moving on to the diagram B we derive

$$\begin{aligned}
\frac{d\sigma^{B(C^*+F^*)+C.C.}(\lambda)}{d^2k_T dy} &= \lambda \frac{4\alpha_s}{(2\pi)^4} \frac{k^-}{p_2^-} \frac{N_c}{N_c^2 - 1} \int d^2x d^2y d^2b e^{-ik \cdot (x-y)} \left\{ \frac{\underline{x}-\underline{b}}{|\underline{x}-\underline{b}|^2} \cdot \frac{\underline{y}-\underline{b}}{|\underline{y}-\underline{b}|^2} \left\langle \text{Tr} \left[U_{\underline{y}}^\dagger U_{\underline{x}}^{\text{G}[1]} \right] - \text{Tr} \left[U_{\underline{b}}^\dagger U_{\underline{x}}^{\text{G}[1]} \right] \right\rangle \right. \\
&\quad \left. + i \int d^2x' \frac{\underline{x}'-\underline{b}}{|\underline{x}'-\underline{b}|^2} \times \frac{\underline{y}-\underline{b}}{|\underline{y}-\underline{b}|^2} \left\langle \text{Tr} \left[U_{\underline{y}}^\dagger U_{\underline{x},\underline{x}'}^{\text{G}[2]} \right] - \text{Tr} \left[U_{\underline{b}}^\dagger U_{\underline{x},\underline{x}'}^{\text{G}[2]} \right] \right\rangle \right\} + \text{c.c.}, \tag{18}
\end{aligned}$$

doubling the contribution in Eq. (14).

Similarly, from the diagram D we obtain

$$\begin{aligned}
\frac{d\sigma^{D A_{\text{eik}}^*+C.C.}(\lambda)}{d^2k_T dy} &= \frac{\lambda}{N_c^2 - 1} \frac{4\alpha_s}{(2\pi)^4} \int d^2x d^2y d^2b e^{-ik \cdot (x-y)} \frac{\underline{x}-\underline{b}}{|\underline{x}-\underline{b}|^2} \cdot \frac{\underline{y}-\underline{b}}{|\underline{y}-\underline{b}|^2} \left\langle \text{Tr} \left[U_{\underline{b}}^\dagger U_{\underline{b}}^{\text{G}[1]} T^a U_{\underline{x}}^\dagger \left(U_{\underline{y}} - U_{\underline{b}} \right) T^a \right] \right\rangle + \text{c.c.} \\
&= -\frac{\lambda}{N_c^2 - 1} \frac{4\alpha_s}{(2\pi)^4} \int d^2x d^2y d^2b e^{-ik \cdot (x-y)} \frac{\underline{x}-\underline{b}}{|\underline{x}-\underline{b}|^2} \cdot \frac{\underline{y}-\underline{b}}{|\underline{y}-\underline{b}|^2} \left\langle \text{Tr} \left[U_{\underline{b}}^\dagger U_{\underline{b}}^{\text{G}[1]} T^a U_{\underline{x}}^\dagger U_{\underline{b}} T^a \right] \right\rangle + \text{c.c.} \\
&= -\lambda \frac{\alpha_s}{4\pi^4} \frac{1}{s} N_c \int d^2x d^2y d^2b e^{-ik \cdot (x-y)} \frac{\underline{x}-\underline{b}}{|\underline{x}-\underline{b}|^2} \cdot \frac{\underline{y}-\underline{b}}{|\underline{y}-\underline{b}|^2} G_{\underline{b},\underline{x}}^{\text{adj}}(2k^- p_1^+), \tag{19}
\end{aligned}$$

where one can readily show that

$$\text{Tr} \left[U_{\underline{b}}^\dagger U_{\underline{b}}^{\text{G}[1]} T^a U_{\underline{x}}^\dagger U_{\underline{y}} T^a \right] + \text{c.c.} \text{ (with } \underline{x} \leftrightarrow \underline{y} \text{)} = 0 \tag{20}$$

and that

$$\text{Tr} \left[U_{\underline{b}}^\dagger U_{\underline{b}}^{\text{G}[1]} T^a U_{\underline{x}}^\dagger U_{\underline{b}} T^a \right] = \frac{N_c}{2} \text{Tr} \left[U_{\underline{x}}^\dagger U_{\underline{b}}^{\text{G}[1]} \right]. \tag{21}$$

The latter relation may be derived by using

$$\text{Tr} \left[U_{\underline{b}}^\dagger T^a U_{\underline{b}}^{\text{G}[1]} T^c \right] \left(U_{\underline{y}} \right)^{ac} = \frac{N_c}{2} \text{Tr} \left[U_{\underline{y}}^\dagger U_{\underline{b}}^{\text{G}[1]} \right], \tag{22}$$

which we will also employ below.

For the diagram E we get the following contribution to the cross section:

$$\begin{aligned}
\frac{d\sigma^{E A_{\text{eik}}^* + \text{c.c.}}(\lambda)}{d^2k_T dy} &= -\frac{\lambda}{N_c^2 - 1} \frac{4\alpha_s}{(2\pi)^4} \int d^2x d^2y d^2b e^{-i\mathbf{k}\cdot(\mathbf{x}-\mathbf{y})} \frac{\mathbf{x}-\mathbf{b}}{|\mathbf{x}-\mathbf{b}|^2} \cdot \frac{\mathbf{y}-\mathbf{b}}{|\mathbf{y}-\mathbf{b}|^2} \left\langle \text{Tr} \left[U_{\mathbf{b}}^\dagger T^a U_{\mathbf{b}}^{G[1]} T^c \right] \left(U_{\mathbf{y}} - U_{\mathbf{b}} \right)^{ac} \right\rangle + \text{c.c.} \\
&= -\frac{\lambda}{N_c^2 - 1} \frac{4\alpha_s}{(2\pi)^4} \int d^2x d^2y d^2b e^{-i\mathbf{k}\cdot(\mathbf{x}-\mathbf{y})} \frac{\mathbf{x}-\mathbf{b}}{|\mathbf{x}-\mathbf{b}|^2} \cdot \frac{\mathbf{y}-\mathbf{b}}{|\mathbf{y}-\mathbf{b}|^2} \left\langle \text{Tr} \left[U_{\mathbf{b}}^\dagger T^a U_{\mathbf{b}}^{G[1]} T^c \right] \left(U_{\mathbf{y}} \right)^{ac} \right\rangle + \text{c.c.} \\
&= -\lambda \frac{\alpha_s}{4\pi^4} \frac{1}{s} N_c \int d^2x d^2y d^2b e^{-i\mathbf{k}\cdot(\mathbf{x}-\mathbf{y})} \frac{\mathbf{x}-\mathbf{b}}{|\mathbf{x}-\mathbf{b}|^2} \cdot \frac{\mathbf{y}-\mathbf{b}}{|\mathbf{y}-\mathbf{b}|^2} G_{\mathbf{b},\mathbf{y}}^{\text{adj}}(2k^- p_1^+),
\end{aligned} \tag{23}$$

where we have used

$$\left(T^a U_{\mathbf{b}}^{G[1]} \right)^{cd} \left(T^a U_{\mathbf{b}} \right)^{cd} = N_c \text{Tr} \left[U_{\mathbf{b}}^\dagger U_{\mathbf{b}}^{G[1]} \right] = 0 \tag{24}$$

along with Eq. (22).

A more careful treatment of the $(D+E) A_{\text{eik}}^* + \text{c.c.}$ contributions, presented in Appendix A, generates the following term, in addition to Eqs. (19) and (23):

$$-\lambda \frac{\alpha_s}{4\pi^4} \frac{1}{s} N_c \int d^2x d^2y d^2b e^{-i\mathbf{k}\cdot(\mathbf{x}-\mathbf{y})} \frac{\mathbf{x}-\mathbf{b}}{|\mathbf{x}-\mathbf{b}|^2} \cdot \frac{\mathbf{y}-\mathbf{b}}{|\mathbf{y}-\mathbf{b}|^2} \left[-2 G_{\mathbf{b},\mathbf{b}'}^{\text{adj}}(2k^- p_1^+) \right], \tag{25}$$

where \mathbf{b} and \mathbf{b}' are the positions of the incoming gluon to the left and to the right of the cut with $|\mathbf{b}' - \mathbf{b}|^2 = 1/(2k^+ p_2^-)$. The notation is illustrated in the last diagram of Fig. 2. The term in Eq. (25) is calculated in the linearized case, appropriate for the DLA used in helicity evolution of [1, 3, 4, 44] which resums powers of $\alpha_s \ln^2(1/x)$. Two different positions of the incoming gluon on the two sides of the cut appear due to the lifetime ordering of emissions [44]: for the x^- -lifetime of the incoming gluon with momentum p_2 to be much longer than the lifetime of the produced gluon with momentum k (see Fig. 2), one requires that

$$\frac{2p_2^-}{p_2^2} \gg \frac{2k^-}{k^2}, \tag{26}$$

which gives $p_2^2 \ll k^2/\beta$, resulting in the position mismatch of $|\mathbf{b}' - \mathbf{b}|^2 = \beta/k^2 = 1/(2k^+ p_2^-)$ for the incoming gluon.¹

This is, indeed, a very small position mismatch, suppressed by a power of energy: one may wonder why we need to keep it. The answer to this question is in the fact that the approach to zero of $\left\langle \text{Tr} \left[U_{\mathbf{b}'}^\dagger U_{\mathbf{b}}^{G[1]} \right] \right\rangle$ as $\mathbf{b}' \rightarrow \mathbf{b}$ is different from what one observes in unpolarized scattering, where the dipole amplitude goes to zero as a positive power of its transverse size [37]: for instance, at Born level one has [2]

$$\left\langle \text{Tr} \left[U_{\mathbf{b}'}^\dagger U_{\mathbf{b}}^{G[1]} \right] \right\rangle_0 (\beta s) \propto \ln(\beta s |\mathbf{b}' - \mathbf{b}|^2), \tag{27}$$

such that zero amplitude is achieved at small but finite dipole size $|\mathbf{b}' - \mathbf{b}|^2 = 1/\beta s$, i.e., this zero is achieved at the dipole size squared given by the ultraviolet (UV) cutoff of the gluon–target scattering — the inverse of the center of mass energy squared (βs). At the same time, the transverse positions mismatch of the incoming gluons is $|\mathbf{b}' - \mathbf{b}|^2 = 1/(2k^+ p_2^-) = 1/\alpha s$ with $\alpha = k^+/p_1^+$, that is, given by the inverse center of mass energy squared αs of the gluon–projectile system. We observe that we have two different (physical) UV cutoffs in the calculation: αs for the gluon–projectile system and βs for the gluon–target system. Due to the existence of these two UV scales, we see that the zero we obtained in Eq. (24) becomes, at Born level,

$$\left\langle \text{Tr} \left[U_{\mathbf{b}'}^\dagger U_{\mathbf{b}}^{G[1]} \right] \right\rangle_0 (\beta s) \Big|_{|\mathbf{b}' - \mathbf{b}|^2 = \frac{1}{\alpha s}} \propto \ln \frac{\beta}{\alpha}. \tag{28}$$

This is, in general, not zero. It becomes zero only when $\alpha = \beta$. Unlike the unpolarized scattering at high energy, where all the transverse distances of the order of the inverse powers of energy can be safely put to zero in a calculation,

¹ One has to distinguish this impact parameter offset resulting from the lifetime ordering condition from the offset in \mathbf{b} and \mathbf{b}' due to the produced gluon having different positions \mathbf{x} and \mathbf{y} on the two sides of the cut (which is, in turn, due to the fixed momentum \mathbf{k} of the produced gluon in our production calculation). The latter offset is $|\mathbf{b}' - \mathbf{b}|^2 = \beta^2 |\mathbf{x} - \mathbf{y}|^2 \approx \beta^2/k^2$ (see, e.g., [122]) and is much smaller than the $|\mathbf{b}' - \mathbf{b}|^2 = \beta/k^2$ offset due to the lifetime ordering, since $\beta \ll 1$: therefore, we will only keep the offset due to the lifetime ordering, neglecting the other much smaller offset.

here we need to keep track of the logarithms of such very short distances, since they contribute to the evolution [1, 3, 4, 63, 70, 71, 73, 123], and, as follows from our calculation, to the production cross section.

Assembling Eqs. (14), (18), (19), (23), and (25) we obtain the helicity-dependent inclusive gluon production cross section in the pure glue sector,

$$\frac{d\sigma(\lambda)}{d^2k_T dy} = \lambda \frac{\alpha_s}{\pi^4} \frac{1}{s} N_c \int d^2x d^2y d^2b e^{-ik \cdot (x-y)} \left\{ \frac{\underline{x}-\underline{b}}{|\underline{x}-\underline{b}|^2} \cdot \frac{\underline{y}-\underline{b}}{|\underline{y}-\underline{b}|^2} \left[G_{\underline{x},\underline{y}}^{\text{adj}}(2k^- p_1^+) - G_{\underline{x},\underline{b}}^{\text{adj}}(2k^- p_1^+) \right. \right. \\ \left. \left. - \frac{1}{4} \left(G_{\underline{b},\underline{y}}^{\text{adj}}(2k^- p_1^+) + G_{\underline{b},\underline{x}}^{\text{adj}}(2k^- p_1^+) - 2 G_{\underline{b},\underline{b}'}^{\text{adj}}(2k^- p_1^+) \right) \right] - 2i k^i \frac{\underline{x}-\underline{b}}{|\underline{x}-\underline{b}|^2} \times \frac{\underline{y}-\underline{b}}{|\underline{y}-\underline{b}|^2} G_{\underline{x},\underline{b}}^{\text{adj}}(2k^- p_1^+) \right\}. \quad (29)$$

C. Target–projectile symmetric form for the gluon production cross section

The expression (29) gives us the helicity-dependent part of the inclusive gluon production cross section in the gluon–target scattering, with the pure-gluon dynamics. By the nature of its derivation, the cross section (29) appears to treat the projectile (gluon) and the target (could be a proton or another gluon) differently: it is not explicitly target–projectile symmetric. At the same time, since both the target and the projectile are assumed to be longitudinally polarized protons, or, for the purpose of our gluon-sector derivation, gluons, and since we are producing a gluon in the central rapidity region, not close in rapidity to either projectile or to target, one would expect the gluon production cross section to be target–projectile symmetric (if one also interchanges the rapidity intervals between the produced gluon and the target/projectile). Therefore, one may wonder whether Eq. (29) can be written in a target–projectile symmetric form. Indeed, the interaction with the target in Eq. (29) is described by the polarized dipole amplitudes, which may include multiple additional gluon emissions due to small- x evolution, while the projectile is simply a gluon emitting the produced gluon, without any evolution corrections at the moment: hence, Eq. (29) is target–projectile asymmetric. However, if the polarized dipole amplitudes in Eq. (29) are taken at the lowest (Born) order, then the expression should become target–projectile symmetric. Conversely, inspired by the inclusive gluon production cross section in the unpolarized case [110], and by the target–projectile symmetry of the physical problem, one may be able to find a form of Eq. (29) where the interaction with the projectile can be also encoded in the polarized dipole amplitudes, which, when taken at Born level, give Eq. (29). Here we will do just that: we will rewrite Eq. (29) in the target–projectile symmetric form, which will facilitate inclusion of evolution corrections in the rapidity interval between the produced gluon and the projectile.

Defining

$$\tilde{x} = \underline{x} - \underline{b}, \quad \tilde{y} = \underline{y} - \underline{b}, \quad (30)$$

we rewrite Eq. (29) as

$$\frac{d\sigma(\lambda)}{d^2k_T dy} = \lambda \frac{\alpha_s}{\pi^4} \frac{1}{s} N_c \int d^2\tilde{x} d^2\tilde{y} d^2b e^{-ik \cdot (\tilde{x}-\tilde{y})} \left\{ \frac{\tilde{x}}{|\tilde{x}|^2} \cdot \frac{\tilde{y}}{|\tilde{y}|^2} \left[G_{\tilde{x}+\underline{b},\tilde{y}+\underline{b}}^{\text{adj}}(2k^- p_1^+) - G_{\tilde{x}+\underline{b},\underline{b}}^{\text{adj}}(2k^- p_1^+) \right. \right. \\ \left. \left. - \frac{1}{4} \left(G_{\underline{b},\tilde{y}+\underline{b}}^{\text{adj}}(2k^- p_1^+) + G_{\underline{b},\tilde{x}+\underline{b}}^{\text{adj}}(2k^- p_1^+) - 2 G_{\underline{b},\underline{b}'}^{\text{adj}}(2k^- p_1^+) \right) \right] - 2i k^i \frac{\tilde{x}}{|\tilde{x}|^2} \times \frac{\tilde{y}}{|\tilde{y}|^2} G_{\tilde{x}+\underline{b},\underline{b}}^{\text{adj}}(2k^- p_1^+) \right\}. \quad (31)$$

Integrating over \underline{b} we obtain

$$\frac{d\sigma(\lambda)}{d^2k_T dy} = \lambda \frac{\alpha_s}{\pi^4} \frac{1}{s} N_c \int d^2\tilde{x} d^2\tilde{y} e^{-ik \cdot (\tilde{x}-\tilde{y})} \frac{\tilde{x}}{|\tilde{x}|^2} \cdot \frac{\tilde{y}}{|\tilde{y}|^2} \left[G^{\text{adj}}(|\tilde{x}-\tilde{y}|^2, 2k^- p_1^+) - G^{\text{adj}}(\tilde{x}_\perp^2, 2k^- p_1^+) \right. \\ \left. - \frac{1}{4} \left(G^{\text{adj}}(\tilde{y}_\perp^2, 2k^- p_1^+) + G^{\text{adj}}(\tilde{x}_\perp^2, 2k^- p_1^+) - 2 G^{\text{adj}}(1/(2k^+ p_2^-), 2k^- p_1^+) \right) - 2 G_2^{\text{adj}}(\tilde{x}_\perp^2, 2k^- p_1^+) \right]. \quad (32)$$

Here $x_\perp = |\underline{x}|$. We have employed the following definition and a decomposition [2, 4, 42]:

$$\int d^2b G_{\underline{b},\underline{b}-\underline{x}}^{\text{adj}}(\beta s) = G^{\text{adj}}(x_\perp^2, \beta s), \quad (33a)$$

$$\int d^2b G_{\underline{b},\underline{b}-\underline{x}}^{\text{adj}}(\beta s) = x^i G_1^{\text{adj}}(x_\perp^2, \beta s) + \epsilon^{ij} x^j G_2^{\text{adj}}(x_\perp^2, \beta s), \quad (33b)$$

along with $|\underline{b}' - \underline{b}|^2 = 1/(2k^+ p_2^-)$.

Note that all the polarized dipole amplitudes, like $G^{\text{adj}}(x_{\perp}^2, \beta s)$, are defined only in the physical region where $x_{\perp}^2 > 1/\beta s$ [1, 3, 4, 44]. Outside this region they are zero. With this in mind we define a ‘‘subtracted’’ dipole amplitude

$$G_{\text{subtr}}^{\text{adj}}(x_{\perp}^2, 2k^- p_1^+) \equiv G^{\text{adj}}(x_{\perp}^2, 2k^- p_1^+) - G^{\text{adj}}(1/(2k^+ p_2^-), 2k^- p_1^+) \quad (34)$$

which is zero at $x_{\perp}^2 = 1/(2k^+ p_2^-) = 1/\alpha s$.

Employing the definition (34) and performing some of the two-dimensional integral we can reduce Eq. (32) to

$$\begin{aligned} \frac{d\sigma(\lambda)}{d^2k_T dy} = & \lambda \frac{2\alpha_s}{\pi^3} \frac{1}{s} N_c \int d^2x e^{-ik \cdot x} \left[\ln \left(\frac{1}{x_{\perp} \Lambda} \right) G_{\text{subtr}}^{\text{adj}}(x_{\perp}^2, 2k^- p_1^+) \right. \\ & \left. - i \frac{x}{|x|^2} \cdot \frac{k}{|k|^2} \left(\frac{3}{2} G_{\text{subtr}}^{\text{adj}}(x_{\perp}^2, 2k^- p_1^+) + 2 G_2^{\text{adj}}(x_{\perp}^2, 2k^- p_1^+) \right) \right], \end{aligned} \quad (35)$$

with Λ the infrared (IR) cutoff.

Our goal is to rewrite the cross section in the target–projectile symmetric form following [37, 110]. We will use the following pure-gluon initial conditions [2, 42]:

$$G^{\text{adj}(0)}(x_{\perp}^2, \alpha s) = 2\alpha_s^2 \pi \frac{N_c}{C_F} \ln(\alpha s x_{\perp}^2), \quad G_2^{\text{adj}(0)}(x_{\perp}^2, \alpha s) = 2\alpha_s^2 \pi \frac{N_c}{C_F} \ln \left(\frac{1}{x_{\perp} \Lambda} \right). \quad (36)$$

The sign of $G^{\text{adj}(0)}$ in Eq. (36) is different from that found in [2]: this is due to the anti-Brodsky-Lepage spinors [121] used in [4] and here (see Eq. (64) below) having polarization index σ different by a minus sign compared to that used in [2, 42]. We have also changed the color factors $C_F/(2N_c) \rightarrow N_c/(2C_F)$, as compared to [2, 42], to account for the gluon–gluon scattering we consider here (with C_F the fundamental Casimir operator of $\text{SU}(N_c)$). In addition, we had to scale up the amplitudes by a factor of 2 due to the difference between the gluon and quark spins (the η -factor in the notation of [46]).

We proceed by rewriting Eq. (35) as

$$\begin{aligned} \frac{d\sigma(\lambda)}{d^2k_T dy} = & \lambda \frac{2\alpha_s}{\pi^3} \frac{1}{s} N_c \int d^2x e^{-ik \cdot x} \left\{ \gamma \left[\ln \left(\frac{1}{x_{\perp} \Lambda} \right) - 2i \frac{x}{|x|^2} \cdot \frac{k}{|k|^2} \right] G_{\text{subtr}}^{\text{adj}}(x_{\perp}^2, 2k^- p_1^+) \right. \\ & + (1 - \gamma) \ln \left(\frac{1}{x_{\perp} \Lambda} \right) G_{\text{subtr}}^{\text{adj}}(x_{\perp}^2, 2k^- p_1^+) - i\delta \frac{x}{|x|^2} \cdot \frac{k}{|k|^2} \left(\frac{3}{2} - 2\gamma \right) G_{\text{subtr}}^{\text{adj}}(x_{\perp}^2, 2k^- p_1^+) \\ & \left. - i(1 - \delta) \frac{x}{|x|^2} \cdot \frac{k}{|k|^2} \left(\frac{3}{2} - 2\gamma \right) G_{\text{subtr}}^{\text{adj}}(x_{\perp}^2, 2k^- p_1^+) - 2i \frac{x}{|x|^2} \cdot \frac{k}{|k|^2} G_2^{\text{adj}}(x_{\perp}^2, 2k^- p_1^+) \right\} \end{aligned} \quad (37)$$

with some unknown constants γ and δ . Since $G_{\text{subtr}}^{\text{adj}}(x_{\perp}^2 = 1/(2k^+ p_2^-), 2k^- p_1^+) = 0$, we can modify the first term in the curly brackets of Eq. (37) as [110]

$$\begin{aligned} & \int d^2x e^{-ik \cdot x} \gamma \left[\ln \left(\frac{1}{x_{\perp} \Lambda} \right) - 2i \frac{x}{|x|^2} \cdot \frac{k}{|k|^2} \right] G_{\text{subtr}}^{\text{adj}}(x_{\perp}^2, 2k^- p_1^+) \\ & = - \int d^2x e^{-ik \cdot x} \gamma \ln \left(\frac{1}{x_{\perp} \Lambda} \right) \frac{1}{k_T^2} \nabla_{\perp}^2 G_{\text{subtr}}^{\text{adj}}(x_{\perp}^2, 2k^- p_1^+). \end{aligned} \quad (38)$$

In addition, we can rewrite the fourth term in the curly brackets as

$$\begin{aligned} & - i(1 - \delta) \frac{x}{|x|^2} \cdot \frac{k}{|k|^2} \left(\frac{3}{2} - 2\gamma \right) G_{\text{subtr}}^{\text{adj}}(x_{\perp}^2, 2k^- p_1^+) \\ & = \int d^2x e^{-ik \cdot x} (1 - \delta) \frac{x^i}{|x|^2} \cdot \frac{1}{k_T^2} \left(\frac{3}{2} - 2\gamma \right) \partial^i G_{\text{subtr}}^{\text{adj}}(x_{\perp}^2, 2k^- p_1^+) \end{aligned} \quad (39)$$

by replacing $k^i \rightarrow -i\partial^i$ with the derivative operator acting on the exponential and integrating by parts. Here we are assuming that the $\ln(1/x_{\perp} \Lambda)$ and $x/|x|^2$ terms in Eq. (37) are associated with the gluon–projectile system, such that their UV scale is $2k^+ p_2^- = \alpha s$. Therefore, we have

$$\nabla_{\perp}^2 \ln \left(\frac{1}{x_{\perp} \Lambda} \right) = \partial^i \frac{x^i}{|x|^2} = -2\pi \delta_{1/\alpha s}^2(x), \quad (40)$$

where $\delta_{1/\alpha_s}^2(\underline{x})$ denotes a two-dimensional delta function with the coarse-graining scale of $1/\sqrt{\alpha_s}$, such that

$$\int d^2x \delta_{1/\alpha_s}^2(\underline{x}) f(x_\perp^2) = f(x_\perp^2 = 1/(2k^+p_2^-) = 1/\alpha_s). \quad (41)$$

After the substitutions (38) and (46), Eq. (37) becomes

$$\begin{aligned} \frac{d\sigma(\lambda)}{d^2k_T dy} &= \lambda \frac{2\alpha_s}{\pi^3} \frac{1}{s} N_c \int d^2x e^{-ik \cdot x} \left\{ -\gamma \ln\left(\frac{1}{x_\perp \Lambda}\right) \frac{1}{k_T^2} \nabla_\perp^2 G_{\text{subtr}}^{\text{adj}}(x_\perp^2, 2k^-p_1^+) \right. \\ &+ (1-\gamma) \ln\left(\frac{1}{x_\perp \Lambda}\right) G_{\text{subtr}}^{\text{adj}}(x_\perp^2, 2k^-p_1^+) - i\delta \frac{x}{|\underline{x}|^2} \cdot \frac{k}{|k|^2} \left(\frac{3}{2} - 2\gamma\right) G_{\text{subtr}}^{\text{adj}}(x_\perp^2, 2k^-p_1^+) \\ &\left. + (1-\delta) \frac{x^i}{|\underline{x}|^2} \cdot \frac{1}{k_T^2} \left(\frac{3}{2} - 2\gamma\right) \partial^i G_{\text{subtr}}^{\text{adj}}(x_\perp^2, 2k^-p_1^+) - 2i \frac{x}{|\underline{x}|^2} \cdot \frac{k}{|k|^2} G_2^{\text{adj}}(x_\perp^2, 2k^-p_1^+) \right\}. \end{aligned} \quad (42)$$

Employing Eq. (36), we make the following replacements in Eq. (42):

$$\ln\left(\frac{1}{x_\perp \Lambda}\right) \rightarrow \frac{C_F}{2\alpha_s^2 \pi N_c} G_2^{\text{adj}(0)}(x_\perp^2, 2k^+p_2^-), \quad (43a)$$

$$\delta \frac{x^i}{|\underline{x}|^2} = \delta \partial^i \ln\left(\frac{1}{x_\perp \Lambda}\right) \rightarrow \frac{C_F}{2\alpha_s^2 \pi N_c} \partial^i \left[\alpha_1 G^{\text{adj}(0)}(x_\perp^2, 2k^+p_2^-) + \beta_1 G_2^{\text{adj}(0)}(x_\perp^2, 2k^+p_2^-) \right], \quad (43b)$$

$$(1-\delta) \frac{x^i}{|\underline{x}|^2} \rightarrow \frac{C_F}{2\alpha_s^2 \pi N_c} \partial^i \left[\alpha_2 G^{\text{adj}(0)}(x_\perp^2, 2k^+p_2^-) + \beta_2 G_2^{\text{adj}(0)}(x_\perp^2, 2k^+p_2^-) \right], \quad (43c)$$

$$\frac{x^i}{|\underline{x}|^2} \rightarrow \frac{C_F}{2\alpha_s^2 \pi N_c} \partial^i \left[\alpha_3 G^{\text{adj}(0)}(x_\perp^2, 2k^+p_2^-) + \beta_3 G_2^{\text{adj}(0)}(x_\perp^2, 2k^+p_2^-) \right], \quad (43d)$$

introducing new unknown parameters $\alpha_1, \beta_2, \dots, \beta_3$ while eliminating δ . Note that the substitutions (43) are valid only when these parameters satisfy

$$\beta_1 + \beta_2 - 2\alpha_1 - 2\alpha_2 = 1, \quad (44a)$$

$$\beta_3 - 2\alpha_3 = 1. \quad (44b)$$

Performing the substitutions (43) in Eq. (42), replacing the remaining $k^i \rightarrow -i\partial^i$ with the derivative acting on the exponential, and integrating by parts, yields

$$\begin{aligned} \frac{d\sigma(\lambda)}{d^2k_T dy} &= \lambda \frac{C_F}{\alpha_s \pi^4} \frac{1}{s k_T^2} \int d^2x e^{-ik \cdot x} \left\{ -\gamma G_{2P}^{\text{adj}} \nabla_\perp^2 G_T^{\text{adj}} + (1-\gamma) G_{2P}^{\text{adj}} G_T^{\text{adj}} \right. \\ &+ \left(\frac{3}{2} - 2\gamma\right) \partial^i \left[\left(\alpha_1 \partial^i G_P^{\text{adj}} + \beta_1 \partial^i G_{2P}^{\text{adj}} \right) G_T^{\text{adj}} \right] + \left(\frac{3}{2} - 2\gamma\right) \left(\alpha_2 \partial^i G_P^{\text{adj}} + \beta_2 \partial^i G_{2P}^{\text{adj}} \right) \partial^i G_T^{\text{adj}} \\ &\left. + 2 \partial^i \left[\left(\alpha_3 \partial^i G_P^{\text{adj}} + \beta_3 \partial^i G_{2P}^{\text{adj}} \right) G_{2T}^{\text{adj}} \right] \right\}. \end{aligned} \quad (45)$$

In arriving at Eq. (45), we have replaced

$$G_{\text{subtr}}^{\text{adj}} \rightarrow G_T^{\text{adj}}, \quad G_2^{\text{adj}} \rightarrow G_{2T}^{\text{adj}}, \quad G^{\text{adj}(0)} \rightarrow G_P^{\text{adj}}, \quad G_2^{\text{adj}(0)} \rightarrow G_{2P}^{\text{adj}}, \quad (46)$$

trying to describe the target and the projectile in terms of the same-type quantities. (The fact that G_T^{adj} denotes a subtracted dipole amplitude while G_P^{adj} denotes the un-subtracted one will be addressed shortly.) We have also suppressed the arguments of the dipole scattering amplitudes for brevity.

Analyzing this expression (45), we notice that the $(1-\gamma) G_{2P}^{\text{adj}} G_T^{\text{adj}}$ has no target–projectile (T \leftrightarrow P) “dual”, i.e., there is no $G_{2T}^{\text{adj}} G_P^{\text{adj}}$ term in the expression. Since we are looking for a T \leftrightarrow P symmetric expression for the cross section, we conclude that this term must vanish, that is,

$$\gamma = 1. \quad (47)$$

Equation (45) then becomes

$$\frac{d\sigma(\lambda)}{d^2k_T dy} = \lambda \frac{C_F}{\alpha_s \pi^4} \frac{1}{s k_T^2} \int d^2x e^{-ik \cdot x} \left\{ -G_{2P}^{\text{adj}} \nabla_\perp^2 G_T^{\text{adj}} - \frac{\alpha_1}{2} \left(\nabla_\perp^2 G_P^{\text{adj}} \right) G_T^{\text{adj}} - \frac{\beta_1}{2} \left(\nabla_\perp^2 G_{2P}^{\text{adj}} \right) G_T^{\text{adj}} \right.$$

$$\begin{aligned}
& -\frac{\alpha_1 + \alpha_2}{2} \partial^i G_P^{\text{adj}} \partial^i G_T^{\text{adj}} - \frac{\beta_1 + \beta_2}{2} \partial^i G_{2P}^{\text{adj}} \partial^i G_T^{\text{adj}} + 2\alpha_3 \left(\nabla_{\perp}^2 G_P^{\text{adj}} \right) G_{2T}^{\text{adj}} + 2\beta_3 \left(\nabla_{\perp}^2 G_{2P}^{\text{adj}} \right) G_{2T}^{\text{adj}} \\
& + 2\alpha_3 \partial^i G_P^{\text{adj}} \partial^i G_{2T}^{\text{adj}} + 2\beta_3 \partial^i G_{2P}^{\text{adj}} \partial^i G_{2T}^{\text{adj}} \Big\}. \tag{48}
\end{aligned}$$

Similar to the above, the $-\frac{\alpha_1}{2} \left(\nabla_{\perp}^2 G_P^{\text{adj}} \right) G_T^{\text{adj}}$, $-\frac{\beta_1}{2} \left(\nabla_{\perp}^2 G_{2P}^{\text{adj}} \right) G_T^{\text{adj}}$ and $2\beta_3 \partial^i G_{2P}^{\text{adj}} \partial^i G_{2T}^{\text{adj}}$ terms have no T \leftrightarrow P “duals”. Hence,

$$\alpha_1 = \beta_1 = \beta_3 = 0. \tag{49}$$

The T \leftrightarrow P imposed on the remaining terms containing ∇_{\perp}^2 yields

$$\alpha_3 = -\frac{1}{2}. \tag{50}$$

Note that $\alpha_3 = -1/2, \beta_3 = 0$ satisfy Eq. (44b).

Further, equating the coefficients of the $\partial^i G_{2P}^{\text{adj}} \partial^i G_T^{\text{adj}}$ and $\partial^i G_P^{\text{adj}} \partial^i G_{2T}^{\text{adj}}$ terms in Eq. (48) in order to achieve the T \leftrightarrow P symmetry gives

$$-\frac{\beta_1 + \beta_2}{2} = 2\alpha_3 \quad \Rightarrow \quad \beta_2 = 2. \tag{51}$$

Finally, employing the condition (44a), we arrive at

$$\alpha_2 = \frac{1}{2}. \tag{52}$$

With all the coefficient fixed, we rewrite Eq. (48) as

$$\begin{aligned}
\frac{d\sigma}{d^2k_T dy} = \frac{C_F}{\alpha_s \pi^4} \frac{1}{s k_T^2} \int d^2x e^{-ik \cdot x} \Big\{ & G_{2P}^{\text{adj}} \nabla_{\perp}^2 G_T^{\text{adj}} + \left(\nabla_{\perp}^2 G_P^{\text{adj}} \right) G_{2T}^{\text{adj}} + \frac{1}{4} \partial^i G_P^{\text{adj}} \partial^i G_T^{\text{adj}} \\
& + \partial^i G_{2P}^{\text{adj}} \partial^i G_T^{\text{adj}} + \partial^i G_P^{\text{adj}} \partial^i G_{2T}^{\text{adj}} \Big\}. \tag{53}
\end{aligned}$$

Here we have absorbed $-\lambda$ into G_P^{adj} and G_{2P}^{adj} , since this is the projectile polarization which is now included in those amplitudes. The minus sign accounts for the fact that the projectile gluon is left-moving, while we have been using the polarization vector basis for a right-moving gluon. Target polarization enters through G_T^{adj} and G_{2T}^{adj} , as before.

Note that the amplitude G_T^{adj} enters Eq. (53) only through its derivatives, i.e., through $\nabla_{\perp}^2 G_T^{\text{adj}}$ and $\partial^i G_T^{\text{adj}}$. As one can readily see from Eq. (34), the difference between the subtracted and un-subtracted dipole amplitudes vanishes after any transverse coordinate differentiation. Therefore, G_T^{adj} in Eq. (53) can be thought of as the “true” un-subtracted polarized dipole amplitude on the target proton.

We observe that Eq. (53) is completely symmetric with respect to the projectile–target interchange. For completeness, let us rewrite it restoring the arguments of the dipole amplitudes. Employing the rapidity variable

$$y = \frac{1}{2} \ln \frac{k^-}{k^+} \tag{54}$$

such that $y = 0$ is mid-rapidity, we get $2p_1^+ k^- = \sqrt{2} p_1^+ k_T e^y$ and $2p_2^- k^+ = \sqrt{2} p_2^- k_T e^{-y}$. In the center-of-mass frame we have $2p_1^+ k^- = \sqrt{s} k_T e^y$ and $2p_2^- k^+ = \sqrt{s} k_T e^{-y}$.

Including the arguments of the dipole amplitudes, we rewrite Eq. (53) as

$$\begin{aligned}
\frac{d\sigma}{d^2k_T dy} = \frac{C_F}{\alpha_s \pi^4} \frac{1}{s k_T^2} \int d^2x e^{-ik \cdot x} \\
\times \left(G_P^{\text{adj}} \quad G_{2P}^{\text{adj}} \right) (x_{\perp}^2, \sqrt{2} p_2^- k_T e^{-y}) \begin{pmatrix} \frac{1}{4} \vec{\nabla}_{\perp} \cdot \vec{\nabla}_{\perp} & \vec{\nabla}_{\perp}^2 + \vec{\nabla}_{\perp} \cdot \vec{\nabla}_{\perp} \\ \vec{\nabla}_{\perp}^2 + \vec{\nabla}_{\perp} \cdot \vec{\nabla}_{\perp} & 0 \end{pmatrix} \begin{pmatrix} G_T^{\text{adj}} \\ G_{2T}^{\text{adj}} \end{pmatrix} (x_{\perp}^2, \sqrt{2} p_1^+ k_T e^y). \tag{55}
\end{aligned}$$

This cross section is the main result of this work. Let us reiterate here that the dipole amplitudes are defined in the regions $x_{\perp}^2 > 1/(\sqrt{2}p_2^- k_T e^{-y})$ for the projectile and $x_{\perp}^2 > 1/(\sqrt{2}p_1^+ k_T e^y)$ for the target. This implies that the integration in Eq. (55) is bounded by

$$x_{\perp}^2 > \max \left\{ \frac{1}{\sqrt{2}p_2^- k_T e^{-y}}, \frac{1}{\sqrt{2}p_1^+ k_T e^y} \right\} \quad (56)$$

from below.

Note that at large N_c we have the following relation between the adjoint and fundamental (G, G_2) polarized dipole amplitudes [3, 4],

$$G^{\text{adj}} = 4G, \quad G_2^{\text{adj}} = 2G_2. \quad (57)$$

We can rewrite Eq. (55) in terms of the gluon transverse-momentum dependent distributions (TMDs). The fundamental-dipole gluon helicity TMD at small x and at large N_c can be written at DLA as (see, e.g., Eq. (41) of [4]; here, in DLA, we have dropped the derivative with respect to the transverse size squared in that formula)

$$g_{1L}^{G \text{ dip}}(x, k_T^2) = \frac{N_c}{\alpha_s 4\pi^4} \int d^2x e^{-i\mathbf{k}\cdot\mathbf{x}} G_2^{\text{adj}} \left(x_{\perp}^2, \frac{Q^2}{x} \right). \quad (58)$$

Thus, the polarized dipole amplitude G_2^{adj} is related to $g_{1L}^{G \text{ dip}}(x, k_T^2)$. (Here Q^2 is the renormalization scale.)

In Appendix B we show that the polarized dipole amplitude G^{adj} is, in turn, related to the twist-three helicity-flip dipole gluon TMD $\Delta H_{3L}^{\perp \text{ dip}}(x, k_T^2)$ [124] at small x and at large N_c by²

$$\Delta H_{3L}^{\perp \text{ dip}}(x, k_T^2) = \frac{N_c}{\alpha_s 16\pi^4} \int d^2x e^{-i\mathbf{k}\cdot\mathbf{x}} G^{\text{adj}} \left(x_{\perp}^2, \frac{Q^2}{x} \right). \quad (59)$$

Using Eqs. (58) and (59) we can rewrite Eq. (55) at large- N_c and at small x as

$$\begin{aligned} \frac{d\sigma}{d^2k_T dy} = & -\frac{32\pi^4 \alpha_s}{N_c} \frac{1}{s k_T^2} \int \frac{d^2q}{(2\pi)^2} \\ & \times \left(\Delta H_{3L}^{\perp \text{ dip } P} \quad g_{1L}^{G \text{ dip } P} \right) \left(q_T^2, \frac{k_T}{\sqrt{2}p_2^-} e^y \right) \begin{pmatrix} \underline{q} \cdot (\underline{k} - \underline{q}) & \underline{q} \cdot \underline{k} \\ \underline{k} \cdot (\underline{k} - \underline{q}) & 0 \end{pmatrix} \begin{pmatrix} \Delta H_{3L}^{\perp \text{ dip } T} \\ g_{1L}^{G \text{ dip } T} \end{pmatrix} \left((\underline{k} - \underline{q})^2, \frac{k_T}{\sqrt{2}p_1^+} e^{-y} \right), \end{aligned} \quad (60)$$

with the renormalization scale chosen to be equal to k_T^2 . The P and T superscripts on the TMDs denote the TMDs of the projectile and of the target, respectively. Eq. (60) is the polarized proton–proton scattering analogue of the unpolarized k_T -factorization formula for gluon production derived in [108, 110]. Just as the result of [108, 110], our k_T -factorization expression (60) is valid in the quasi-classical GGM/MV approximation and, as we will show below, for the leading-order small- x evolution of the dipole amplitudes (that is, in DLA for helicity evolution). We do not expect Eq. (60) to apply beyond the small- x regime.

D. Lowest-order calculations

Let us cross-check our main result (55) by performing the lowest-order gluon production calculation in the polarized parton–parton scattering. For simplicity, we will work in the large- N_c approximation. Even in this approximation, finding the lowest non-trivial contribution to the polarization-dependent part of the $GG \rightarrow GGG$ process can be a significant calculation. Our strategy is to do the calculation of the polarization-dependent part of the $qq \rightarrow qqG$ process instead, and then use the observations obtained in [46] to deduce the (large- N_c part of) of the polarization-dependent $GG \rightarrow GGG$ cross section.

The diagrams contributing to gluon production amplitude in the $qq \rightarrow qqG$ process at large N_c are shown in Fig. 3. The diagrams we are neglecting here may not be immediately seen as N_c -suppressed, but they lead to N_c -suppressed contributions in the polarization-dependent part of the cross section at the sub-eikonal level of our calculation.

As before, our incoming “projectile” quark has a large minus momentum component p_2^- , while the “target” quark has a large plus momentum p_1^+ . We will work in the multi-peripheral regime for particle production, defined by

$$(p_2 + q - k)^- \gg k^- \gg (p_1 - q)^-, \quad (p_2 + q - k)^+ \ll k^+ \ll (p_1 - q)^+. \quad (61)$$

² Note that our definition of ΔH_{3L}^{\perp} is equal to $-2x$ times the definition of this TMD in [124].

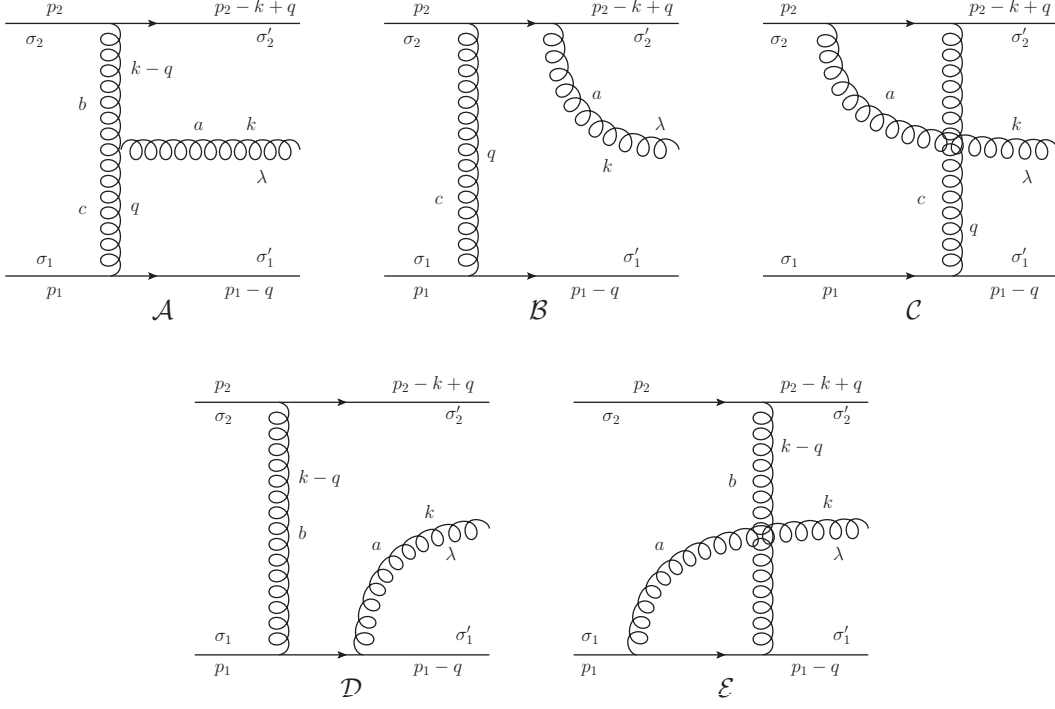


FIG. 3. Diagrams contributing to the leading- N_c gluon production cross section in the polarized quark-quark scattering.

It requires that $\alpha \ll 1$ and $\beta \ll 1$, along with

$$q_T^2 \ll \beta s, \quad (\underline{k} - \underline{q})^2 \ll \alpha s, \quad (62)$$

where $\alpha = k^+/p_1^+$, $\beta = k^-/p_2^-$ and $s = 2p_1^+p_2^-$. Note that $k_T^2 = \alpha\beta s$, which is much smaller than αs and βs , such that the upper bound on q_T becomes

$$q_T^2 \ll \min\{\alpha, \beta\} s. \quad (63)$$

For the plus-moving (target) quark line we use the Brodsky-Lepage spinors [121]. For the minus-moving (projectile) quark line we use the (\pm) -interchanged Brodsky-Lepage spinors, which we will refer to as the anti-BL spinors following [3, 61]. These are

$$u_\sigma(p) = \frac{1}{\sqrt{\sqrt{2}p^-}} [\sqrt{2}p^- + m\gamma^0 + \gamma^0 \underline{\gamma} \cdot \underline{p}] \rho(\sigma), \quad v_\sigma(p) = \frac{1}{\sqrt{\sqrt{2}p^-}} [\sqrt{2}p^- - m\gamma^0 + \gamma^0 \underline{\gamma} \cdot \underline{p}] \rho(-\sigma), \quad (64)$$

with $p^\mu = \left(\frac{p^2 + m^2}{2p^-}, p^-, \underline{p} \right)$ and

$$\rho(+1) = \frac{1}{\sqrt{2}} \begin{pmatrix} 1 \\ 0 \\ -1 \\ 0 \end{pmatrix}, \quad \rho(-1) = \frac{1}{\sqrt{2}} \begin{pmatrix} 0 \\ 1 \\ 0 \\ 1 \end{pmatrix}. \quad (65)$$

Calculating the diagrams in Fig. 3 in $A^- = 0$ gauge while including only the sub-eikonal helicity-dependent terms, we get the following contributions to the scattering amplitude:

$$i M_{\mathcal{A}} = g^3 f^{abc} (t^b)_2 (t^c)_1 \delta_{\sigma_1 \sigma'_1} \delta_{\sigma_2 \sigma'_2} \frac{1}{q^2 (\underline{k} - \underline{q})^2} \left\{ -4s \underline{\epsilon}_\lambda^* \cdot (\underline{k} - \underline{q}) + 2i \frac{p_1^+}{k^+} \sigma_2 [2 \underline{k} \times \underline{q} \underline{\epsilon}_\lambda^* \cdot \underline{k} - (k_T^2 - q_T^2) \underline{\epsilon}_\lambda^* \times \underline{q}] \right. \\ \left. + 4ip_2^- k^+ \sigma_1 \underline{\epsilon}_\lambda^* \times (\underline{k} - \underline{q}) + 2\sigma_1 \sigma_2 [\underline{\epsilon}_\lambda^* \cdot \underline{q} \underline{q} \cdot (\underline{k} - \underline{q}) + \underline{\epsilon}_\lambda^* \times \underline{k} \underline{k} \times \underline{q}] \right\}, \quad (66a)$$

$$i M_B = ig^3 (t^a t^c)_2 (t^c)_1 \delta_{\sigma_1 \sigma'_1} \delta_{\sigma_2 \sigma'_2} \frac{1}{q_T^2 2p_1^+ k^-} \left\{ 4 \frac{p_1^+}{k^+} s \underline{\epsilon}_\lambda^* \cdot \underline{k} - 2is \underline{\epsilon}_\lambda^* \times \underline{k} \sigma_1 - 2p_1^+ \sigma_1 \sigma_2 \left[\underline{\epsilon}_\lambda^* \cdot \underline{k} \frac{q_T^2}{k^+} - \underline{\epsilon}_\lambda^* \cdot \underline{q} k^- \right] \right\}, \quad (66b)$$

$$i M_C = -ig^3 (t^c t^a)_2 (t^c)_1 \delta_{\sigma_1 \sigma'_1} \delta_{\sigma_2 \sigma'_2} \frac{1}{q_T^2 2p_1^+ k^-} \left\{ 4 \frac{p_1^+}{k^+} s \underline{\epsilon}_\lambda^* \cdot \underline{k} - 2is \underline{\epsilon}_\lambda^* \times \underline{k} \sigma_1 - 2p_1^+ \sigma_1 \sigma_2 \left[\underline{\epsilon}_\lambda^* \cdot \underline{k} \frac{q_T^2}{k^+} - \underline{\epsilon}_\lambda^* \cdot \underline{q} k^- \right] \right\}, \quad (66c)$$

$$i M_D = ig^3 (t^b)_2 (t^a t^b)_1 \delta_{\sigma_1 \sigma'_1} \delta_{\sigma_2 \sigma'_2} \frac{1}{2p_2^- k^+ (\underline{q} - \underline{k})^2} \left\{ 2is \sigma_2 \underline{\epsilon}_\lambda^* \times (\underline{q} - \underline{k}) + \sigma_1 \sigma_2 2p_2^- k^+ \underline{\epsilon}_\lambda^* \cdot (\underline{k} - \underline{q}) \right\}, \quad (66d)$$

$$i M_E = -ig^3 (t^b)_2 (t^b t^a)_1 \delta_{\sigma_1 \sigma'_1} \delta_{\sigma_2 \sigma'_2} \frac{1}{2p_2^- k^+ (\underline{q} - \underline{k})^2} \left\{ 2is \sigma_2 \underline{\epsilon}_\lambda^* \times (\underline{q} - \underline{k}) + \sigma_1 \sigma_2 2p_2^- k^+ \underline{\epsilon}_\lambda^* \cdot (\underline{k} - \underline{q}) \right\}. \quad (66e)$$

All momenta, colors and polarizations are as labeled in Fig. 3. We also keep only the leading term in each channel (with the channels defined by their σ -structure). The subscripts 1 and 2 on the (products of) color matrices indicate the color spaces of quarks 1 and 2.

Adding up the contributions in Eqs. (66) we get

$$\begin{aligned} i M = i (M_A + M_B + M_C + M_D + M_E) = g^3 f^{abc} (t^b)_2 (t^c)_1 \delta_{\sigma_1 \sigma'_1} \delta_{\sigma_2 \sigma'_2} & \left\{ -\frac{4s}{q_T^2} \underline{\epsilon}_\lambda^* \cdot \left(\frac{\underline{k} - \underline{q}}{(\underline{k} - \underline{q})^2} - \frac{\underline{k}}{k^2} \right) \right. \\ & + 2i\sigma_2 \frac{p_1^+}{k^+} \frac{2\underline{k} \times \underline{q} \underline{\epsilon}_\lambda^* \cdot \underline{k} - k_T^2 \underline{\epsilon}_\lambda^* \times \underline{q} + q_T^2 \underline{\epsilon}_\lambda^* \times \underline{k}}{q^2 (\underline{k} - \underline{q})^2} + 2i\sigma_1 \frac{p_2^-}{k^-} \frac{k_T^2 \underline{\epsilon}_\lambda^* \times (\underline{k} - \underline{q}) - (\underline{k} - \underline{q})^2 \underline{\epsilon}_\lambda^* \times \underline{k}}{q^2 (\underline{k} - \underline{q})^2} \\ & \left. + \sigma_1 \sigma_2 \left[2 \frac{\underline{\epsilon}_\lambda^* \cdot \underline{q} \underline{q} \cdot (\underline{k} - \underline{q}) + \underline{\epsilon}_\lambda^* \times \underline{k} \underline{k} \times \underline{q}}{q^2 (\underline{k} - \underline{q})^2} - \underline{\epsilon}_\lambda^* \cdot \left(2 \frac{\underline{k}}{k^2} - \frac{\underline{q}}{q^2} + \frac{\underline{k} - \underline{q}}{(\underline{k} - \underline{q})^2} \right) \right] \right\}. \quad (67) \end{aligned}$$

The corresponding $\sigma_1 \sigma_2$ -dependent part of the amplitude squared (and averaged over the incoming quarks' colors) is

$$\langle |M|^2 \rangle = -4g^6 C_F \sigma_1 \sigma_2 s \frac{k^2 + q^2 + (\underline{k} - \underline{q})^2}{k^2 q^2 (\underline{k} - \underline{q})^2}. \quad (68)$$

This agrees, up to an overall sign, with Eq. (B4) in [2], where the same process was calculated in Feynman gauge. The sign difference is due to the fact that the anti-BL spinors (64) have a different sign convention for the quark polarization σ compared to the extraction of the polarization-dependent part of the cross section using the projection with the $\sigma_2 \gamma^5 / 2$ operator employed in [2].

The amplitude squared in Eq. (68) is for the polarization-dependent part of the $qq \rightarrow qqG$ process, while we are interested in the $GG \rightarrow GGG$ process. To construct the latter, we first concentrate on the contribution of diagrams \mathcal{B} and \mathcal{C} from Fig. 3. If we replace the quark lines by gluons in those diagrams, the $qq \rightarrow qq$ sub-process would become $GG \rightarrow GG$, which, at the sub-eikonal level, can proceed through the s - and u -channel exchange, along with a 4-gluon vertex contribution, in addition to the t -channel exchange shown in Fig. 3, as demonstrated in [46]. The effect of the s - and u -channel exchanges and the 4-gluon vertex contribution is to reduce the t -channel exchange contribution in half [46]. Thus, before scaling Eq. (68) up by the factors appropriate to the conversion from incoming quarks to gluons, we need to reduce the contribution of diagrams \mathcal{B} and \mathcal{C} by 2.

The $\sigma_1 \sigma_2$ -dependent part of the diagrams \mathcal{B} and \mathcal{C} from Fig. 3, interfering with the eikonal (first in the curly brackets) term in Eq. (67), gives the following contribution to $\langle |M|^2 \rangle$,

$$4g^6 C_F \sigma_1 \sigma_2 s \frac{1}{q^2} \left(\frac{\underline{k} - \underline{q}}{(\underline{k} - \underline{q})^2} - \frac{\underline{k}}{k^2} \right) \cdot \left(2 \frac{\underline{k}}{k^2} - \frac{\underline{q}}{q^2} \right). \quad (69)$$

The last \underline{q}/q^2 term in the second parentheses can be neglected: indeed,

$$\int d^2 q_\perp \frac{1}{q^2} \frac{\underline{k}}{k^2} \cdot \frac{\underline{q}}{q^2} = 0, \quad (70)$$

while

$$\int d^2 q_\perp \frac{1}{q^2} \frac{\underline{k} - \underline{q}}{(\underline{k} - \underline{q})^2} \cdot \frac{\underline{q}}{q^2} = -\frac{\pi}{k_T^2} \quad (71)$$

and is non-logarithmic, suppressed by a power of the logarithm compared to the rest of the expression (integrated over q). Such contribution probably corresponds to emission from inside the shock wave in the shock wave formalism.

The remainder of Eq. (69) gives

$$-4g^6 C_F \sigma_1 \sigma_2 s \frac{-\underline{k}^2 + \underline{q}^2 + (\underline{k} - \underline{q})^2}{\underline{k}^2 \underline{q}^2 (\underline{k} - \underline{q})^2}. \quad (72)$$

To go from $qq \rightarrow qqG$ to $GG \rightarrow GGG$, we need to subtract Eq. (72) from Eq. (68), and add 1/2 of Eq. (72) to the resulting expression: this amounts to subtracting 1/2 of Eq. (72) from Eq. (68). In addition, we need to multiply everything by 4 to account for the color factor difference between $qq \rightarrow qqG$ and $GG \rightarrow GGG$ (at large N_c) and by 4 to account for the spin difference between gluons and quarks (see [46]). We get (at large N_c)

$$\langle |M|^2 \rangle_{GG \rightarrow GGG} = -32g^6 C_F \sigma_1 \sigma_2 s \frac{3\underline{k}^2 + \underline{q}^2 + (\underline{k} - \underline{q})^2}{\underline{k}^2 \underline{q}^2 (\underline{k} - \underline{q})^2} \quad (73)$$

with the corresponding cross section

$$\frac{d\sigma_{LO}^{GG \rightarrow GGG}}{d^2 k_T dy} = -\frac{4\alpha_s^3 N_c}{\pi^2 s} \int d^2 q \frac{3\underline{k}^2 + \underline{q}^2 + (\underline{k} - \underline{q})^2}{\underline{k}^2 \underline{q}^2 (\underline{k} - \underline{q})^2}. \quad (74)$$

The q integral is bounded from above by the limits stated in Eq. (63). We will use the IR cutoff Λ to regulate the singularities at $q = 0$ and $q = k$. Performing the q integration in Eq. (74) yields

$$\frac{d\sigma_{LO}^{GG \rightarrow GGG}}{d^2 k_T dy} = -\frac{8\alpha_s^3 N_c}{\pi s k_T^2} \left\{ 3 \ln \frac{k_T^2}{\Lambda^2} + \ln \left(\frac{\min\{\alpha, \beta\} s}{\Lambda^2} \right) \right\}. \quad (75)$$

This result needs to be compared to our main result (55) evaluated at the lowest non-trivial order. Indeed, substituting the Born-level polarized dipole amplitudes from Eq. (36) into Eq. (55), both for the projectile and for the target (while replacing $\alpha \rightarrow \beta$ for the latter), and integrating over \underline{x} while keeping the lower bound (56) in mind, such that

$$\nabla_{\perp}^2 \ln(\alpha s x_{\perp}^2) = \nabla_{\perp}^2 \ln(\beta s x_{\perp}^2) = 4\pi \delta_{\max\{1/\alpha s, 1/\beta s\}}^2(\underline{x}), \quad (76)$$

we readily arrive at Eq. (75) (up to the minus sign mentioned before due to the anti-BL spinor convention from [3, 61]). This accomplishes the cross check of Eq. (55) at the lowest non-trivial order.

Let us add that the inclusive gluon production cross section in unpolarized gluon-gluon collisions at the same lowest order in the coupling (order- α_s^3) is (see [37] and references therein)

$$\frac{d\sigma_{LO, \text{unpolarized}}^{GG \rightarrow GGG}}{d^2 k_T dy} = \frac{4\alpha_s^3 N_c^2}{\pi C_F} \frac{1}{k_T^4} \ln \frac{k_T^2}{\Lambda^2}. \quad (77)$$

Using this result, along with Eq. (75) in Eq. (1), we conclude that, at this lowest order, the double-spin asymmetry scales as

$$A_{LL} \sim \frac{k_T^2}{s}, \quad (78)$$

in qualitative agreement with the experimental data reported at RHIC [104, 105, 125, 126].

III. INCLUDING SMALL- x EVOLUTION

The aim of this Section is to show that our main result (55) for the gluon production cross section in polarized proton-proton collisions in the pure glue sector is valid when the DLA small- x helicity evolution [1–4] is included in the rapidity intervals between the produced gluon and the projectile and between the produced gluon and the target. We will show that the evolution would just enter the polarized dipole amplitudes in Eq. (55), both for the dipole scattering on the projectile and on the target.

The evolution is easier to discuss in terms of rapidity variables. Assuming that both the projectile and the target are characterized by the same transverse momentum scale Λ , our IR cutoff, we define the rapidity of the projectile as

$$Y_P = \frac{1}{2} \ln \frac{p_2^-}{p_2^+} = \ln \frac{\sqrt{2} p_2^-}{\Lambda} \quad (79)$$

and the rapidity of the target as

$$Y_T = \frac{1}{2} \ln \frac{p_1^-}{p_1^+} = \ln \frac{\Lambda}{\sqrt{2} p_1^+}. \quad (80)$$

Using these two variables, we rewrite Eq. (55) as

$$\begin{aligned} \frac{d\sigma}{d^2k_T dy} &= \frac{C_F}{\alpha_s \pi^4} \frac{1}{s k_T^2} \int d^2x e^{-i\mathbf{k}\cdot\mathbf{x}} \\ &\times (G_P^{\text{adj}} \ G_{2P}^{\text{adj}})(x_\perp^2, \Lambda k_T e^{Y_P-y}) \begin{pmatrix} \frac{1}{4} \vec{\nabla}_\perp \cdot \vec{\nabla}_\perp & \vec{\nabla}_\perp^2 + \vec{\nabla}_\perp \cdot \vec{\nabla}_\perp \\ \vec{\nabla}_\perp^2 + \vec{\nabla}_\perp \cdot \vec{\nabla}_\perp & 0 \end{pmatrix} \begin{pmatrix} G_T^{\text{adj}} \\ G_{2T}^{\text{adj}} \end{pmatrix} (x_\perp^2, \Lambda k_T e^{y-Y_T}). \end{aligned} \quad (81)$$

Hence, the evolution in the target dipole amplitudes will correspond to the evolution in the $y - Y_T$ rapidity interval, while the evolution in the projectile dipole amplitudes would be given by the evolution in the $Y_P - y$ rapidity interval.

A. Target side

Including the DLA evolution [1–4] in the $y - Y_T$ rapidity interval is quite straightforward. For the central rapidity gluon production in unpolarized proton–proton or proton–nucleus collisions, the inclusion of small- x evolution between the gluon and the target was done in [110]. For that unpolarized case, this is now a standard procedure in the field, detailed in [37]: one can show that to include small- x evolution in the $y - Y_T$ rapidity interval, one has to simply evolve the unpolarized dipole amplitude N on the target with the non-linear small- x evolution equations [21–30], leaving the expression for the production cross section the same. This conclusion is perhaps easiest to see in the operator language: writing the dipole amplitude as a correlator of light-cone Wilson line operators makes the expression equally valid with and without the small- x evolution.

The same logic applies to the helicity evolution at hand. While the target-projectile symmetric expression (55) treats the target and projectile polarized dipole amplitudes on the same footing by the virtue of substitutions (43) and (46), the expression we derived above in the operator language is Eq. (29). In Eq. (29) the gluon production cross section is expressed in terms of the target polarized dipole amplitudes, defined via correlators of polarized and regular Wilson line operators in Eqs. (16). These operator matrix elements can be evaluated in the quasi-classical approximation of the helicity-dependent MV (hMV) model [46], or by including the small- x helicity evolution [1–4] into them. In this sense, the effects of the DLA helicity evolution are already included into Eq. (55) (or, equivalently, into Eq. (81)) if we evaluate G_T^{adj} and G_{2T}^{adj} in those expressions by solving the equations derived in [4]. Since the helicity evolution equations [1–4] close only in the large- N_c and large- $N_c \& N_f$ limits, and as the large- N_c limit is the one appropriate for our gluons-only calculation here, the relations in Eq. (57) are needed to connect the adjoint dipole amplitudes G_T^{adj} and G_{2T}^{adj} to the fundamental ones, G_T and G_{2T} , entering the large- N_c helicity evolution equations in [4]. For finite N_c , the polarized dipole amplitudes G_T^{adj} and G_{2T}^{adj} can be evaluated using the helicity-dependent extension [44] of the Jalilian-Marian–Iancu–McLerran–Weigert–Leonidov–Kovner (JIMWLK) evolution equation [25–30].

To summarize this Subsection, we see that the small- x evolution effects in the $y - Y_T$ rapidity interval are already included in Eq. (55) if the target polarized dipole amplitudes are evaluated using the DLA helicity evolution from [1–4].

B. Projectile side

Including the small- x evolution on the projectile side, in the $Y_P - y$ rapidity interval, is less straightforward than on the target side. Here we will follow the strategy applied in [110], with more details provided in Chapter 8 of [37]. We will also work in the large- N_c limit: while this may be a little less general than the any- N_c applicability of Eq. (55), currently the helicity evolution equations are solved in the large- N_c limit [4, 49] (and at large- $N_c \& N_f$ [5]), with the solution of helicity-JIMWLK (hJIMWLK) evolution [44] still lacking (and, with the hJIMWLK evolution [44] itself in need of revisiting in light of the corrections found in [4]).

Following [110], we first argue that, in the shock wave picture, the gluon emissions in the $Y_P - y$ rapidity interval take place *before* the interaction with the shock wave. The argument completely parallels that in [110] and will not be repeated here: we just remark that the hard gluon emissions (that is, emissions in the $Y_P - y$ rapidity interval) happening after the interaction with the shock wave cancel after squaring the amplitude (see [37] for more details). The result is illustrated in Fig. 4, where the emission of gluons harder (in the longitudinal momentum fraction β) than the produced gluon are shown for a gluon projectile. Per the above-mentioned argument, the surviving emissions all take place to the left of the shock wave (before the shock wave interaction).

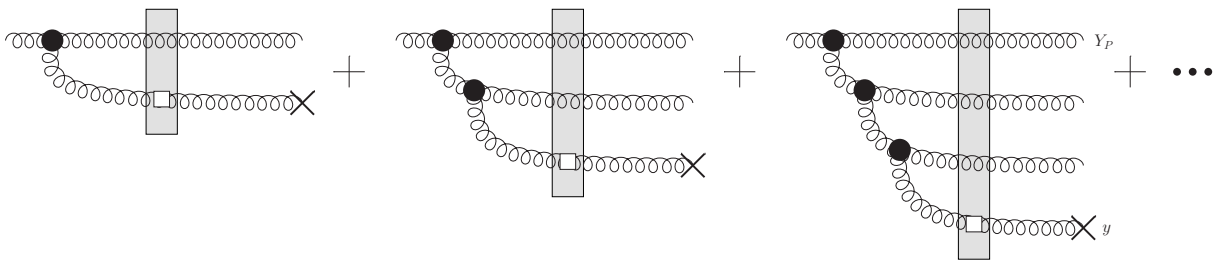


FIG. 4. Diagrams illustrating gluon emissions in the rapidity interval $Y_P - y$ between the projectile gluon at rapidity Y_P and the produced gluon at rapidity y . The produced gluon is marked by a cross.

In the large- N_c limit, these early emissions of harder in β gluons result in a dipole cascade, with the produced gluon being emitted from one of the dipoles formed this way. Unlike the eikonal unpolarized evolution, where there is only one type of dipoles [21–24, 51–53], in the sub-eikonal helicity evolution case in the gluon sector we have two types of dipole amplitudes, as given by Eqs. (16). Therefore, the produced gluon can be emitted by either of the two possible dipoles, constructed out of the \mathcal{F}^{12} and $\mathcal{D}^i - \tilde{\mathcal{D}}^i$ operators, respectively. These emissions are a generalization of the above calculation for a single projectile gluon and are considered in detail in Appendix C below. In Appendix C we demonstrate that when the produced gluon is emitted by a color-dipole made using either the \mathcal{F}^{12} or $\mathcal{D}^i - \tilde{\mathcal{D}}^i$ operators, the gluon production cross section still factorizes into the part describing the gluon emission by the projectile dipole, and the interaction of the system with the target. Importantly, the interaction with the target is described by the same dipole amplitudes $G_T^{\text{adj}}(\beta s)$ and $G_T^{i\text{adj}}(\beta s)$ from Eqs. (16), just like in the gluon projectile case of Eq. (29). We can then conclude that the interaction with the target for the single gluon inclusive production cross section with multiple higher- β gluon emissions (generating a dipole cascade to the left of the shock wave) is also described by $G_T^{\text{adj}}(\beta s)$ and $G_T^{i\text{adj}}(\beta s)$ dipole amplitudes. Owing to Eq. (33b), this means that the interaction with the target is expressible in terms of $G_T^{\text{adj}}(\beta s)$ and $G_{2T}^{\text{adj}}(\beta s)$.

We now employ the following argument: based on the above observation, we can write the inclusive gluon production cross section with the the full higher- β gluon cascade at large N_c as

$$\frac{d\sigma}{d^2k_T dy} = C_1(\alpha s) \otimes G_T^{\text{adj}}(\beta s) + C_2(\alpha s) \otimes G_{2T}^{\text{adj}}(\beta s), \quad (82)$$

with some unknown functions C_1 and C_2 resulting from re-summing the higher- β cascade in the DLA. The convolution (\otimes) is over the dipole sizes which are not shown explicitly. If we now “turn off” the evolution between the produced gluon and the target by replacing $G_T^{\text{adj}}(\beta s) \rightarrow G_T^{\text{adj}(0)}(\beta s)$ and $G_{2T}^{\text{adj}}(\beta s) \rightarrow G_{2T}^{\text{adj}(0)}(\beta s)$ in Eq. (82), we would reduce the cross section to that for the scattering of an un-evolved target on the projectile, that is, to Eq. (29) with the target and projectile interchanged. Following the above calculations, we can then rewrite this cross section as in Eq. (55), but with $G_T^{\text{adj}(0)}$ and $G_{2T}^{\text{adj}(0)}$ instead of G_T^{adj} and G_{2T}^{adj} . At this point, we readily observe that we can simply reverse the earlier replacement of the dipole amplitudes, $G_T^{\text{adj}(0)}(\beta s) \rightarrow G_T^{\text{adj}}(\beta s)$ and $G_{2T}^{\text{adj}(0)}(\beta s) \rightarrow G_{2T}^{\text{adj}}(\beta s)$, reinstating the evolution on the target side, and arriving at Eq. (55) with the DLA small- x helicity evolution included both on the target and on the projectile side.

We thus conclude that our main result (55) for the projectile and target polarization-dependent inclusive gluon production cross section is still valid when the small- x DLA helicity evolution [1–4] is included both on the target and on the projectile sides. This makes our result (55) more general, and, potentially, applicable to the hadron or jet production phenomenology in the central rapidity region of the polarized proton–proton collisions at RHIC [13, 14, 104, 105].

IV. CONCLUSIONS AND OUTLOOK

In this paper we have derived the inclusive gluon production cross section for the scattering of a longitudinally polarized projectile on a longitudinally polarized target. The cross section was calculated in the pure gluon sector, with the inclusion of quarks left for the future work. Our main result, written in a k_T -factorized form, is shown in Eq. (55). It employs the impact-parameter integrated polarized dipole amplitudes $G_T^{\text{adj}}(2k^- p_1^+)$ and $G_{2T}^{\text{adj}}(2k^- p_1^+)$ for a gluon dipole scattering on the target and the dipole amplitudes $G_P^{\text{adj}}(2k^+ p_2^-)$ and $G_{2P}^{\text{adj}}(2k^+ p_2^-)$ for the scattering on the projectile. These dipole amplitudes can be found by solving the DLA evolution equations from [1–4]. We have, therefore, constructed a theoretical prediction for the small- x gluon production in the central rapidity region

of longitudinally polarized nucleon–nucleon collisions. Our result parallels that of [108, 110] for the small- x gluon production at mid-rapidity in unpolarized scattering.

While our calculation was done for gluon production only, it may still be applicable to phenomenology of hadron and jet production at mid-rapidity in the polarized proton–proton collisions at RHIC [13, 14, 104, 105], where gluon contribution is known to dominate over the quark one. The data analysis can be done following the approach pioneered in [85] for polarized DIS at small x , which has recently been extended to polarized SIDIS in [50]. Our cross section (55), when convoluted with the appropriate fragmentation functions, would give the numerator of the double spin asymmetry A_{LL} for hadron production measured in the polarized proton–proton collisions at RHIC.

In the future, our result needs to be expanded to include the contribution of quarks, both to inclusive gluon production and to inclusive quark production at central rapidity in polarized proton–proton collisions. This can be done along the lines of [1, 3, 4, 47]. Such calculation would lead to a complete expression for the inclusive small- x parton production cross section in longitudinally polarized nucleon–nucleon scattering. It would allow to fully complete the small- x polarized data analysis program started in [50, 85] and to make as precise a prediction as possible (based on the small- x formalism) for the longitudinal spin observables to be measured at the EIC.

ACKNOWLEDGMENTS

The authors would like to thank Daniel Adamiak for his contributions at the early stages of this project. We are also grateful to Nicholas Baldonado, Daniel Pitonyak, and Matthew Sievert for helpful and encouraging discussions.

This material is based upon work supported by the U.S. Department of Energy, Office of Science, Office of Nuclear Physics under Award Number DE-SC0004286 and within the framework of the Saturated Glue (SURGE) Topical Theory Collaboration.

Appendix A: Ultraviolet contribution to $(D + E) A_{\text{eik}}^* + \text{c.c.}$ interference terms

The mismatch between the transverse positions of the incoming gluon to the left and to the right of the final state cut only affects the $(D + E) A_{\text{eik}}^* + \text{c.c.}$ contributions to the production cross section calculated in Sec. II B in the main text, as follows from an analysis of the diagrams shown in Fig. 2. Indeed, in Fig. 2, only diagrams D and E come in with the sub-eikonal interaction, denoted by the white square, taking place when the gluon at position \underline{b} crosses the shock wave, potentially leading to the issue discussed around Eq. (28) above.

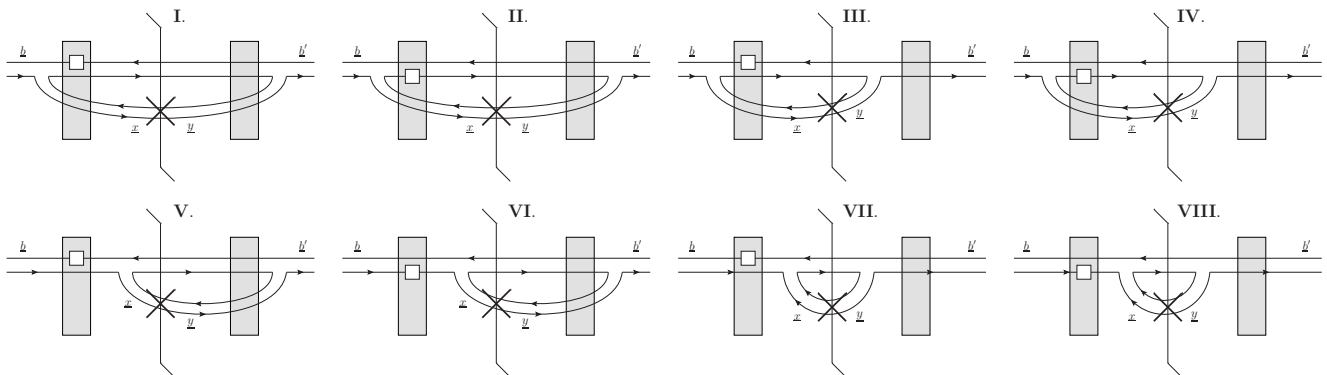


FIG. 5. Large- N_c diagrams contributing to $(D + E) A_{\text{eik}}^*$ interference terms. The shaded rectangle represents the shock wave, the white square denotes the sub-eikonal interactions, while the cross denotes the produced gluon. All double lines represent gluons at large- N_c [68]. The complex conjugate terms are not shown explicitly.

Here we analyse the $(D + E) A_{\text{eik}}^*$ diagrams a little more carefully. Our discussion employs the large- N_c limit, which is exact for the pure-gluon diagrams of Fig. 2, as can be readily checked. The $(D + E) A_{\text{eik}}^*$ diagrams from Fig. 2 are depicted again in Fig. 5, utilizing the large- N_c limit (with the gluons shown as double lines). The top row of diagrams in Fig. 5 corresponds to the $D A_{\text{eik}}^*$ interference, while the bottom row corresponds to $E A_{\text{eik}}^*$ contributions.

Working in the large- N_c limit, we immediately observe that diagrams IV and VI (and their complex conjugates) in Fig. 5 do not contain a color-dipole or quadrupole involving both lines at \underline{b} and \underline{b}' . These contributions are included in equations (19) and (23) and have no potential new terms arising from the $\underline{b}' \rightarrow \underline{b}$ limit. Therefore, we do not need to consider those further.

Moreover, combining diagrams I, III, V, and VII, along with their complex conjugates, we notice that their contribution is proportional to the unpolarized gluon production cross section (see [37, 106]), such that

$$\text{I} + \text{III} + \text{V} + \text{VII} \propto \left\langle \text{tr} \left[V_{\underline{b}}^{\text{G}[1]\dagger} V_{\underline{b}'} \right] \right\rangle \left[S_{\underline{x}, \underline{y}} - (S_{\underline{x}, \underline{b}})^2 - (S_{\underline{b}, \underline{y}})^2 + 1 \right]. \quad (\text{A1})$$

Here $S_{\underline{x}, \underline{y}}$ is the unpolarized dipole S -matrix [21, 23] and we put $\underline{b}' = \underline{b}$ in the second square brackets, since this limit is regular for the unpolarized dipole S -matrices. With the DLA accuracy of our calculation, all $S = 1$ in Eq. (A1), giving

$$\text{I} + \text{III} + \text{V} + \text{VII} = 0. \quad (\text{A2})$$

We can thus discard diagrams I, III, V, and VII, along with their complex conjugates. It appears that those diagrams would contribute if one includes single-logarithmic corrections (that is, powers of $\alpha_s \ln(1/x)$) into the gluon production calculation. However, while some of these single-logarithmic corrections to small- x helicity evolution were found in [48], it appears that for a complete calculation of small- x helicity evolution at the single logarithmic order one would need to go beyond the shock-wave picture we are employing here.

We are left with the diagrams II and VIII from Fig. 5. While the diagram II contains a polarized color-quadrupole amplitude made out of the $\underline{x}, \underline{y}, \underline{b}, \underline{b}'$ lines, the part of diagram II giving new terms in the $\underline{b}' \rightarrow \underline{b}$ limit is obtained when the \underline{x} and \underline{y} lines do not interact and the quadrupole amplitude reduces to the $\underline{b}, \underline{b}'$ polarized dipole. This part of diagram II is identical to diagram VII. Therefore, in the DLA, we conclude that the $\underline{b}' \rightarrow \underline{b}$ limit of the diagrams in Fig. 5, not accounted for in Eqs. (19) and (23), is given by the sum of diagrams VII and VIII (and their complex conjugates). This is a part of the $E A_{\text{eik}}^*$ interference, which follows from Eq. (23) and is given by

$$\begin{aligned} & -\frac{\lambda}{N_c^2 - 1} \frac{4\alpha_s}{(2\pi)^4} \int d^2x d^2y d^2b e^{-ik \cdot (\underline{x} - \underline{y})} \frac{\underline{x} - \underline{b}}{|\underline{x} - \underline{b}|^2} \cdot \frac{\underline{y} - \underline{b}}{|\underline{y} - \underline{b}|^2} \left\langle \text{Tr} \left[U_{\underline{b}'}^\dagger T^a U_{\underline{b}}^{\text{G}[1]} T^c \right] (-U_{\underline{b}'})^{ac} \right\rangle + \text{c.c.} \\ & = \frac{\lambda}{N_c^2 - 1} \frac{4\alpha_s}{(2\pi)^4} \int d^2x d^2y d^2b e^{-ik \cdot (\underline{x} - \underline{y})} \frac{\underline{x} - \underline{b}}{|\underline{x} - \underline{b}|^2} \cdot \frac{\underline{y} - \underline{b}}{|\underline{y} - \underline{b}|^2} \left\langle \text{Tr} \left[T^a U_{\underline{b}}^{\text{G}[1]} U_{\underline{b}'}^\dagger T^a \right] \right\rangle + \text{c.c.} \\ & = -\lambda \frac{\alpha_s}{4\pi^4} \frac{1}{s} N_c \int d^2x d^2y d^2b e^{-ik \cdot (\underline{x} - \underline{y})} \frac{\underline{x} - \underline{b}}{|\underline{x} - \underline{b}|^2} \cdot \frac{\underline{y} - \underline{b}}{|\underline{y} - \underline{b}|^2} \left[-2 G_{\underline{b}, \underline{b}'}^{\text{adj}} (2k^- p_1^+) \right]. \end{aligned} \quad (\text{A3})$$

This is exactly the result in Eq. (25) of the main text.

Appendix B: Small- x limit of twist-3 gluon helicity-flip TMD

The general gauge-invariant two-gluon correlation functions are defined as [124]

$$\Gamma^{\mu\nu; \rho\sigma}(k, P, S) = \int \frac{d^4\xi}{(2\pi)^4} e^{ik \cdot \xi} \langle P, S | \text{Tr} \left[F^{\mu\nu}(0) \mathcal{U}^{[+]}(0, \xi) F^{\rho\sigma}(\xi) \mathcal{U}^{[-]}(\xi, 0) \right] | P, S \rangle. \quad (\text{B1})$$

We choose the future- ($\mathcal{U}^{[+]}$) and past-pointing ($\mathcal{U}^{[-]}$) fundamental Wilson line staples relevant to the gluon production process under consideration. This way, the TMDs one can construct out of the correlator (B1) will be the dipole TMDs. Here $|P, S\rangle$ is the proton state with momentum P and spin S .

Among all the possible values of μ, ν, ρ, σ , the leading twist-2 gluon correlation function

$$\Gamma^{+i; +j}(k, P, S) = \int \frac{d^4\xi}{(2\pi)^4} e^{ik \cdot \xi} \langle P, S | \text{Tr} \left[F^{+i}(0) \mathcal{U}^{[+]}(0, \xi) F^{+j}(\xi) \mathcal{U}^{[-]}(\xi, 0) \right] | P, S \rangle \quad (\text{B2})$$

is related to the gluon helicity TMD for a longitudinally polarized proton and if projected onto ϵ^{ij} . For longitudinally polarized proton states, the small x limit of Eq. (B2) (projected onto ϵ^{ij}) was derived in [4].

In this Appendix, we derive the small x limit of a twist-3 gluon helicity-flip TMD, which results from the correlator

$$\Gamma^{ij; l+}(k; P, S_L) = \int \frac{d^4\xi}{(2\pi)^4} e^{ik \cdot \xi} \langle P, S_L | \text{Tr} \left[F^{ij}(0) \mathcal{U}^{[+]}(0, \xi) F^{l+}(\xi) \mathcal{U}^{[-]}(\xi, 0) \right] | P, S_L \rangle \quad (\text{B3})$$

with the longitudinally polarized proton state having spin S_L . Further, following [124], we define

$$M \Gamma_L^{ij; l}(x, \underline{k}) = \int dk^- \Gamma^{ij; l+}(k; P, S_L) \quad (\text{B4})$$

with $k^+ = xP^+$. Here M is the mass of the proton.

For a longitudinally polarized proton state, the twist-3 gluon helicity-flip TMD $\Delta H_{3L}^\perp(x, k_T^2)$ is defined by

$$M \Gamma_L^{ij;l}(x, \underline{k}) = -\frac{i}{4} S_L \epsilon^{ij} k^l \Delta H_{3L}^\perp(x, k_T^2). \quad (\text{B5})$$

Note that we do not include the additional factor x on the right of Eq. (B5) compared to that in [124] and we use the normalization in [4] which differs from that in [124] by a factor of $(-1/2)$ on the right of (B5): overall, our Eq. (B5) differs from Eq. (22) in [124] by an additional factor of $-1/(2x)$ on its right-hand side. Removing the factor of x gives the resulting TMD ΔH_{3L}^\perp the right ‘‘eikonality’’: as will become apparent shortly, this is a sub-eikonal quantity, and should scale as $(1/x)^0$ at small x before the evolution corrections are included.

Inverting Eq. (B5) we get

$$\Delta H_{3L}^\perp(x, k_T^2) = 2i \epsilon^{ij} \frac{k^l}{\underline{k}^2} \frac{1}{2} \sum_{S_L} S_L M \Gamma_L^{ij;l}(x, \underline{k}). \quad (\text{B6})$$

Using the definition (B3), one can show that

$$\Gamma^{l+;ij}(k; P, S_L) = \Gamma^{ij;l+*}(k; P, S_L). \quad (\text{B7})$$

Since the definition (B5) implies that the TMD is real, and, hence, $\Gamma_L^{ij;l}$ is imaginary, then so is $\Gamma^{ij;l+}$. Therefore, Eq. (B7) implies that

$$\Gamma^{l+;ij}(k; P, S_L) = -\Gamma^{ij;l+}(k; P, S_L) \quad (\text{B8})$$

allowing us to rewrite Eq. (B4) as

$$M \Gamma_L^{ij;l}(x, \underline{k}) = \int dk^- \frac{1}{2} [\Gamma^{ij;l+}(k; P, S_L) - \Gamma^{l+;ij}(k; P, S_L)]. \quad (\text{B9})$$

Combining Eqs. (B5) and (B9) we obtain

$$\begin{aligned} \Delta H_{3L}^\perp(x, k_T^2) &= \frac{2i}{V^-(2\pi)^3} \epsilon^{ij} \frac{k^l}{\underline{k}^2} \sum_{S_L} \frac{1}{2} S_L \int d\xi^- d^2\xi d\zeta^- d^2\zeta e^{ik^+(\xi^- - \zeta^-)} e^{-i\underline{k}\cdot(\underline{\xi} - \underline{\zeta})} \\ &\times \frac{1}{2} \left[\langle P, S_L | \text{Tr} \left[F^{ij}(\zeta) \mathcal{U}^{l+}(\zeta, \xi) F^{l+}(\xi) \mathcal{U}^{[-]}(\xi, \zeta) \right] | P, S_L \rangle \Big|_{\xi^+ = \zeta^+ = 0} \right. \\ &\left. - \langle P, S_L | \text{Tr} \left[F^{l+}(\zeta) \mathcal{U}^{l+}(\zeta, \xi) F^{ij}(\xi) \mathcal{U}^{[-]}(\xi, \zeta) \right] | P, S_L \rangle \Big|_{\xi^+ = \zeta^+ = 0} \right]. \end{aligned} \quad (\text{B10})$$

Here $V^- = \int dx^- d^2x$.

To obtain the small- x limit of $\Delta H_{3L}^\perp(x, k_T^2)$, we first note that in any gauge where $A_\perp \rightarrow 0$ as $x^- \rightarrow \pm\infty$, we can write the gauge links as

$$\mathcal{U}^{l+}(\zeta, \xi) = V_\zeta^+[\zeta^-, \infty] V_\xi^+[\infty, \xi^-], \quad \mathcal{U}^{[-]}(\xi, \zeta) = V_\xi^+[\xi^-, -\infty] V_\zeta^+[-\infty, \zeta^-]. \quad (\text{B11})$$

We then can approximate (cf. Eq. (22) in [4])

$$\begin{aligned} &\frac{k^l}{\underline{k}^2} \int d^2\xi e^{-i\underline{k}\cdot\underline{\xi}} \int_{-\infty}^{\infty} d\xi^- e^{ixP^+\xi^-} V_\xi^+[\infty, \xi^-] F^{l+}(\xi^-, \underline{\xi}) V_\xi^+[\xi^-, -\infty] \\ &= \frac{k^l}{\underline{k}^2} \int d^2\xi e^{-i\underline{k}\cdot\underline{\xi}} \int_{-\infty}^{\infty} d\xi^- e^{ixP^+\xi^-} V_\xi^+[\infty, \xi^-] [\partial^l A^+(\xi^-, \underline{\xi}) + ixP^+ A^l(\xi^-, \underline{\xi})] V_\xi^+[\xi^-, -\infty] \\ &\approx \frac{1}{ig} \frac{k^l}{\underline{k}^2} \int d^2\xi e^{-i\underline{k}\cdot\underline{\xi}} \partial^l V_\xi^+ = -\frac{1}{g} \int d^2\xi e^{-i\underline{k}\cdot\underline{\xi}} V_\xi^+. \end{aligned} \quad (\text{B12})$$

In the last line of the above derivation we have neglected terms suppressed by powers of $x \ll 1$.

On the other hand, one gets, again by expanding in x ,

$$\begin{aligned}
& \epsilon^{ij} \int d\zeta^- e^{-ixP^+\zeta^-} V_{\underline{\zeta}}[-\infty, \zeta^-] F^{ij}(\zeta^-, \underline{\zeta}) V_{\underline{\zeta}}[\zeta^-, \infty] \\
& \approx 2 \int d\zeta^- V_{\underline{\zeta}}[-\infty, \zeta^-] F^{12}(\zeta^-, \underline{\zeta}) V_{\underline{\zeta}}[\zeta^-, \infty] \\
& = \frac{4k^-}{-ig} V_{\underline{\zeta}}^{G[1]\dagger},
\end{aligned} \tag{B13}$$

where (cf. Eq. (5a)) [4]

$$V_{\underline{x}}^{G[1]} = \frac{igP^+}{s} \int_{-\infty}^{\infty} dx^- V_{\underline{x}}[\infty, x^-] F^{12}(x^-, \underline{x}) V_{\underline{x}}[x^-, -\infty]. \tag{B14}$$

Employing Eqs. (B11), (B12), and (B13) in Eq. (B10), and remembering that

$$\langle \dots \rangle \equiv \frac{1}{2} \sum_{S_L} S_L \frac{1}{2^{P+V^-}} \langle P, S_L | \dots | P, S_L \rangle \tag{B15}$$

and $\langle\langle \dots \rangle\rangle = s \langle \dots \rangle$, we obtain the final expression for the small x limit of $\Delta H_{3L}^\perp(x, k_T^2)$,

$$\begin{aligned}
\Delta H_{3L}^\perp(x, k_T^2) &= \frac{8}{g^2(2\pi)^3} \int d^2\xi d^2\zeta e^{-ik\cdot(\xi-\zeta)} \frac{1}{2} \langle\langle \text{tr} [V_{\underline{\xi}} V_{\underline{\zeta}}^{G[1]\dagger} + V_{\underline{\zeta}}^\dagger V_{\underline{\xi}}^{G[1]}] \rangle\rangle \\
&= \frac{N_c}{\alpha_s 4\pi^4} \int d^2x e^{-ik\cdot\underline{x}} G\left(x_\perp^2, \frac{Q^2}{x}\right),
\end{aligned} \tag{B16}$$

where

$$G(x_\perp^2, s) = \int d^2b G_{b+\underline{x}, \underline{b}}(s) \tag{B17}$$

with

$$G_{\underline{x}, \underline{y}}(s) \equiv \frac{1}{2N_c} \text{Re} \langle\langle \text{T tr} [V_{\underline{x}} V_{\underline{y}}^{G[1]\dagger}] + \text{T tr} [V_{\underline{y}}^{G[1]} V_{\underline{x}}^\dagger] \rangle\rangle(s). \tag{B18}$$

Since, at large N_c , $G^{\text{adj}} = 4G$, Eq. (B16) is equivalent to Eq. (59) in the main text.

To conclude, the small- x limit of the twist-3 gluon helicity-flip TMD is given by the dipole amplitude containing the chromo-magnetically polarized Wilson line $V^{G[1]}$.

Appendix C: Gluon production in an adjoint dipole scattering on a polarized target

In this Appendix we show that gluon production cross section for the scattering on a longitudinally polarized target is expressible in terms of the G_T^{adj} and G_{2T}^{adj} polarized dipole amplitudes for the incoming projectile being either an \mathcal{F}^{12} - or $(\mathcal{D}^i - \tilde{\mathcal{D}}^i)$ -type dipole.

1. \mathcal{F}^{12} -type dipole projectile

We start with the eikonal gluon production for the dipole projectile, as shown in Fig. 6. The corresponding amplitude is

$$A_{\text{eik}}^{\text{LO}}(\underline{x}, \underline{b}) = \frac{g}{\pi} \delta_{\lambda, \lambda'} \left(U_{\underline{b}_1} T^b U_{\underline{b}_0}^\dagger \right)^{cd} \left\{ \frac{\epsilon_{\lambda_2}^* \cdot (\underline{x} - \underline{b}_1)}{|\underline{x} - \underline{b}_1|^2} \left[(U_{\underline{x}})^{ab} - (U_{\underline{b}_1})^{ab} \right] - \frac{\epsilon_{\lambda_2}^* \cdot (\underline{x} - \underline{b}_0)}{|\underline{x} - \underline{b}_0|^2} \left[(U_{\underline{x}})^{ab} - (U_{\underline{b}_0})^{ab} \right] \right\}. \tag{C1}$$

Next, let us consider inclusive gluon production amplitudes for a projectile being a gluon dipole. If we choose the polarized gluon line to be at \underline{b}_1 in the transverse plane, we would need to generalize diagrams B, D and E to include

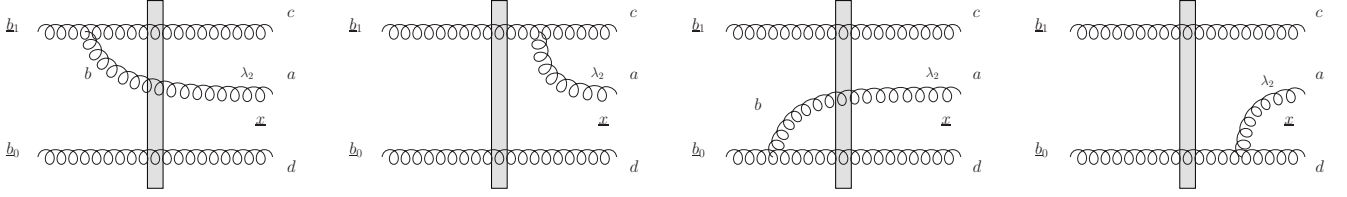


FIG. 6. Diagrams contributing to eikonal inclusive gluon production for the gluon dipole projectile.

emission from the eikonal gluon line at \underline{b}_0 , as shown in Fig. 7. As before, the black circle denotes the insertion of the \mathcal{F}^{12} operator from Eq. (5a), while the white boxes in the diagrams D_1, D_0, E_1 and E_0 denote $U^{G[1]}$. The white boxes in B_1 and B_0 denote the entire sub-eikonal polarized Wilson line (with the gluon background fields only).

Calculating the diagrams in Fig. 7 in a similar way to the calculation in the main text, we can write

$$\begin{aligned}
 \frac{d\sigma^{AA^*_{\text{eik}}+\text{c.c.}}(\lambda)}{d^2k_T dy} &= \lambda \frac{4\alpha_s}{(2\pi)^4} \frac{k^-}{p_2^-} \frac{N_c}{N_c^2 - 1} \int d^2x d^2y d^2b_1 e^{-ik \cdot (x-y)} \sum_{i=0}^1 (-1)^{i+1} \left\{ \frac{\underline{x} - \underline{b}_1}{|\underline{x} - \underline{b}_1|^2} \cdot \frac{\underline{y} - \underline{b}_i}{|\underline{y} - \underline{b}_i|^2} \right. \\
 &\times \left\langle \text{Tr} \left[U_{\underline{y}}^\dagger U_{\underline{x}}^{G[1]} \right] - \text{Tr} \left[U_{\underline{b}_i}^\dagger U_{\underline{x}}^{G[1]} \right] \right\rangle + i \int d^2x' \frac{\underline{x}' - \underline{b}_1}{|\underline{x}' - \underline{b}_1|^2} \times \frac{\underline{y} - \underline{b}_i}{|\underline{y} - \underline{b}_i|^2} \left\langle \text{Tr} \left[U_{\underline{y}}^\dagger U_{\underline{x}, \underline{x}'}^{G[2]} \right] - \text{Tr} \left[U_{\underline{b}_i}^\dagger U_{\underline{x}, \underline{x}'}^{G[2]} \right] \right\rangle \left. \right\} + \text{c.c.} \\
 &= \lambda \frac{\alpha_s}{2\pi^4} \frac{1}{s} N_c \int d^2x d^2y d^2b_1 e^{-ik \cdot (x-y)} \sum_{i=0}^1 (-1)^{i+1} \left\{ \frac{\underline{x} - \underline{b}_1}{|\underline{x} - \underline{b}_1|^2} \cdot \frac{\underline{y} - \underline{b}_i}{|\underline{y} - \underline{b}_i|^2} \left[G_{\underline{x}, \underline{y}}^{\text{adj}}(2k^- p_1^+) - G_{\underline{x}, \underline{b}_i}^{\text{adj}}(2k^- p_1^+) \right] \right. \\
 &\quad \left. - 2i k^j \frac{\underline{x} - \underline{b}_1}{|\underline{x} - \underline{b}_1|^2} \times \frac{\underline{y} - \underline{b}_i}{|\underline{y} - \underline{b}_i|^2} G_{\underline{x}, \underline{b}_i}^{j \text{ adj}}(2k^- p_1^+) \right\}. \tag{C2}
 \end{aligned}$$

Note that when integrating d^2b_1 we keep \underline{b}_{10} fixed (and, hence, \underline{b}_0 varies). Calculating the diagrams B_1 and B_0 from

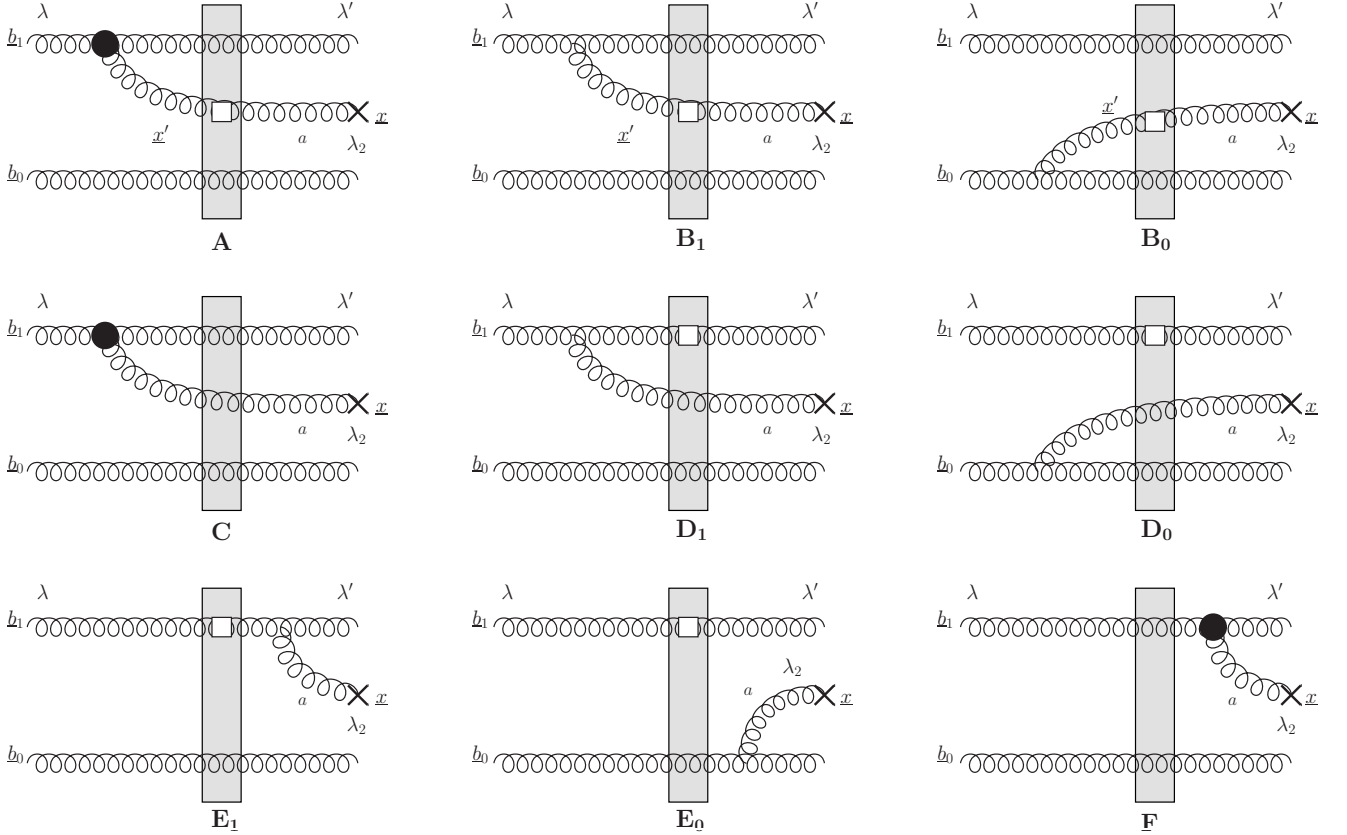


FIG. 7. Diagrams contributing to inclusive sub-eikonal gluon production for the gluon dipole projectile.

Fig. 7 we find their contribution to the cross section to be

$$\begin{aligned}
\frac{d\sigma^{(B_1+B_0)(C^*+F^*)+c.c.}(\lambda)}{d^2k_T dy} &= \lambda \frac{4\alpha_s}{(2\pi)^4} \frac{k^-}{p_2^-} \frac{N_c}{N_c^2-1} \int d^2x d^2y d^2b_1 e^{-ik\cdot(x-y)} \sum_{i=0}^1 (-1)^{i+1} \left\{ \frac{\underline{x}-\underline{b}_i}{|\underline{x}-\underline{b}_i|^2} \cdot \frac{\underline{y}-\underline{b}_1}{|\underline{y}-\underline{b}_1|^2} \right. \\
&\times \left. \left\langle \text{Tr} \left[U_{\underline{y}}^\dagger U_{\underline{x}}^{\text{G}[1]} \right] - \text{Tr} \left[U_{\underline{b}_1}^\dagger U_{\underline{x}}^{\text{G}[1]} \right] \right\rangle + i \int d^2x' \frac{\underline{x}'-\underline{b}_i}{|\underline{x}'-\underline{b}_i|^2} \times \frac{\underline{y}-\underline{b}_1}{|\underline{y}-\underline{b}_1|^2} \left\langle \text{Tr} \left[U_{\underline{y}}^\dagger U_{\underline{x},\underline{x}'}^{\text{G}[2]} \right] - \text{Tr} \left[U_{\underline{b}_1}^\dagger U_{\underline{x},\underline{x}'}^{\text{G}[2]} \right] \right\rangle \right\} + \text{c.c.} \\
&= \lambda \frac{\alpha_s}{2\pi^4} \frac{1}{s} N_c \int d^2x d^2y d^2b_1 e^{-ik\cdot(x-y)} \sum_{i=0}^1 (-1)^{i+1} \left\{ \frac{\underline{x}-\underline{b}_i}{|\underline{x}-\underline{b}_i|^2} \cdot \frac{\underline{y}-\underline{b}_1}{|\underline{y}-\underline{b}_1|^2} \left[G_{\underline{x},\underline{y}}^{\text{adj}}(2k^-p_1^+) - G_{\underline{x},\underline{b}_1}^{\text{adj}}(2k^-p_1^+) \right] \right. \\
&\quad \left. - 2i k^j \frac{\underline{x}-\underline{b}_i}{|\underline{x}-\underline{b}_i|^2} \times \frac{\underline{y}-\underline{b}_1}{|\underline{y}-\underline{b}_1|^2} G_{\underline{x},\underline{b}_1}^{\text{adj}}(2k^-p_1^+) \right\}. \tag{C3}
\end{aligned}$$

Diagrams D_1 and D_0 give

$$\begin{aligned}
\frac{d\sigma^{(D_1+D_0)A_{\text{eik}}^*+c.c.}(\lambda)}{d^2k_T dy} &= \frac{\lambda}{N_c^2-1} \frac{4\alpha_s}{(2\pi)^4} \int d^2x d^2y d^2b_1 e^{-ik\cdot(x-y)} \sum_{i,j=0}^1 (-1)^{i+j} \frac{\underline{x}-\underline{b}_i}{|\underline{x}-\underline{b}_i|^2} \cdot \frac{\underline{y}-\underline{b}_j}{|\underline{y}-\underline{b}_j|^2} \\
&\times \left\langle \text{Tr} \left[U_{\underline{b}_1}^\dagger U_{\underline{b}_1}^{\text{G}[1]} T^a U_{\underline{x}}^\dagger \left(U_{\underline{y}} - U_{\underline{b}_j} \right) T^a \right] \right\rangle + \text{c.c.} \\
&= -\frac{\lambda}{N_c^2-1} \frac{4\alpha_s}{(2\pi)^4} \int d^2x d^2y d^2b_1 e^{-ik\cdot(x-y)} \sum_{i,j=0}^1 (-1)^{i+j} \frac{\underline{x}-\underline{b}_i}{|\underline{x}-\underline{b}_i|^2} \cdot \frac{\underline{y}-\underline{b}_j}{|\underline{y}-\underline{b}_j|^2} \\
&\times \left\langle \text{Tr} \left[U_{\underline{b}_1}^\dagger U_{\underline{b}_1}^{\text{G}[1]} T^a U_{\underline{x}}^\dagger U_{\underline{b}_j} T^a \right] \right\rangle + \text{c.c.} \\
&= -\frac{\lambda}{N_c^2-1} \frac{4\alpha_s}{(2\pi)^4} \int d^2x d^2y d^2b_1 e^{-ik\cdot(x-y)} \left(\frac{\underline{x}-\underline{b}_1}{|\underline{x}-\underline{b}_1|^2} - \frac{\underline{x}-\underline{b}_0}{|\underline{x}-\underline{b}_0|^2} \right) \cdot \frac{\underline{y}-\underline{b}_1}{|\underline{y}-\underline{b}_1|^2} \\
&\times \left\langle \text{Tr} \left[U_{\underline{b}_1}^\dagger U_{\underline{b}_1}^{\text{G}[1]} T^a U_{\underline{x}}^\dagger U_{\underline{b}_1} T^a \right] \right\rangle + \text{c.c.} \\
&= -\lambda \frac{\alpha_s}{4\pi^4} \frac{1}{s} N_c \int d^2x d^2y d^2b_1 e^{-ik\cdot(x-y)} \left(\frac{\underline{x}-\underline{b}_1}{|\underline{x}-\underline{b}_1|^2} - \frac{\underline{x}-\underline{b}_0}{|\underline{x}-\underline{b}_0|^2} \right) \cdot \frac{\underline{y}-\underline{b}_1}{|\underline{y}-\underline{b}_1|^2} G_{\underline{b}_1,\underline{x}}^{\text{adj}}(2k^-p_1^+), \tag{C4}
\end{aligned}$$

where we have employed cancellations of some of the contributions with parts of $(E_1+E_0)A_{\text{eik}}^*+c.c.$, which, in turn, is

$$\begin{aligned}
\frac{d\sigma^{(E_1+E_0)A_{\text{eik}}^*+c.c.}(\lambda)}{d^2k_T dy} &= -\frac{\lambda}{N_c^2-1} \frac{4\alpha_s}{(2\pi)^4} \int d^2x d^2y d^2b_1 e^{-ik\cdot(x-y)} \left\langle \left[(T^a U_{\underline{b}_1}^{\text{G}[1]} U_{\underline{b}_0}^\dagger)^{cd} \frac{\underline{x}-\underline{b}_1}{|\underline{x}-\underline{b}_1|^2} - (U_{\underline{b}_1}^{\text{G}[1]} U_{\underline{b}_0}^\dagger T^a)^{cd} \right. \right. \\
&\times \left. \left. \frac{\underline{x}-\underline{b}_0}{|\underline{x}-\underline{b}_0|^2} \right] \cdot \left[\left[(U_{\underline{y}})^{ac} - (U_{\underline{b}_1})^{ac} \right] \frac{\underline{y}-\underline{b}_1}{|\underline{y}-\underline{b}_1|^2} - \left[(U_{\underline{y}})^{ac} - (U_{\underline{b}_0})^{ac} \right] \frac{\underline{y}-\underline{b}_0}{|\underline{y}-\underline{b}_0|^2} \right] (U_{\underline{b}_1} T^{*c} U_{\underline{b}_0}^\dagger)^{cd} \right\rangle + \text{c.c.} \\
&= -\frac{\lambda N_c}{N_c^2-1} \frac{2\alpha_s}{(2\pi)^4} \int d^2x d^2y d^2b_1 e^{-ik\cdot(x-y)} \left\{ \frac{\underline{x}-\underline{b}_1}{|\underline{x}-\underline{b}_1|^2} \cdot \left(\frac{\underline{y}-\underline{b}_1}{|\underline{y}-\underline{b}_1|^2} - \frac{\underline{y}-\underline{b}_0}{|\underline{y}-\underline{b}_0|^2} \right) \left\langle \text{Tr} \left[U_{\underline{y}}^\dagger U_{\underline{b}_1}^{\text{G}[1]} \right] \right\rangle \right. \\
&+ \left. \left(\frac{\underline{x}-\underline{b}_1}{|\underline{x}-\underline{b}_1|^2} \cdot \frac{\underline{y}-\underline{b}_0}{|\underline{y}-\underline{b}_0|^2} + \frac{\underline{x}-\underline{b}_0}{|\underline{x}-\underline{b}_0|^2} \cdot \frac{\underline{y}-\underline{b}_1}{|\underline{y}-\underline{b}_1|^2} \right) \left\langle \text{Tr} \left[U_{\underline{b}_0}^\dagger U_{\underline{b}_1}^{\text{G}[1]} \right] \right\rangle \right\} + \text{c.c.} \\
&= -\lambda \frac{\alpha_s}{4\pi^4} \frac{1}{s} N_c \int d^2x d^2y d^2b_1 e^{-ik\cdot(x-y)} \left\{ \frac{\underline{x}-\underline{b}_1}{|\underline{x}-\underline{b}_1|^2} \cdot \left(\frac{\underline{y}-\underline{b}_1}{|\underline{y}-\underline{b}_1|^2} - \frac{\underline{y}-\underline{b}_0}{|\underline{y}-\underline{b}_0|^2} \right) G_{\underline{b}_1,\underline{y}}^{\text{adj}}(2k^-p_1^+) \right. \\
&+ \left. \left(\frac{\underline{x}-\underline{b}_1}{|\underline{x}-\underline{b}_1|^2} \cdot \frac{\underline{y}-\underline{b}_0}{|\underline{y}-\underline{b}_0|^2} + \frac{\underline{x}-\underline{b}_0}{|\underline{x}-\underline{b}_0|^2} \cdot \frac{\underline{y}-\underline{b}_1}{|\underline{y}-\underline{b}_1|^2} \right) G_{\underline{b}_1,\underline{b}_0}^{\text{adj}}(2k^-p_1^+) \right\}. \tag{C5}
\end{aligned}$$

Assembling all the above contributions together and adding Eq. (A3) with $\underline{b} \rightarrow \underline{b}_1$ to account for the UV-divergent terms calculated in Appendix A (such that $|\underline{b}'_1 - \underline{b}_1|^2 = 1/(2k^+p_2^-)$) yields

$$\begin{aligned}
\frac{d\sigma(\lambda)}{d^2k_T dy} &= \lambda \frac{\alpha_s}{4\pi^4} \frac{1}{s} N_c \int d^2x d^2y d^2b_1 e^{-ik\cdot(x-y)} \\
&\times \left\{ \frac{\underline{x}-\underline{b}_1}{|\underline{x}-\underline{b}_1|^2} \cdot \frac{\underline{y}-\underline{b}_1}{|\underline{y}-\underline{b}_1|^2} \left[4G_{\underline{x},\underline{y}}^{\text{adj}}(2k^-p_1^+) - 4G_{\underline{x},\underline{b}_1}^{\text{adj}}(2k^-p_1^+) - G_{\underline{b}_1,\underline{y}}^{\text{adj}}(2k^-p_1^+) - G_{\underline{b}_1,\underline{x}}^{\text{adj}}(2k^-p_1^+) + 2G_{\underline{b}_1,\underline{b}_1}^{\text{adj}}(2k^-p_1^+) \right] \right.
\end{aligned}$$

$$\begin{aligned}
& - \frac{\underline{x} - \underline{b}_1}{|\underline{x} - \underline{b}_1|^2} \cdot \frac{\underline{y} - \underline{b}_0}{|\underline{y} - \underline{b}_0|^2} \left[2 G_{\underline{x}, \underline{y}}^{\text{adj}}(2k^- p_1^+) - 2 G_{\underline{x}, \underline{b}_0}^{\text{adj}}(2k^- p_1^+) - G_{\underline{b}_1, \underline{y}}^{\text{adj}}(2k^- p_1^+) + G_{\underline{b}_1, \underline{b}_0}^{\text{adj}}(2k^- p_1^+) \right] \\
& - \frac{\underline{x} - \underline{b}_0}{|\underline{x} - \underline{b}_0|^2} \cdot \frac{\underline{y} - \underline{b}_1}{|\underline{y} - \underline{b}_1|^2} \left[2 G_{\underline{x}, \underline{y}}^{\text{adj}}(2k^- p_1^+) - 2 G_{\underline{x}, \underline{b}_1}^{\text{adj}}(2k^- p_1^+) - G_{\underline{b}_1, \underline{x}}^{\text{adj}}(2k^- p_1^+) + G_{\underline{b}_1, \underline{b}_0}^{\text{adj}}(2k^- p_1^+) \right] \\
& - 8i k^j \frac{\underline{x} - \underline{b}_1}{|\underline{x} - \underline{b}_1|^2} \times \frac{\underline{y} - \underline{b}_1}{|\underline{y} - \underline{b}_1|^2} G_{\underline{x}, \underline{b}_1}^{\text{adj}}(2k^- p_1^+) + 4i k^j \frac{\underline{x} - \underline{b}_1}{|\underline{x} - \underline{b}_1|^2} \times \frac{\underline{y} - \underline{b}_0}{|\underline{y} - \underline{b}_0|^2} G_{\underline{x}, \underline{b}_0}^{\text{adj}}(2k^- p_1^+) \\
& + 4i k^j \frac{\underline{x} - \underline{b}_0}{|\underline{x} - \underline{b}_0|^2} \times \frac{\underline{y} - \underline{b}_1}{|\underline{y} - \underline{b}_1|^2} G_{\underline{x}, \underline{b}_1}^{\text{adj}}(2k^- p_1^+) \Big\}. \tag{C6}
\end{aligned}$$

We see that the inclusive gluon production cross section (C6) is expressed in terms of the polarized dipole amplitudes G_T^{adj} and $G_T^{i\text{adj}}$. Since the amplitudes $G_T^{i\text{adj}}$ enter Eq. (C6) multiplied by the cross-product, which contains ϵ^{ij} , we need another Levy-Civita symbol for the term to survive. The decomposition Eq. (33b) indicates that only the dipole amplitude G_{2T}^{adj} comes in with the needed Levy-Civita symbol. We thus conclude that the inclusive gluon production cross section (C6) for the \mathcal{F}^{21} -type gluon dipole projectile is expressed in terms of G_T^{adj} and G_{2T}^{adj} .

2. $(\mathcal{G}^i - \tilde{\mathcal{G}}^i)$ -type dipole projectile

Next we consider inclusive gluon production for the projectile dipole with a type-2 operator. That is, we consider the same diagrams in Fig. 7, except that now the black circles of the diagrams A, C and F come in with the $(\mathcal{G}^i - \tilde{\mathcal{G}}^i)$ operator (and with the prefactor) from Eq. (17). The white boxes in diagrams D_1, D_0, E_1 and E_0 denote $U^{iG[2]}$, while the same boxes in diagrams B_1 and B_0 still denote the entire sub-eikonal polarized Wilson line. This means that all diagrams, when squared, give contributions which carry a transverse index i , which we will use to distinguish them from the diagrams in the previous Subsection of this Appendix.

Our goal here is to show that even for the projectile being a dipole with a type-2 sub-eikonal operator, the corresponding cross section would still depend only on G_T^{adj} and G_{2T}^{adj} . We demonstrate this by an explicit calculation. Similar to the above we write³

$$\begin{aligned}
\frac{d\sigma^{A^i A_{\text{eik}}^* + \text{c.c.}}}{d^2 k_T dy} &= \frac{\alpha_s}{(2\pi)^4} \frac{k^-}{p_2^-} \frac{N_c}{N_c^2 - 1} \int d^2 x d^2 y d^2 b_1 e^{-ik \cdot (\underline{x} - \underline{y})} \sum_{m=0}^1 (-1)^{m+1} \tag{C7} \\
& \left\{ \epsilon^{kj} \left(\delta^{ik} - \frac{2(x - b_1)^i (x - b_1)^k}{|\underline{x} - \underline{b}_1|^2} \right) \frac{(y - b_m)^j}{|\underline{y} - \underline{b}_m|^2} \left\langle \text{Tr} \left[U_{\underline{y}}^\dagger U_{\underline{x}}^{G[1]} \right] - \text{Tr} \left[U_{\underline{b}_m}^\dagger U_{\underline{x}}^{G[1]} \right] \right\rangle \right. \\
& \left. - i \int d^2 x' \left(\delta^{ij} - \frac{2(x' - b_1)^i (x' - b_1)^j}{|\underline{x}' - \underline{b}_1|^2} \right) \frac{(y - b_m)^j}{|\underline{y} - \underline{b}_m|^2} \left\langle \text{Tr} \left[U_{\underline{y}}^\dagger U_{\underline{x}, \underline{x}'}^{G[2]} \right] - \text{Tr} \left[U_{\underline{b}_m}^\dagger U_{\underline{x}, \underline{x}'}^{G[2]} \right] \right\rangle \right\} + \text{c.c.}
\end{aligned}$$

The $m = 1$ term vanishes for the following reason: $U_{\underline{x}}^{G[1]}$ is real, while $U_{\underline{x}, \underline{x}'}^{G[2]}$ is imaginary. Hence, the first correlator in (C7) is real, and “ i ” times the second one is real too. The object in the curly brackets of (C7) is, therefore, also real, and has one Lorentz index i . Integration over the impact parameters yields, for $m = 1$,

$$\int d^2 b_1 d^2 \left(\frac{\underline{x} + \underline{y}}{2} \right) \{ \dots \}_{m=1}^i = (x - y)^i f_1 [(\underline{x} - \underline{y})^2] + \epsilon^{im} (x - y)^m f_2 [(\underline{x} - \underline{y})^2] \tag{C8}$$

with some real functions f_1 and f_2 . Fourier-transforming Eq. (C8) yields a purely imaginary expression, which is cancelled in Eq. (C7) when we add the complex conjugate term.

We are left with the $m = 0$ term in Eq. (C7) giving

$$\begin{aligned}
\frac{d\sigma^{A^i A_{\text{eik}}^* + \text{c.c.}}}{d^2 k_T dy} &= - \frac{\alpha_s}{(2\pi)^4} \frac{k^-}{p_2^-} \frac{N_c}{N_c^2 - 1} \int d^2 x d^2 y d^2 b_1 e^{-ik \cdot (\underline{x} - \underline{y})} \left\{ \epsilon^{kj} \left(\delta^{ik} - \frac{2(x - b_1)^i (x - b_1)^k}{|\underline{x} - \underline{b}_1|^2} \right) \frac{(y - b_0)^j}{|\underline{y} - \underline{b}_0|^2} \right. \tag{C9} \\
& \left. \left\langle \text{Tr} \left[U_{\underline{y}}^\dagger U_{\underline{x}}^{G[1]} \right] - \text{Tr} \left[U_{\underline{b}_0}^\dagger U_{\underline{x}}^{G[1]} \right] \right\rangle - i \int d^2 x' \left(\delta^{ij} - \frac{2(x' - b_1)^i (x' - b_1)^j}{|\underline{x}' - \underline{b}_1|^2} \right) \frac{(y - b_0)^j}{|\underline{y} - \underline{b}_0|^2} \right.
\end{aligned}$$

³ Indeed it is not quite right to call the object in Eq. (C7) a cross section, since the projectile here is not a physical object, but a dipole made with the (17) polarized Wilson line, which carries a transverse index i . We will proceed with this notation, however, with the understanding that this cross section has to be convoluted with some i -dependent function describing how the polarized Wilson line (17) arises in the projectile through small- x evolution.

$$\times \left\langle \text{Tr} \left[U_{\underline{y}}^\dagger U_{\underline{x}, \underline{x}'}^{\text{G}[2]} \right] - \text{Tr} \left[U_{\underline{b}_0}^\dagger U_{\underline{x}, \underline{x}'}^{\text{G}[2]} \right] \right\rangle + \text{c.c.}$$

Next we look at the interference of B with $C^i + F^i$,

$$\begin{aligned} \frac{d\sigma^{B(C^{i*}+F^{i*})+\text{c.c.}}}{d^2k_T dy} &= \frac{\alpha_s}{(2\pi)^4} \frac{k^-}{p_2^-} \frac{N_c}{N_c^2 - 1} \int d^2x d^2y d^2b_1 e^{-ik \cdot (\underline{x}-\underline{y})} \sum_{m=0}^1 (-1)^{m+1} \\ &\times \left\{ \epsilon^{kj} \left(\delta^{ik} - \frac{2(y-b_1)^i (y-b_1)^k}{|\underline{y}-\underline{b}_1|^2} \right) \frac{(x-b_m)^j}{|\underline{x}-\underline{b}_m|^2} \left\langle \text{Tr} \left[U_{\underline{y}}^\dagger U_{\underline{x}}^{\text{G}[1]} \right] - \text{Tr} \left[U_{\underline{b}_1}^\dagger U_{\underline{x}}^{\text{G}[1]} \right] \right\rangle \right. \\ &+ i \int d^2x' \left(\delta^{ij} - \frac{2(y-b_1)^i (y-b_1)^j}{|\underline{y}-\underline{b}_1|^2} \right) \frac{(x'-b_m)^j}{|\underline{x}'-\underline{b}_m|^2} \left\langle \text{Tr} \left[U_{\underline{y}}^\dagger U_{\underline{x}, \underline{x}'}^{\text{G}[2]} \right] - \text{Tr} \left[U_{\underline{b}_1}^\dagger U_{\underline{x}, \underline{x}'}^{\text{G}[2]} \right] \right\rangle \left. \right\} + \text{c.c.} \\ &= -\frac{\alpha_s}{(2\pi)^4} \frac{k^-}{p_2^-} \frac{N_c}{N_c^2 - 1} \int d^2x d^2y d^2b_1 e^{-ik \cdot (\underline{x}-\underline{y})} \\ &\times \left\{ \epsilon^{kj} \left(\delta^{ik} - \frac{2(y-b_1)^i (y-b_1)^k}{|\underline{y}-\underline{b}_1|^2} \right) \frac{(x-b_0)^j}{|\underline{x}-\underline{b}_0|^2} \left\langle \text{Tr} \left[U_{\underline{y}}^\dagger U_{\underline{x}}^{\text{G}[1]} \right] - \text{Tr} \left[U_{\underline{b}_1}^\dagger U_{\underline{x}}^{\text{G}[1]} \right] \right\rangle \right. \\ &+ i \int d^2x' \left(\delta^{ij} - \frac{2(y-b_1)^i (y-b_1)^j}{|\underline{y}-\underline{b}_1|^2} \right) \frac{(x'-b_0)^j}{|\underline{x}'-\underline{b}_0|^2} \left\langle \text{Tr} \left[U_{\underline{y}}^\dagger U_{\underline{x}, \underline{x}'}^{\text{G}[2]} \right] - \text{Tr} \left[U_{\underline{b}_1}^\dagger U_{\underline{x}, \underline{x}'}^{\text{G}[2]} \right] \right\rangle \left. \right\} + \text{c.c.} \end{aligned} \quad (\text{C10})$$

Let us take a closer look at the $U_{\underline{x}, \underline{x}'}^{\text{G}[2]}$ -containing terms in the above expressions. In doing so, let us assume that the cross sections we are calculating will be convoluted with

$$\int d^2b_{10} \epsilon^{ii'} b_{10}^{i'} f(b_{10}^2), \quad (\text{C11})$$

where $f(b_{10}^2)$ is some real-valued function. Indeed, after integrating over the impact parameters (transverse positions) of the (evolved) projectile, we would be left with some function of b_{10} with one transverse index i , necessitating the form in Eq. (C11). Since the Levi-Civita symbol always appears in helicity calculations, we have included it into Eq. (C11).

We are interested in the following object

$$\begin{aligned} &\int d^2b_{10} \epsilon^{ii'} b_{10}^{i'} f(b_{10}^2) \left[\frac{d\sigma^{A^i A_{\text{eik}}^* + \text{c.c.}}}{d^2k_T dy} + \frac{d\sigma^{B(C^{i*}+F^{i*})+\text{c.c.}}}{d^2k_T dy} \right]_{U_{\underline{x}, \underline{x}'}^{\text{G}[2]} \text{-terms}} = i \frac{\alpha_s}{(2\pi)^4} \frac{k^-}{p_2^-} \frac{N_c}{N_c^2 - 1} \int d^2b_{10} \epsilon^{ii'} b_{10}^{i'} f(b_{10}^2) \\ &\times \int d^2x d^2y d^2b_1 e^{-ik \cdot (\underline{x}-\underline{y})} \left\{ \int d^2x' \left(\delta^{ij} - \frac{2(x'-b_1)^i (x'-b_1)^j}{|\underline{x}'-\underline{b}_1|^2} \right) \frac{(y-b_0)^j}{|\underline{y}-\underline{b}_0|^2} \left\langle \text{Tr} \left[\left(U_{\underline{y}}^\dagger - U_{\underline{b}_0}^\dagger \right) U_{\underline{x}, \underline{x}'}^{\text{G}[2]} \right] \right\rangle \right. \\ &\left. - \int d^2x' \left(\delta^{ij} - \frac{2(y-b_1)^i (y-b_1)^j}{|\underline{y}-\underline{b}_1|^2} \right) \frac{(x'-b_0)^j}{|\underline{x}'-\underline{b}_0|^2} \left\langle \text{Tr} \left[\left(U_{\underline{y}}^\dagger - U_{\underline{b}_1}^\dagger \right) U_{\underline{x}, \underline{x}'}^{\text{G}[2]} \right] \right\rangle \right\} + \text{c.c.} \end{aligned} \quad (\text{C12})$$

We will next follow the calculations in [4] and in Appendix A of [127]. Writing

$$\delta^{ij} - \frac{2(x'-b_1)^i (x'-b_1)^j}{|\underline{x}'-\underline{b}_1|^2} = -4\pi \int \frac{d^2q}{(2\pi)^2} e^{iq \cdot (\underline{x}'-\underline{b}_1)} \frac{1}{q_\perp^2} \left[\delta^{ij} - \frac{2q^i q^j}{q_\perp^2} \right], \quad (\text{C13a})$$

$$\frac{(y-b_0)^j}{|\underline{y}-\underline{b}_0|^2} = -2\pi i \int \frac{d^2l}{(2\pi)^2} e^{il \cdot (\underline{y}-\underline{b}_0)} \frac{l^j}{l_\perp^2} \quad (\text{C13b})$$

and using the definition (5c) of $U_{\underline{x}, \underline{x}'}^{\text{G}[2]}$ we get

$$\begin{aligned} &\int d^2b_{10} \epsilon^{ii'} b_{10}^{i'} f(b_{10}^2) \left[\frac{d\sigma^{A^i A_{\text{eik}}^* + \text{c.c.}}}{d^2k_T dy} + \frac{d\sigma^{B(C^{i*}+F^{i*})+\text{c.c.}}}{d^2k_T dy} \right]_{U_{\underline{x}, \underline{x}'}^{\text{G}[2]} \text{-terms}} = i \frac{\alpha_s}{(2\pi)^4} \frac{k^-}{p_2^-} \frac{N_c}{N_c^2 - 1} \int d^2b_{10} \epsilon^{ii'} b_{10}^{i'} f(b_{10}^2) \\ &\times \frac{2(2\pi)^2}{2k^-} \int_{-\infty}^{\infty} dz^- \int d^2x d^2y d^2b_1 e^{-ik \cdot (\underline{x}-\underline{y})} \left\{ \int \frac{d^2q}{(2\pi)^2} e^{iq \cdot (\underline{x}-\underline{b}_1)} \frac{1}{q_\perp^2} \left[\delta^{ij} - \frac{2q^i q^j}{q_\perp^2} \right] \int \frac{d^2l}{(2\pi)^2} e^{il \cdot (\underline{y}-\underline{b}_0)} \frac{l^j}{l_\perp^2} \right. \\ &\times \left[\left\langle \text{Tr} \left[\left(U_{\underline{y}}^\dagger - U_{\underline{b}_0}^\dagger \right) \left((\mathcal{D}^p + i k^p) U_{\underline{x}}[\infty, z^-] \right) \left((\mathcal{D}^p - i q^p) U_{\underline{x}}[z^-, -\infty] \right) \right] \right\rangle \right. \end{aligned}$$

$$\begin{aligned}
& + \left\langle \text{Tr} \left[\left(U_{\underline{y}} - U_{b_0} \right) \left((\mathcal{D}^p - i q^p) U_{\underline{x}}[-\infty, z^-] \right) \left((\mathcal{D}^p + i k^p) U_{\underline{x}}[z^-, \infty] \right) \right] \right\rangle \\
& - \int \frac{d^2 q}{(2\pi)^2} e^{iq \cdot (\underline{y} - b_1)} \frac{1}{q_{\perp}^2} \left[\delta^{ij} - \frac{2q^i q^j}{q_{\perp}^2} \right] \int \frac{d^2 l}{(2\pi)^2} e^{il \cdot (\underline{x} - b_0)} \frac{l^j}{l_{\perp}^2} \\
& \times \left[\left\langle \text{Tr} \left[\left(U_{\underline{y}}^{\dagger} - U_{b_1}^{\dagger} \right) \left((\mathcal{D}^p + i k^p) U_{\underline{x}}[\infty, z^-] \right) \left((\mathcal{D}^p - i l^p) U_{\underline{x}}[z^-, -\infty] \right) \right] \right\rangle \right. \\
& \left. + \left\langle \text{Tr} \left[\left(U_{\underline{y}} - U_{b_1} \right) \left((\mathcal{D}^i - i l^i) U_{\underline{x}}[-\infty, z^-] \right) \left((\mathcal{D}^p + i k^p) U_{\underline{x}}[z^-, \infty] \right) \right] \right\rangle \right] \Bigg\}, \tag{C14}
\end{aligned}$$

where we explicitly show the c.c. terms, having employed the fact that the cross section, along with each term in the above expression, are symmetric under $\underline{k} \rightarrow -\underline{k}$: this simplified the complex conjugation.

Now, let us employ the passive PT transformation. Under this transformation we have

$$U_{\underline{x}} \xrightarrow{\text{PT}} U_{-\underline{x}}^{\dagger}, \quad U_{\underline{x}}[\infty, z^-] \xrightarrow{\text{PT}} U_{-\underline{x}}[-\infty, -z^-], \quad U_{\underline{x}}[z^-, -\infty] \xrightarrow{\text{PT}} U_{-\underline{x}}[-z^-, \infty], \quad \int_{-\infty}^{\infty} dz^- \xrightarrow{\text{PT}} \int_{\infty}^{-\infty} dz^-. \tag{C15}$$

Note that the sign of the integration variables can always be reverted, compensating for the sign change in the integrand due to PT transformation: for instance, in the arguments of Wilson lines in Eq. (C15) we have $\underline{x} \xrightarrow{\text{PT}} -\underline{x}$, which can be eliminated by redefining the integration variable $\underline{x} \rightarrow -\underline{x}$, generating no overall minus sign. Therefore, one needs to pay attention to the sign change in the integration limits only.

Under such a passive PT transformation, Eq. (C14) becomes

$$\begin{aligned}
& \int d^2 b_{10} \epsilon^{ii'} b_{10}^{i'} f(b_{10}^2) \left[\frac{d\sigma^{A^i A_{\text{eik}}^* + \text{c.c.}}}{d^2 k_T dy} + \frac{d\sigma^{B^{(C^{i*} + F^{i*}) + \text{c.c.}}}}{d^2 k_T dy} \right]_{U_{\underline{x}, \underline{x}'}^{G[2]} \text{-terms}} \xrightarrow{\text{PT}} -i \frac{\alpha_s}{(2\pi)^4} \frac{k^-}{p_2^-} \frac{N_c}{N_c^2 - 1} \int d^2 b_{10} \epsilon^{ii'} b_{10}^{i'} f(b_{10}^2) \\
& \times \frac{2(2\pi)^2}{2k^-} \int_{-\infty}^{\infty} dz^- \int d^2 x d^2 y d^2 b_1 e^{-ik \cdot (\underline{x} - \underline{y})} \left\{ \int \frac{d^2 q}{(2\pi)^2} e^{iq \cdot (\underline{x} - b_1)} \frac{1}{q_{\perp}^2} \left[\delta^{ij} - \frac{2q^i q^j}{q_{\perp}^2} \right] \int \frac{d^2 l}{(2\pi)^2} e^{il \cdot (\underline{y} - b_0)} \frac{l^j}{l_{\perp}^2} \right. \\
& \times \left[\left\langle \text{Tr} \left[\left(U_{\underline{y}} - U_{b_0} \right) \left((\mathcal{D}^p + i k^p) U_{\underline{x}}[-\infty, z^-] \right) \left((\mathcal{D}^p - i q^p) U_{\underline{x}}[z^-, \infty] \right) \right] \right\rangle \right. \\
& \left. + \left\langle \text{Tr} \left[\left(U_{\underline{y}}^{\dagger} - U_{b_0}^{\dagger} \right) \left((\mathcal{D}^p - i q^p) U_{\underline{x}}[\infty, z^-] \right) \left((\mathcal{D}^p + i k^p) U_{\underline{x}}[z^-, -\infty] \right) \right] \right\rangle \right] \\
& - \int \frac{d^2 q}{(2\pi)^2} e^{iq \cdot (\underline{y} - b_1)} \frac{1}{q_{\perp}^2} \left[\delta^{ij} - \frac{2q^i q^j}{q_{\perp}^2} \right] \int \frac{d^2 l}{(2\pi)^2} e^{il \cdot (\underline{x} - b_0)} \frac{l^j}{l_{\perp}^2} \\
& \times \left[\left\langle \text{Tr} \left[\left(U_{\underline{y}} - U_{b_1} \right) \left((\mathcal{D}^p + i k^p) U_{\underline{x}}[-\infty, z^-] \right) \left((\mathcal{D}^p - i l^p) U_{\underline{x}}[z^-, \infty] \right) \right] \right\rangle \right. \\
& \left. + \left\langle \text{Tr} \left[\left(U_{\underline{y}}^{\dagger} - U_{b_1}^{\dagger} \right) \left((\mathcal{D}^p - i l^p) U_{\underline{x}}[\infty, z^-] \right) \left((\mathcal{D}^p + i k^p) U_{\underline{x}}[z^-, -\infty] \right) \right] \right\rangle \right] \Bigg\}. \tag{C16}
\end{aligned}$$

Comparing Eqs. (C16) and (C14), we see that the terms containing $\mathcal{D}^p \mathcal{D}^p$, $q^p k^p$, and $l^p k^p$ are PT-odd (note the overall sign change between these two equations). Since the cross section (and the double spin asymmetry A_{LL}) should be PT-even, such terms must be zero. Therefore, we drop them. Concentrating on the terms containing one power of momentum and one covariant derivative, we see that the first trace in Eq. (C14) contains

$$ik^p \mathcal{D}^p - iq^p \tilde{\mathcal{D}}^p = \frac{i}{2} (k^p + q^p) \left(\mathcal{D}^p - \tilde{\mathcal{D}}^p \right) + \frac{i}{2} (k^p - q^p) \left(\mathcal{D}^p + \tilde{\mathcal{D}}^p \right). \tag{C17}$$

This term should be compared to that contained in the second trace of Eq. (C16), which, otherwise, has the same Wilson line structure as the first trace in Eq. (C14),

$$ik^p \tilde{\mathcal{D}}^p - iq^p \mathcal{D}^p = -\frac{i}{2} (k^p + q^p) \left(\mathcal{D}^p - \tilde{\mathcal{D}}^p \right) + \frac{i}{2} (k^p - q^p) \left(\mathcal{D}^p + \tilde{\mathcal{D}}^p \right). \tag{C18}$$

Combining this with the overall sign change between Eqs. (C16) and (C14), we conclude that the $\frac{i}{2} (k^p + q^p) \left(\mathcal{D}^p - \tilde{\mathcal{D}}^p \right)$ term is PT-even and should be kept, while the $\frac{i}{2} (k^p - q^p) \left(\mathcal{D}^p + \tilde{\mathcal{D}}^p \right)$ term is PT-odd and should be zero: we can neglect this term.

Applying similar treatment to other terms in Eqs. (C16) and (C14) containing one power of momentum and one covariant derivative, we arrive at

$$\begin{aligned}
& \int d^2 b_{10} \epsilon^{ii'} b_{10}^{i'} f(b_{10}^2) \left[\frac{d\sigma^{A^i A_{\text{eik}}^* + \text{C.C.}}}{d^2 k_T dy} + \frac{d\sigma^{B(C^{i*} + F^{i*}) + \text{C.C.}}}{d^2 k_T dy} \right]_{U_{\underline{x}, \underline{x}'}^{\text{G}[2]} \text{-terms}} = i \frac{\alpha_s}{(2\pi)^4} \frac{k^-}{p_2^-} \frac{N_c}{N_c^2 - 1} \int d^2 b_{10} \epsilon^{ii'} b_{10}^{i'} f(b_{10}^2) \\
& \times \frac{2(2\pi)^2}{2k^-} \int_{-\infty}^{\infty} dz^- \int d^2 x d^2 y d^2 b_1 e^{-ik \cdot (\underline{x} - \underline{y})} \left\{ \int \frac{d^2 q}{(2\pi)^2} e^{iq \cdot (\underline{x} - b_1)} \frac{1}{q_1^2} \left[\delta^{ij} - \frac{2q^i q^j}{q_1^2} \right] \int \frac{d^2 l}{(2\pi)^2} e^{il \cdot (\underline{y} - b_0)} \frac{l^j}{l_1^2} \right. \\
& \times \left[\frac{i}{2} (k^p + q^p) \left\langle \text{Tr} \left[\left(U_{\underline{y}}^\dagger - U_{b_0}^\dagger \right) U_{\underline{x}}[\infty, z^-] \left(\mathcal{D}^p - \tilde{\mathcal{D}}^p \right) U_{\underline{x}}[z^-, -\infty] \right] \right\rangle \right. \\
& \left. - \frac{i}{2} (k^p + q^p) \left\langle \text{Tr} \left[\left(U_{\underline{y}} - U_{b_0} \right) U_{\underline{x}}[-\infty, z^-] \left(\mathcal{D}^p - \tilde{\mathcal{D}}^p \right) U_{\underline{x}}[z^-, \infty] \right] \right\rangle \right] \\
& - \int \frac{d^2 q}{(2\pi)^2} e^{iq \cdot (\underline{y} - b_1)} \frac{1}{q_1^2} \left[\delta^{ij} - \frac{2q^i q^j}{q_1^2} \right] \int \frac{d^2 l}{(2\pi)^2} e^{il \cdot (\underline{x} - b_0)} \frac{l^j}{l_1^2} \\
& \times \left[\frac{i}{2} (k^p + l^p) \left\langle \text{Tr} \left[\left(U_{\underline{y}}^\dagger - U_{b_1}^\dagger \right) U_{\underline{x}}[\infty, z^-] \left(\mathcal{D}^p - \tilde{\mathcal{D}}^p \right) U_{\underline{x}}[z^-, -\infty] \right] \right\rangle \right. \\
& \left. - \frac{i}{2} (k^p + l^p) \left\langle \text{Tr} \left[\left(U_{\underline{y}} - U_{b_1} \right) U_{\underline{x}}[-\infty, z^-] \left(\mathcal{D}^p - \tilde{\mathcal{D}}^p \right) U_{\underline{x}}[z^-, \infty] \right] \right\rangle \right\}, \tag{C19}
\end{aligned}$$

which we can rewrite using the definition of $U_{\underline{x}}^{\text{G}[2]}$ in Eq. (17) as

$$\begin{aligned}
& \int d^2 b_{10} \epsilon^{ii'} b_{10}^{i'} f(b_{10}^2) \left[\frac{d\sigma^{A^i A_{\text{eik}}^* + \text{C.C.}}}{d^2 k_T dy} + \frac{d\sigma^{B(C^{i*} + F^{i*}) + \text{C.C.}}}{d^2 k_T dy} \right]_{U_{\underline{x}, \underline{x}'}^{\text{G}[2]} \text{-terms}} = -\frac{\alpha_s}{(2\pi)^4} \frac{k^-}{p_2^-} \frac{N_c}{N_c^2 - 1} \int d^2 b_{10} \epsilon^{ii'} b_{10}^{i'} f(b_{10}^2) \\
& \times 2(2\pi)^2 \int d^2 x d^2 y d^2 b_1 e^{-ik \cdot (\underline{x} - \underline{y})} \left\{ \int \frac{d^2 q}{(2\pi)^2} e^{iq \cdot (\underline{x} - b_1)} \frac{1}{q_1^2} \left[\delta^{ij} - \frac{2q^i q^j}{q_1^2} \right] (k^p + q^p) \int \frac{d^2 l}{(2\pi)^2} e^{il \cdot (\underline{y} - b_0)} \frac{l^j}{l_1^2} \right. \\
& \times \left[\left\langle \text{Tr} \left[\left(U_{\underline{y}}^\dagger - U_{b_0}^\dagger \right) U_{\underline{x}}^{\text{G}[2]} \right] \right\rangle + \left\langle \text{Tr} \left[\left(U_{\underline{y}} - U_{b_0} \right) \left(U_{\underline{x}}^{\text{G}[2]} \right)^\dagger \right] \right\rangle \right] \\
& - \int \frac{d^2 q}{(2\pi)^2} e^{iq \cdot (\underline{y} - b_1)} \frac{1}{q_1^2} \left[\delta^{ij} - \frac{2q^i q^j}{q_1^2} \right] \int \frac{d^2 l}{(2\pi)^2} e^{il \cdot (\underline{x} - b_0)} \frac{l^j}{l_1^2} (k^p + l^p) \\
& \times \left[\left\langle \text{Tr} \left[\left(U_{\underline{y}}^\dagger - U_{b_1}^\dagger \right) U_{\underline{x}}^{\text{G}[2]} \right] \right\rangle + \left\langle \text{Tr} \left[\left(U_{\underline{y}} - U_{b_1} \right) \left(U_{\underline{x}}^{\text{G}[2]} \right)^\dagger \right] \right\rangle \right] \left. \right\}. \tag{C20}
\end{aligned}$$

Note that in our expressions here we did not explicitly include the time-ordering and anti-time-ordering signs T and $\bar{\text{T}}$. Since each term in, say, Eq. (C14) contains both the operators from the scattering amplitude and from the complex conjugate amplitude, some of the operators in each term should be time-ordered, while others should be anti-time-ordered. While strictly-speaking we should keep track of such (anti-)time-ordering, since both the PT transformation and the complex conjugation interchange the two orderings, $\text{T} \leftrightarrow \bar{\text{T}}$, our above argument would be unaffected by using the more lengthy notation with T and $\bar{\text{T}}$.

We can rewrite Eq. (C20) as

$$\begin{aligned}
& \int d^2 b_{10} \epsilon^{ii'} b_{10}^{i'} f(b_{10}^2) \left[\frac{d\sigma^{A^i A_{\text{eik}}^* + \text{C.C.}}}{d^2 k_T dy} + \frac{d\sigma^{B(C^{i*} + F^{i*}) + \text{C.C.}}}{d^2 k_T dy} \right]_{U_{\underline{x}, \underline{x}'}^{\text{G}[2]} \text{-terms}} = -\frac{\alpha_s N_c}{(2\pi)^4} \frac{1}{s} \int d^2 b_{10} \epsilon^{ii'} b_{10}^{i'} f(b_{10}^2) \\
& \times 4(2\pi)^2 \int d^2 x d^2 y d^2 b_1 e^{-ik \cdot (\underline{x} - \underline{y})} \left\{ \int \frac{d^2 q}{(2\pi)^2} e^{iq \cdot (\underline{x} - b_1)} \frac{1}{q_1^2} \left[\delta^{ij} - \frac{2q^i q^j}{q_1^2} \right] (k^p + q^p) \int \frac{d^2 l}{(2\pi)^2} e^{il \cdot (\underline{y} - b_0)} \frac{l^j}{l_1^2} \right. \\
& \times \left[G_{\underline{x}, \underline{y}}^{\text{p adj}}(2k^- p_1^+) - G_{\underline{x}, b_0}^{\text{p adj}}(2k^- p_1^+) \right] \\
& \left. - \int \frac{d^2 q}{(2\pi)^2} e^{iq \cdot (\underline{y} - b_1)} \frac{1}{q_1^2} \left[\delta^{ij} - \frac{2q^i q^j}{q_1^2} \right] \int \frac{d^2 l}{(2\pi)^2} e^{il \cdot (\underline{x} - b_0)} \frac{l^j}{l_1^2} (k^p + l^p) \left[G_{\underline{x}, \underline{y}}^{\text{p adj}}(2k^- p_1^+) - G_{\underline{x}, b_1}^{\text{p adj}}(2k^- p_1^+) \right] \right\}. \tag{C21}
\end{aligned}$$

Performing the Fourier transformations we arrive at

$$\begin{aligned}
& \int d^2 b_{10} \epsilon^{ii'} b_{10}^{j'} f(b_{10}^2) \left[\frac{d\sigma^{A^i A_{\text{eik}}^* + \text{c.c.}}}{d^2 k_T dy} + \frac{d\sigma^{B^{(C^{i*} + F^{i*}) + \text{c.c.}}}}{d^2 k_T dy} \right]_{U_{\underline{x}, \underline{x}'}^{G[2]}\text{-terms}} = -\frac{\alpha_s N_c}{(2\pi)^4} \frac{1}{s} \int d^2 b_{10} \epsilon^{ii'} b_{10}^{j'} f(b_{10}^2) \\
& \times 2 \int d^2 x d^2 y d^2 b_1 e^{-ik \cdot (\underline{x} - \underline{y})} \left\{ \left[(\partial_x^p - i k^p) \left(\delta^{ij} - \frac{2(x - b_1)^i (x - b_1)^j}{|\underline{x} - \underline{b}_1|^2} \right) \right] \frac{(y - b_0)^j}{|\underline{y} - \underline{b}_0|^2} \right. \\
& \times \left[G_{\underline{x}, \underline{y}}^{p \text{ adj}}(2k^- p_1^+) - G_{\underline{x}, \underline{b}_0}^{p \text{ adj}}(2k^- p_1^+) \right] \\
& \left. - \left[(\partial_x^p - i k^p) \frac{(x - b_0)^j}{|\underline{x} - \underline{b}_0|^2} \right] \left(\delta^{ij} - \frac{2(y - b_1)^i (y - b_1)^j}{|\underline{y} - \underline{b}_1|^2} \right) \left[G_{\underline{x}, \underline{y}}^{p \text{ adj}}(2k^- p_1^+) - G_{\underline{x}, \underline{b}_1}^{p \text{ adj}}(2k^- p_1^+) \right] \right\}. \tag{C22}
\end{aligned}$$

Adding the $U_{\underline{x}}^{G[1]}$ -containing terms from Eqs. (C9) and (C10) to Eq. (C22) and dropping $\int d^2 b_{10} \epsilon^{ii'} b_{10}^{j'} f(b_{10}^2)$ in the latter yields

$$\begin{aligned}
& \frac{d\sigma^{A^i A_{\text{eik}}^* + \text{c.c.}}}{d^2 k_T dy} + \frac{d\sigma^{B^{(C^{i*} + F^{i*}) + \text{c.c.}}}}{d^2 k_T dy} = -\frac{2\alpha_s N_c}{(2\pi)^4} \frac{1}{s} \int d^2 x d^2 y d^2 b_1 e^{-ik \cdot (\underline{x} - \underline{y})} \\
& \times \left\{ \epsilon^{kj} \left(\delta^{ik} - \frac{2(y - b_1)^i (y - b_1)^k}{|\underline{y} - \underline{b}_1|^2} \right) \frac{(x - b_0)^j}{|\underline{x} - \underline{b}_0|^2} \left[G_{\underline{x}, \underline{y}}^{\text{adj}}(2k^- p_1^+) - G_{\underline{x}, \underline{b}_0}^{\text{adj}}(2k^- p_1^+) \right] \right. \\
& + \epsilon^{kj} \left(\delta^{ik} - \frac{2(x - b_1)^i (x - b_1)^k}{|\underline{x} - \underline{b}_1|^2} \right) \frac{(y - b_0)^j}{|\underline{y} - \underline{b}_0|^2} \left[G_{\underline{x}, \underline{y}}^{\text{adj}}(2k^- p_1^+) - G_{\underline{x}, \underline{b}_1}^{\text{adj}}(2k^- p_1^+) \right] \\
& \left[(\partial_x^p - i k^p) \left(\delta^{ij} - \frac{2(x - b_1)^i (x - b_1)^j}{|\underline{x} - \underline{b}_1|^2} \right) \right] \frac{(y - b_0)^j}{|\underline{y} - \underline{b}_0|^2} \left[G_{\underline{x}, \underline{y}}^{p \text{ adj}}(2k^- p_1^+) - G_{\underline{x}, \underline{b}_0}^{p \text{ adj}}(2k^- p_1^+) \right] \\
& \left. - \left[(\partial_x^p - i k^p) \frac{(x - b_0)^j}{|\underline{x} - \underline{b}_0|^2} \right] \left(\delta^{ij} - \frac{2(y - b_1)^i (y - b_1)^j}{|\underline{y} - \underline{b}_1|^2} \right) \left[G_{\underline{x}, \underline{y}}^{p \text{ adj}}(2k^- p_1^+) - G_{\underline{x}, \underline{b}_1}^{p \text{ adj}}(2k^- p_1^+) \right] \right\}. \tag{C23}
\end{aligned}$$

Indeed, everything in Eq. (C23) is expressed in terms of the polarized dipole amplitudes G_T^{adj} and $G_T^{i \text{ adj}}$.

Lastly, the $(D^i + E^i) A_{\text{eik}}^*$ terms depend on the $\mathcal{P}^p - \check{\mathcal{P}}^p$ operator by definition, that is, diagrams D^i and E^i already have the $\mathcal{P}^p - \check{\mathcal{P}}^p$ operator in the black circle. Therefore, such contribution depends on $G_T^{i \text{ adj}}$. For completeness, let us quote the $(D^i + E^i) A_{\text{eik}}^* + \text{c.c.}$ contribution, which can be read from Eqs. (C4) and (C5) by replacing $G^{\text{adj}} \rightarrow G^{i \text{ adj}}$ in them and dropping the overall factor of λ . We get

$$\begin{aligned}
& \frac{d\sigma^{D^i A_{\text{eik}}^* + \text{c.c.}}}{d^2 k_T dy} + \frac{d\sigma^{E^i A_{\text{eik}}^* + \text{c.c.}}}{d^2 k_T dy} \\
& = -\frac{\alpha_s}{4\pi^4} \frac{1}{s} N_c \int d^2 x d^2 y d^2 b_1 e^{-ik \cdot (\underline{x} - \underline{y})} \left\{ \left(\frac{\underline{x} - \underline{b}_1}{|\underline{x} - \underline{b}_1|^2} - \frac{\underline{x} - \underline{b}_0}{|\underline{x} - \underline{b}_0|^2} \right) \cdot \frac{\underline{y} - \underline{b}_1}{|\underline{y} - \underline{b}_1|^2} G_{\underline{b}_1, \underline{x}}^{i \text{ adj}}(2k^- p_1^+) \right. \\
& + \frac{\underline{x} - \underline{b}_1}{|\underline{x} - \underline{b}_1|^2} \cdot \left(\frac{\underline{y} - \underline{b}_1}{|\underline{y} - \underline{b}_1|^2} - \frac{\underline{y} - \underline{b}_0}{|\underline{y} - \underline{b}_0|^2} \right) G_{\underline{b}_1, \underline{y}}^{i \text{ adj}}(2k^- p_1^+) \\
& \left. + \left(\frac{\underline{x} - \underline{b}_1}{|\underline{x} - \underline{b}_1|^2} \cdot \frac{\underline{y} - \underline{b}_0}{|\underline{y} - \underline{b}_0|^2} + \frac{\underline{x} - \underline{b}_0}{|\underline{x} - \underline{b}_0|^2} \cdot \frac{\underline{y} - \underline{b}_1}{|\underline{y} - \underline{b}_1|^2} \right) G_{\underline{b}_1, \underline{b}_0}^{i \text{ adj}}(2k^- p_1^+) \right\}. \tag{C24}
\end{aligned}$$

Adding Eqs. (C23) and (C24) together we arrive at the final result for the polarization-independent dipole producing a gluon at the sub-eikonal order:

$$\begin{aligned}
& \frac{d\sigma^i}{d^2 k_T dy} = -\frac{\alpha_s}{4\pi^4} \frac{1}{s} N_c \int d^2 x d^2 y d^2 b_1 e^{-ik \cdot (\underline{x} - \underline{y})} \\
& \times \left\{ 2 \epsilon^{kj} \left(\delta^{ik} - \frac{2(y - b_1)^i (y - b_1)^k}{|\underline{y} - \underline{b}_1|^2} \right) \frac{(x - b_0)^j}{|\underline{x} - \underline{b}_0|^2} \left[G_{\underline{x}, \underline{y}}^{\text{adj}}(2k^- p_1^+) - G_{\underline{x}, \underline{b}_0}^{\text{adj}}(2k^- p_1^+) \right] \right. \\
& + 2 \epsilon^{kj} \left(\delta^{ik} - \frac{2(x - b_1)^i (x - b_1)^k}{|\underline{x} - \underline{b}_1|^2} \right) \frac{(y - b_0)^j}{|\underline{y} - \underline{b}_0|^2} \left[G_{\underline{x}, \underline{y}}^{\text{adj}}(2k^- p_1^+) - G_{\underline{x}, \underline{b}_1}^{\text{adj}}(2k^- p_1^+) \right] \\
& \left. 2 \left[(\partial_x^p - i k^p) \left(\delta^{ij} - \frac{2(x - b_1)^i (x - b_1)^j}{|\underline{x} - \underline{b}_1|^2} \right) \right] \frac{(y - b_0)^j}{|\underline{y} - \underline{b}_0|^2} \left[G_{\underline{x}, \underline{y}}^{p \text{ adj}}(2k^- p_1^+) - G_{\underline{x}, \underline{b}_0}^{p \text{ adj}}(2k^- p_1^+) \right] \right\}
\end{aligned}$$

$$\begin{aligned}
& - 2 \left[(\partial_x^p - i k^p) \frac{(x - b_0)^j}{|x - b_0|^2} \right] \left(\delta^{ij} - \frac{2(y - b_1)^i (y - b_1)^j}{|y - b_1|^2} \right) \left[G_{\underline{x}, \underline{y}}^{p \text{ adj}}(2k^- p_1^+) - G_{\underline{x}, b_1}^{p \text{ adj}}(2k^- p_1^+) \right] \\
& + \left(\frac{x - b_1}{|x - b_1|^2} - \frac{x - b_0}{|x - b_0|^2} \right) \cdot \frac{y - b_1}{|y - b_1|^2} G_{b_1, \underline{x}}^{i \text{ adj}}(2k^- p_1^+) \\
& + \frac{x - b_1}{|x - b_1|^2} \cdot \left(\frac{y - b_1}{|y - b_1|^2} - \frac{y - b_0}{|y - b_0|^2} \right) G_{b_1, \underline{y}}^{i \text{ adj}}(2k^- p_1^+) \\
& + \left(\frac{x - b_1}{|x - b_1|^2} \cdot \frac{y - b_0}{|y - b_0|^2} + \frac{x - b_0}{|x - b_0|^2} \cdot \frac{y - b_1}{|y - b_1|^2} \right) G_{b_1, b_0}^{i \text{ adj}}(2k^- p_1^+) \Bigg\}. \tag{C25}
\end{aligned}$$

Once again, we see that everything is expressed in terms of the \mathcal{F}^{12} and $\mathcal{D}^p - \tilde{\mathcal{D}}^p$ operators, and, therefore, in terms of G_T^{adj} and $G_T^{i \text{ adj}}$. After convolution with Eq. (C11), we see that only the part of the decomposition (33b) containing G_{2T}^{adj} survives.

We have thus shown that the interaction with the target in the cross section of small- x evolved longitudinally polarized projectile on a longitudinally polarized target is expressible in terms of $G_T^{\text{adj}}(2k^- p_1^+)$ and $G_{2T}^{\text{adj}}(2k^- p_1^+)$, as desired.

-
- [1] Y. V. Kovchegov, D. Pitonyak and M. D. Sievert, *Helicity Evolution at Small- x* , *JHEP* **01** (2016) 072, [[1511.06737](#)].
 - [2] Y. V. Kovchegov, D. Pitonyak and M. D. Sievert, *Helicity Evolution at Small x : Flavor Singlet and Non-Singlet Observables*, *Phys. Rev.* **D95** (2017) 014033, [[1610.06197](#)].
 - [3] Y. V. Kovchegov and M. D. Sievert, *Small- x Helicity Evolution: an Operator Treatment*, *Phys. Rev.* **D99** (2019) 054032, [[1808.09010](#)].
 - [4] F. Cougoulic, Y. V. Kovchegov, A. Tarasov and Y. Tawabutr, *Quark and gluon helicity evolution at small x : revised and updated*, *JHEP* **07** (2022) 095, [[2204.11898](#)].
 - [5] D. Adamiak, N. Baldonado, Y. V. Kovchegov, W. Melnitchouk, D. Pitonyak, N. Sato et al., *Global analysis of polarized DIS & SIDIS data with improved small- x helicity evolution*, **2308.07461**.
 - [6] EUROPEAN MUON collaboration, J. Ashman et al., *A Measurement of the Spin Asymmetry and Determination of the Structure Function $g(1)$ in Deep Inelastic Muon-Proton Scattering*, *Phys. Lett. B* **206** (1988) 364.
 - [7] R. L. Jaffe and A. Manohar, *The $G(1)$ Problem: Fact and Fantasy on the Spin of the Proton*, *Nucl. Phys.* **B337** (1990) 509–546.
 - [8] X.-D. Ji, *Gauge-Invariant Decomposition of Nucleon Spin*, *Phys. Rev. Lett.* **78** (1997) 610–613, [[hep-ph/9603249](#)].
 - [9] D. Boer et al., *Gluons and the quark sea at high energies: Distributions, polarization, tomography*, **1108.1713**.
 - [10] C. A. Aidala, S. D. Bass, D. Hasch and G. K. Mallot, *The Spin Structure of the Nucleon*, *Rev. Mod. Phys.* **85** (2013) 655–691, [[1209.2803](#)].
 - [11] A. Accardi et al., *Electron Ion Collider: The Next QCD Frontier*, *Eur. Phys. J.* **A52** (2016) 268, [[1212.1701](#)].
 - [12] E. Leader and C. Lorcé, *The angular momentum controversy: What’s it all about and does it matter?*, *Phys. Rept.* **541** (2014) 163–248, [[1309.4235](#)].
 - [13] E. C. Aschenauer et al., *The RHIC Spin Program: Achievements and Future Opportunities*, **1304.0079**.
 - [14] E.-C. Aschenauer et al., *The RHIC SPIN Program: Achievements and Future Opportunities*, **1501.01220**.
 - [15] A. Prokudin, Y. Hatta, Y. Kovchegov and C. Marquet, eds., *Proceedings, Probing Nucleons and Nuclei in High Energy Collisions: Dedicated to the Physics of the Electron Ion Collider: Seattle (WA), United States, October 1 - November 16, 2018*, WSP, 2020. 10.1142/11684.
 - [16] X. Ji, F. Yuan and Y. Zhao, *What we know and what we don’t know about the proton spin after 30 years*, *Nature Rev. Phys.* **3** (2021) 27–38, [[2009.01291](#)].
 - [17] R. Abdul Khalek et al., *Science Requirements and Detector Concepts for the Electron-Ion Collider: EIC Yellow Report*, **2103.05419**.
 - [18] E. A. Kuraev, L. N. Lipatov and V. S. Fadin, *The Pomernanchuk singularity in non-Abelian gauge theories*, *Sov. Phys. JETP* **45** (1977) 199–204.
 - [19] I. Balitsky and L. Lipatov, *The Pomernanchuk Singularity in Quantum Chromodynamics*, *Sov.J.Nucl.Phys.* **28** (1978) 822–829.
 - [20] L. V. Gribov, E. M. Levin and M. G. Ryskin, *Singlet structure function at small x : Unitarization of gluon ladders*, *Nucl. Phys.* **B188** (1981) 555–576.
 - [21] I. Balitsky, *Operator expansion for high-energy scattering*, *Nucl. Phys.* **B463** (1996) 99–160, [[hep-ph/9509348](#)].
 - [22] I. Balitsky, *Factorization and high-energy effective action*, *Phys. Rev.* **D60** (1999) 014020, [[hep-ph/9812311](#)].
 - [23] Y. V. Kovchegov, *Small- x F_2 structure function of a nucleus including multiple pomeron exchanges*, *Phys. Rev.* **D60** (1999) 034008, [[hep-ph/9901281](#)].
 - [24] Y. V. Kovchegov, *Unitarization of the BFKL pomeron on a nucleus*, *Phys. Rev.* **D61** (2000) 074018, [[hep-ph/9905214](#)].
 - [25] J. Jalilian-Marian, A. Kovner and H. Weigert, *The Wilson renormalization group for low x physics: Gluon evolution at finite parton density*, *Phys. Rev.* **D59** (1998) 014015, [[hep-ph/9709432](#)].

- [26] J. Jalilian-Marian, A. Kovner, A. Leonidov and H. Weigert, *The Wilson renormalization group for low x physics: Towards the high density regime*, *Phys. Rev.* **D59** (1998) 014014, [[hep-ph/9706377](#)].
- [27] H. Weigert, *Unitarity at small Bjorken x* , *Nucl. Phys.* **A703** (2002) 823–860, [[hep-ph/0004044](#)].
- [28] E. Iancu, A. Leonidov and L. D. McLerran, *The renormalization group equation for the color glass condensate*, *Phys. Lett.* **B510** (2001) 133–144.
- [29] E. Iancu, A. Leonidov and L. D. McLerran, *Nonlinear gluon evolution in the color glass condensate. I*, *Nucl. Phys.* **A692** (2001) 583–645, [[hep-ph/0011241](#)].
- [30] E. Ferreiro, E. Iancu, A. Leonidov and L. McLerran, *Nonlinear gluon evolution in the color glass condensate. II*, *Nucl. Phys.* **A703** (2002) 489–538, [[hep-ph/0109115](#)].
- [31] L. V. Gribov, E. M. Levin and M. G. Ryskin, *Semihard Processes in QCD*, *Phys. Rept.* **100** (1983) 1–150.
- [32] E. Iancu and R. Venugopalan, *The Color glass condensate and high-energy scattering in QCD*, pp. 249–3363. 3, 2003. [[hep-ph/0303204](#)]. 10.1142/9789812795533_0005.
- [33] H. Weigert, *Evolution at small x_{bj} : The Color Glass Condensate*, *Prog. Part. Nucl. Phys.* **55** (2005) 461–565, [[hep-ph/0501087](#)].
- [34] J. Jalilian-Marian and Y. V. Kovchegov, *Saturation physics and deuteron-Gold collisions at RHIC*, *Prog. Part. Nucl. Phys.* **56** (2006) 104–231, [[hep-ph/0505052](#)].
- [35] F. Gelis, E. Iancu, J. Jalilian-Marian and R. Venugopalan, *The Color Glass Condensate*, *Ann.Rev.Nucl.Part.Sci.* **60** (2010) 463–489, [[1002.0333](#)].
- [36] J. L. Albacete and C. Marquet, *Gluon saturation and initial conditions for relativistic heavy ion collisions*, *Prog.Part.Nucl.Phys.* **76** (2014) 1–42, [[1401.4866](#)].
- [37] Y. V. Kovchegov and E. Levin, *Quantum chromodynamics at high energy*, vol. 33. Cambridge University Press, 2012.
- [38] A. Morreale and F. Salazar, *Mining for Gluon Saturation at Colliders*, *Universe* **7** (2021) 312, [[2108.08254](#)].
- [39] Y. Hatta, Y. Nakagawa, F. Yuan, Y. Zhao and B. Xiao, *Gluon orbital angular momentum at small- x* , *Phys. Rev.* **D95** (2017) 114032, [[1612.02445](#)].
- [40] Y. V. Kovchegov, D. Pitonyak and M. D. Sievert, *Small- x asymptotics of the quark helicity distribution*, *Phys. Rev. Lett.* **118** (2017) 052001, [[1610.06188](#)].
- [41] Y. V. Kovchegov, D. Pitonyak and M. D. Sievert, *Small- x Asymptotics of the Quark Helicity Distribution: Analytic Results*, *Phys. Lett.* **B772** (2017) 136–140, [[1703.05809](#)].
- [42] Y. V. Kovchegov, D. Pitonyak and M. D. Sievert, *Small- x Asymptotics of the Gluon Helicity Distribution*, *JHEP* **10** (2017) 198, [[1706.04236](#)].
- [43] Y. V. Kovchegov, *Orbital Angular Momentum at Small x* , *JHEP* **03** (2019) 174, [[1901.07453](#)].
- [44] F. Cougoulic and Y. V. Kovchegov, *Helicity-dependent generalization of the JIMWLK evolution*, *Phys. Rev.* **D100** (2019) 114020, [[1910.04268](#)].
- [45] Y. V. Kovchegov and Y. Tawabutr, *Helicity at Small x : Oscillations Generated by Bringing Back the Quarks*, *JHEP* **08** (2020) 014, [[2005.07285](#)].
- [46] F. Cougoulic and Y. V. Kovchegov, *Helicity-dependent extension of the McLerran-Venugopalan model*, *Nucl. Phys. A* **1004** (2020) 122051, [[2005.14688](#)].
- [47] G. A. Chirilli, *High-energy operator product expansion at sub-eikonal level*, *JHEP* **06** (2021) 096, [[2101.12744](#)].
- [48] Y. V. Kovchegov, A. Tarasov and Y. Tawabutr, *Helicity evolution at small x : the single-logarithmic contribution*, *JHEP* **03** (2022) 184, [[2104.11765](#)].
- [49] J. Borden and Y. V. Kovchegov, *Analytic solution for the revised helicity evolution at small x and large N_c : New resummed gluon-gluon polarized anomalous dimension and intercept*, *Phys. Rev. D* **108** (2023) 014001, [[2304.06161](#)].
- [50] D. Adamiak, Y. V. Kovchegov and Y. Tawabutr, *Helicity evolution at small x : Revised asymptotic results at large N_c and N_f* , *Phys. Rev. D* **108** (2023) 054005, [[2306.01651](#)].
- [51] A. H. Mueller, *Soft gluons in the infinite momentum wave function and the BFKL pomeron*, *Nucl. Phys.* **B415** (1994) 373–385.
- [52] A. H. Mueller and B. Patel, *Single and double BFKL pomeron exchange and a dipole picture of high-energy hard processes*, *Nucl. Phys.* **B425** (1994) 471–488, [[hep-ph/9403256](#)].
- [53] A. H. Mueller, *Unitarity and the BFKL pomeron*, *Nucl. Phys.* **B437** (1995) 107–126, [[hep-ph/9408245](#)].
- [54] T. Altinoluk, N. Armesto, G. Beuf, M. Martinez and C. A. Salgado, *Next-to-eikonal corrections in the CGC: gluon production and spin asymmetries in pA collisions*, *JHEP* **07** (2014) 068, [[1404.2219](#)].
- [55] I. Balitsky and A. Tarasov, *Rapidity evolution of gluon TMD from low to moderate x* , *JHEP* **10** (2015) 017, [[1505.02151](#)].
- [56] I. Balitsky and A. Tarasov, *Gluon TMD in particle production from low to moderate x* , *JHEP* **06** (2016) 164, [[1603.06548](#)].
- [57] G. A. Chirilli, *Sub-eikonal corrections to scattering amplitudes at high energy*, *JHEP* **01** (2019) 118, [[1807.11435](#)].
- [58] J. Jalilian-Marian, *Quark jets scattering from a gluon field: from saturation to high p_t* , *Phys. Rev.* **D99** (2019) 014043, [[1809.04625](#)].
- [59] J. Jalilian-Marian, *Rapidity loss, spin and angular asymmetries in scattering of a quark from color field of a proton (nucleus)*, [[1912.08878](#)].
- [60] T. Altinoluk, G. Beuf, A. Czajka and A. Tymowska, *Quarks at next-to-eikonal accuracy in the CGC: Forward quark-nucleus scattering*, *Phys. Rev. D* **104** (2021) 014019, [[2012.03886](#)].
- [61] Y. V. Kovchegov and M. G. Santiago, *Quark sivers function at small x : spin-dependent odderon and the sub-eikonal evolution*, *JHEP* **11** (2021) 200, [[2108.03667](#)].
- [62] T. Altinoluk and G. Beuf, *Quark and scalar propagators at next-to-eikonal accuracy in the CGC through a dynamical*

- background gluon field, *Phys. Rev. D* **105** (2022) 074026, [2109.01620].
- [63] Y. V. Kovchegov and M. G. Santiago, *T-odd leading-twist quark TMDs at small x*, *JHEP* **11** (2022) 098, [2209.03538].
- [64] T. Altinoluk, G. Beuf, A. Czakajka and A. Tymowska, *DIS dijet production at next-to-eikonal accuracy in the CGC*, *Phys. Rev. D* **107** (2023) 074016, [2212.10484].
- [65] T. Altinoluk, N. Armesto and G. Beuf, *Probing quark transverse momentum distributions in the color glass condensate: Quark-gluon dijets in deep inelastic scattering at next-to-eikonal accuracy*, *Phys. Rev. D* **108** (2023) 074023, [2303.12691].
- [66] T. Altinoluk, G. Beuf and J. Jalilian-Marian, *Renormalization of the gluon distribution function in the background field formalism*, **2305.11079**.
- [67] M. Li, *Small x physics beyond eikonal approximation: an effective Hamiltonian approach*, *JHEP* **07** (2023) 158, [2304.12842].
- [68] G. 't Hooft, *A Planar Diagram Theory for Strong Interactions*, *Nucl. Phys. B* **72** (1974) 461.
- [69] G. Veneziano, *Some Aspects of a Unified Approach to Gauge, Dual and Gribov Theories*, *Nucl. Phys. B* **117** (1976) 519–545.
- [70] J. Bartels, B. Ermolaev and M. Ryskin, *Nonsinglet contributions to the structure function g_1 at small x*, *Z.Phys.* **C70** (1996) 273–280, [hep-ph/9507271].
- [71] J. Bartels, B. Ermolaev and M. Ryskin, *Flavor singlet contribution to the structure function $G(1)$ at small x*, *Z.Phys.* **C72** (1996) 627–635, [hep-ph/9603204].
- [72] V. G. Gorshkov, V. N. Gribov, L. N. Lipatov and G. V. Frolov, *Doubly logarithmic asymptotic behavior in quantum electrodynamics*, *Sov. J. Nucl. Phys.* **6** (1968) 95.
- [73] R. Kirschner and L. Lipatov, *Double Logarithmic Asymptotics and Regge Singularities of Quark Amplitudes with Flavor Exchange*, *Nucl. Phys.* **B213** (1983) 122–148.
- [74] R. Kirschner, *Reggeon interactions in perturbative QCD*, *Z.Phys.* **C65** (1995) 505–510, [hep-th/9407085].
- [75] R. Kirschner, *Regge asymptotics of scattering with flavor exchange in QCD*, *Z.Phys.* **C67** (1995) 459–466, [hep-th/9404158].
- [76] J. Blumlein and A. Vogt, *On the behavior of nonsinglet structure functions at small x*, *Phys. Lett. B* **370** (1996) 149–155, [hep-ph/9510410].
- [77] S. Griffiths and D. Ross, *Studying the perturbative Reggeon*, *Eur.Phys.J.* **C12** (2000) 277–286, [hep-ph/9906550].
- [78] S. Moch, J. A. M. Vermaseren and A. Vogt, *The Three-Loop Splitting Functions in QCD: The Helicity-Dependent Case*, *Nucl. Phys. B* **889** (2014) 351–400, [1409.5131].
- [79] J. Blümlein, P. Marquard, C. Schneider and K. Schönwald, *The three-loop polarized singlet anomalous dimensions from off-shell operator matrix elements*, *JHEP* **01** (2022) 193, [2111.12401].
- [80] J. Blümlein and A. Vogt, *The Singlet contribution to the structure function $g_1(x, Q^{*2})$ at small x*, *Phys. Lett. B* **386** (1996) 350–358, [hep-ph/9606254].
- [81] B. I. Ermolaev, M. Greco and S. I. Troian, *QCD running coupling effects for the nonsinglet structure function at small x*, *Nucl. Phys.* **B571** (2000) 137–150, [hep-ph/9906276].
- [82] B. I. Ermolaev, M. Greco and S. I. Troyan, *Intercepts of the nonsinglet structure functions*, *Nucl. Phys.* **B594** (2001) 71–88, [hep-ph/0009037].
- [83] B. I. Ermolaev, M. Greco and S. I. Troyan, *Running coupling effects for the singlet structure function g_1 at small x*, *Phys. Lett.* **B579** (2004) 321–330, [hep-ph/0307128].
- [84] B. I. Ermolaev, M. Greco and S. I. Troyan, *Overview of the spin structure function g_1 at arbitrary x and Q^2* , *Riv. Nuovo Cim.* **33** (2010) 57–122, [0905.2841].
- [85] JEFFERSON LAB ANGULAR MOMENTUM collaboration, D. Adamiak, Y. V. Kovchegov, W. Melnitchouk, D. Pitonyak, N. Sato and M. D. Sievert, *First analysis of world polarized DIS data with small-x helicity evolution*, *Phys. Rev. D* **104** (2021) L031501, [2102.06159].
- [86] M. Gluck, E. Reya, M. Stratmann and W. Vogelsang, *Models for the polarized parton distributions of the nucleon*, *Phys. Rev. D* **63** (2001) 094005, [hep-ph/0011215].
- [87] E. Leader, A. V. Sidorov and D. B. Stamenov, *Longitudinal polarized parton densities updated*, *Phys. Rev.* **D73** (2006) 034023, [hep-ph/0512114].
- [88] D. de Florian, R. Sassot, M. Stratmann and W. Vogelsang, *Extraction of Spin-Dependent Parton Densities and Their Uncertainties*, *Phys. Rev.* **D80** (2009) 034030, [0904.3821].
- [89] E. Leader, A. V. Sidorov and D. B. Stamenov, *Determination of Polarized PDFs from a QCD Analysis of Inclusive and Semi-inclusive Deep Inelastic Scattering Data*, *Phys. Rev.* **D82** (2010) 114018, [1010.0574].
- [90] P. Jimenez-Delgado, A. Accardi and W. Melnitchouk, *Impact of hadronic and nuclear corrections on global analysis of spin-dependent parton distributions*, *Phys. Rev.* **D89** (2014) 034025, [1310.3734].
- [91] NNPDF collaboration, R. D. Ball, S. Forte, A. Guffanti, E. R. Nocera, G. Ridolfi and J. Rojo, *Unbiased determination of polarized parton distributions and their uncertainties*, *Nucl. Phys.* **B874** (2013) 36–84, [1303.7236].
- [92] NNPDF collaboration, E. R. Nocera, R. D. Ball, S. Forte, G. Ridolfi and J. Rojo, *A first unbiased global determination of polarized PDFs and their uncertainties*, *Nucl. Phys.* **B887** (2014) 276–308, [1406.5539].
- [93] D. de Florian, R. Sassot, M. Stratmann and W. Vogelsang, *Evidence for polarization of gluons in the proton*, *Phys. Rev. Lett.* **113** (2014) 012001, [1404.4293].
- [94] E. Leader, A. V. Sidorov and D. B. Stamenov, *New analysis concerning the strange quark polarization puzzle*, *Phys. Rev.* **D91** (2015) 054017, [1410.1657].
- [95] JEFFERSON LAB ANGULAR MOMENTUM collaboration, N. Sato, W. Melnitchouk, S. E. Kuhn, J. J. Ethier and A. Accardi, *Iterative Monte Carlo analysis of spin-dependent parton distributions*, *Phys. Rev.* **D93** (2016) 074005,

- [1601.07782].
- [96] J. Ethier, N. Sato and W. Melnitchouk, *First simultaneous extraction of spin-dependent parton distributions and fragmentation functions from a global QCD analysis*, *Phys. Rev. Lett.* **119** (2017) 132001, [1705.05889].
- [97] D. De Florian, G. A. Lucero, R. Sassot, M. Stratmann and W. Vogelsang, *Monte Carlo sampling variant of the DSSV14 set of helicity parton densities*, *Phys. Rev. D* **100** (2019) 114027, [1902.10548].
- [98] I. Borsa, G. Lucero, R. Sassot, E. C. Aschenauer and A. S. Nunes, *Revisiting helicity parton distributions at a future electron-ion collider*, *Phys. Rev. D* **102** (2020) 094018, [2007.08300].
- [99] JAM COLLABORATION collaboration, Y. Zhou, N. Sato and W. Melnitchouk, *How well do we know the gluon polarization in the proton?*, *Phys. Rev. D* **105** (2022) 074022, [2201.02075].
- [100] JAM COLLABORATION collaboration, C. Cocuzza, W. Melnitchouk, A. Metz and N. Sato, *Polarized antimatter in the proton from a global QCD analysis*, *Phys. Rev. D* **106** (2022) L031502, [2202.03372].
- [101] V. N. Gribov and L. N. Lipatov, *Deep inelastic e p scattering in perturbation theory*, *Sov. J. Nucl. Phys.* **15** (1972) 438–450.
- [102] G. Altarelli and G. Parisi, *Asymptotic Freedom in Parton Language*, *Nucl. Phys.* **B126** (1977) 298.
- [103] Y. L. Dokshitzer, *Calculation of the Structure Functions for Deep Inelastic Scattering and e^+e^- Annihilation by Perturbation Theory in Quantum Chromodynamics*, *Sov. Phys. JETP* **46** (1977) 641–653.
- [104] STAR collaboration, L. Adamczyk et al., *Precision Measurement of the Longitudinal Double-spin Asymmetry for Inclusive Jet Production in Polarized Proton Collisions at $\sqrt{s} = 200$ GeV*, *Phys. Rev. Lett.* **115** (2015) 092002, [1405.5134].
- [105] PHENIX collaboration, A. Adare et al., *Inclusive cross section and double-helicity asymmetry for π^0 production at midrapidity in p + p collisions at $\sqrt{s} = 510$ GeV*, *Phys. Rev. D* **93** (2016) 011501, [1510.02317].
- [106] Y. V. Kovchegov and A. H. Mueller, *Gluon production in current nucleus and nucleon nucleus collisions in a quasi-classical approximation*, *Nucl. Phys.* **B529** (1998) 451–479, [hep-ph/9802440].
- [107] B. Z. Kopeliovich, A. V. Tarasov and A. Schafer, *Bremsstrahlung of a quark propagating through a nucleus*, *Phys. Rev. C* **59** (1999) 1609–1619, [hep-ph/9808378].
- [108] M. A. Braun, *Inclusive jet production on the nucleus in the perturbative QCD with $N_c \rightarrow \infty$* , *Phys. Lett.* **B483** (2000) 105–114, [hep-ph/0003003].
- [109] A. Dumitru and L. D. McLerran, *How protons shatter colored glass*, *Nucl. Phys.* **A700** (2002) 492–508, [hep-ph/0105268].
- [110] Y. V. Kovchegov and K. Tuchin, *Inclusive gluon production in dis at high parton density*, *Phys. Rev.* **D65** (2002) 074026, [hep-ph/0111362].
- [111] D. Kharzeev, Y. V. Kovchegov and K. Tuchin, *Cronin effect and high-p(t) suppression in p a collisions*, *Phys. Rev.* **D68** (2003) 094013, [hep-ph/0307037].
- [112] I. Balitsky, *Scattering of shock waves in QCD*, *Phys. Rev.* **D70** (2004) 114030, [hep-ph/0409314].
- [113] G. A. Chirilli, Y. V. Kovchegov and D. E. Wertepny, *Classical Gluon Production Amplitude for Nucleus-Nucleus Collisions: First Saturation Correction in the Projectile*, *JHEP* **03** (2015) 015, [1501.03106].
- [114] M. Li and V. V. Skokov, *First saturation correction in high energy proton-nucleus collisions. Part I. Time evolution of classical Yang-Mills fields beyond leading order*, *JHEP* **06** (2021) 140, [2102.01594].
- [115] M. Li and V. V. Skokov, *First saturation correction in high energy proton-nucleus collisions. Part II. Single inclusive semi-hard gluon production*, *JHEP* **06** (2021) 141, [2104.01879].
- [116] M. Li and V. V. Skokov, *First saturation correction in high energy proton-nucleus collisions. Part III. Ensemble averaging*, *JHEP* **01** (2022) 160, [2111.05304].
- [117] A. H. Mueller, *Small x Behavior and Parton Saturation: A QCD Model*, *Nucl. Phys.* **B335** (1990) 115.
- [118] L. D. McLerran and R. Venugopalan, *Computing quark and gluon distribution functions for very large nuclei*, *Phys. Rev.* **D49** (1994) 2233–2241, [hep-ph/9309289].
- [119] L. D. McLerran and R. Venugopalan, *Gluon distribution functions for very large nuclei at small transverse momentum*, *Phys. Rev.* **D49** (1994) 3352–3355, [hep-ph/9311205].
- [120] L. D. McLerran and R. Venugopalan, *Green’s functions in the color field of a large nucleus*, *Phys. Rev.* **D50** (1994) 2225–2233, [hep-ph/9402335].
- [121] G. P. Lepage and S. J. Brodsky, *Exclusive processes in perturbative quantum chromodynamics*, *Phys. Rev.* **D22** (1980) 2157.
- [122] Y. V. Kovchegov and M. D. Sievert, *A New Mechanism for Generating a Single Transverse Spin Asymmetry*, *Phys.Rev.* **D86** (2012) 034028, [1201.5890].
- [123] K. Itakura, Y. V. Kovchegov, L. McLerran and D. Teaney, *Baryon stopping and valence quark distribution at small x*, *Nucl. Phys.* **A730** (2004) 160–190, [hep-ph/0305332].
- [124] P. J. Mulders and J. Rodrigues, *Transverse momentum dependence in gluon distribution and fragmentation functions*, *Phys. Rev.* **D63** (2001) 094021, [hep-ph/0009343].
- [125] PHENIX collaboration, A. Adare et al., *Inclusive double-helicity asymmetries in neutral-pion and eta-meson production in $\vec{p} + \vec{p}$ collisions at $\sqrt{s} = 200$ GeV*, *Phys. Rev. D* **90** (2014) 012007, [1402.6296].
- [126] STAR collaboration, M. S. Abdallah et al., *Longitudinal double-spin asymmetry for inclusive jet and dijet production in polarized proton collisions at $\sqrt{s} = 510$ GeV*, *Phys. Rev. D* **105** (2022) 092011, [2110.11020].
- [127] Y. V. Kovchegov and B. Manley, *Orbital angular momentum at small x revisited*, *JHEP* **02** (2024) 060, [2310.18404].